EERA DTOC calculation of scenarios

Gerard Schepers, Alfredo Pena, Alice Ely, Ana Palomares, Ayman Attiya, Giorgos Sieros, Gregor Giebel, Harald Svendsen, Ilona Bastigkeit, Ioanna Karagali, Ivan Moya, Olimpo Anaya Lara, Pablo Ledesma, Pedro M. Fernandes Correia, Vitar Gosta Gomez, Wei He

June, 2015

Document information

Document Name:	EERA DTOC Calculation of scenarios
Document Number:	D5.12
Author:	Gerard Schepers, Alfredo Pena, Alice Ely, Ana Palomares, Ayman Attiya, Giorgos Sieros, Gregor Giebel, Harald Svendsen, Ilona Bastigkeit, Ioanna Karagali, Ivan Moya, Olimpo Anaya Lara, Pablo Ledesma, Pedro M. Fernandes Correia, Vitar Gosta Gomez, Wei He
Date:	June 2015
WP:	5
Task:	5.3

TABLE OF CONTENTS

Deliverable 5.12 EERA DTOC calculation of scenarios

Deliverable 5.12 EERA DTOC calculation of scenarios

SUMMARY

This report describes the calculation of scenarios which have been defined to demonstrate the value of the EERA-DTOC tool. Thereto it should be realized that the value of the EERA-DTOC tool could best be demonstrated by a comparison with measurements but the intended clusters for which the tool is developed are still mainly in the planning phase by which measurements to validate the tool are lacking. However, by the calculation of likely scenarios, the industrial usefulness of the tool can still be tested where moreover an 'expert view' on the results will be carried out in order to check their degree of reality.

Therefore several scenarios are described which are denoted as the 'base and the near future scenario', i.e. scenarios which are still relatively close to the present state of the art wind farm (clusters). This is in particular true for the base scenario which is described as a scenario which reflects 'the current way of thinking'. The near future scenario goes beyond the current way of thinking by using upscaled turbines. The description of these scenarios is given in D5.2

The base scenario considers a 500MW wind farm which consists of hundred turbines with a rated power of 5 MW at the location where the Race Bank wind farm is planned under the UK Round 2. This farm is planned 27 km from the North Norfolk coast at the Eastern part of England. The Race Bank farm is surrounded by several other wind farms which are either operational or under construction. The turbine which is selected for this farm is the reference turbine from the former EU project Upwind, since this turbine is described in detail in public literature and reflects the current state of the art wind turbine technology.

The near future scenario assumes a 1 GW wind farm and is located at the Dogger Bank in the North Sea. It consists of 100 turbines with a rated power of 10 MW. Although 10 MW turbines are not on the market yet the INNWIND.EU reference wind turbine has been selected since a full description of this turbine is available.

Moreover a far future scenario is defined which refers to a time line of some 15 year. It consists of large clusters (up to 10 GW) where some of the farms in the cluster are differently sized and contain floating turbines. The far future scenario includes several grid planning options, both for the export to the mainland as for interconnecting wind farms in the cluster. It even includes interconnections with other development zones or even to other countries, combining wind power export and cross-border electricity trade.

The far future scenario is reported in D5.7.

Deliverable 5.12 EERA DTOC calculation of scenarios

1. INTRODUCTION

1.1 Background

In WP5.3 of the EERA-DTOC project the integrated offshore wind farm design tool as delivered from WP4 [2] is demonstrated for and by the industry on the basis of likely scenarios. The scenarios as described in this document are denoted as the 'base and the near future scenario', i.e. scenarios which are still relatively close to the present state of the art wind farm (clusters). This is in particular true for the base scenario which is described as a scenario which reflects 'the current way of thinking'. The near future scenario goes beyond the current way of thinking by using upscaled turbines. The far future scenario has a time line in the order of 15 years.

.

.

1.2 Goal of scenarios and document

It is important to realize that validation of the integrated design tool by means of measurements is still difficult to do on the scale of clusters because large wind farm clusters are in planning rather than in operation. Nevertheless the demonstration of the EERA-DTOC tool by means of likely scenarios enables a check on the industrial usefulness of the tool on basis of the user requirements as defined in the start-up phase of the project and reported in D4.1 [12]. These user stories, together with the global definition of the scenario formed the starting point of the present calculation. More specifically it should be shown that the tool is useful, easy to use, complete and robust. Moreover the 'steepness' of the learning curve will be determined and it will be checked which tutorials would have be added (e.g. simple case, videos?). Although a comparison with measurements cannot be made an expert view is carried out on the results in order to assess their degree of reality.

An important requirement for the scenario calculation is that all EERA-DTOC main modules (i.e. the wind module, the wake module, the grid module, the energy yield module and the cost module) are activated.

1.3 Approach

As explained in section 1.1., the so-called base and near future scenario are mainly used for the testing of the EERA-DTOC tool.

Base Scenario

The base scenario is connected to the planned Race Bank wind farm at the Eastern coast of England, see http://www.4coffshore.com/windfarms/race-bank-united-kingdom-uk18.html and https://mapsengine.google.com/map/edit?hl=nl&mid=zBjDdqwq1tDE.kInbPPDGvF7U which shows this farm to be scheduled 27 km from the North Norfolk coast. The planned capacity is 580 MW realized though 94-116 turbines in the range of 5-6.15 MW. Since the turbine type is not decided yet and because the eventual turbine data will anyhow be confidential the present scenario assumes the farm to consist of 100 UPWIND 5MW reference turbine since the UPWIND turbine is well documented in the public domain. The Race Bank wind farm is surrounded by several other wind farms which are either in operation already or they are in the planning phase. These surrounding farms are included in the scenario description.

Near future scenario

The near future scenario is connected to (aspects of) the plans for an off-shore cluster at Dogger Bank. It starts with a 1GW wind farm consisting of 100 turbines with a rated power of 10 MW using the well documented INNWIND.EU reference turbine. The farm is assumed to be located at the southern part of the Doggersbank area and it is surrounded by other wind farms similar to the planned situation for Doggersbank of figure 3.

Deliverable 5.12 EERA DTOC calculation of scenarios

Some preliminary calculations on this near future scenario have already been done in an early stage by ECN to check the suitability of the scenario definition.

Far future scenario

A far future scenario is defined which refers to a time line of some 15 year. It consists of large clusters (up to 10 GW) where some of the farms in the cluster are differently sized and contain floating turbines. The far future scenario includes several grid planning options, both for the export to the mainland as for interconnecting wind farms in the cluster. It even includes interconnections with other development zones or even to other countries, combining wind power export and cross-border electricity trade.

Deliverable 5.12 EERA DTOC calculation of scenarios

2. APPROACH

As mentioned before, the previously defined users stories and the global definition of scenarios formed the starting point of the calculations. Thereto it should be known that the wind climate is calculated with the mesoscale model WRF by DTU, CENER and CIEMAT (with and without wind farms) for the areas under consideration.

- For the base scenario IWES, DTU, RES, Fraunhofer,Uporto were running the following user stories:
  - *"As strategic planner or developer I can determine the wake impact of individual wind farms within a cluster on each other (just meso)"*
    - *"As a developer I can determine the wake effects of neighbouring wind farm clusters on a single wind farm (meso scale and micro scale modelling)"*
  - *"As a developer I can determine the wake effects due to turbines within a wind farm"*
  - *"As a developer I can determine the net energy yield of a wind farm"*
- For the near future scenario ECN, DTU, CRES, Fraunhofer were running user stories
  - *"As a developer I can determine the wake effects of neighbouring wind farm clusters on a single wind farm (meso scale and micro scale modelling)"*
  - *"As a developer I can determine the optimum spacing, turbine model and hub height of turbines within off-shore farms"*
  - *"As a developer I want to use wind farm lay-out scenarios of my target wind farm with respect to nr of turbines, turbine types, thrust curves etc"*
- The far future scenario was Run off-line
- Iberdrola was planning to run its own calculations

All participants were asked to provide user reports of their calculations. The user reports should have the following format:
- 1 Objective/user story
  - *1.1 Objective*
  - *1.2 User story and scenario*
  - *[Please remove the scenarios or user stories you do not use.]*
    - Base scenario (Race Bank)
    - Near future scenario (Doggersbank)
    - Far future scenario
    - Other (please describe):
  - User story
    - 1.1 As strategic planner or developer I can determine the wake impact of individual wind farms within a cluster on each other (just meso)
    - 1.2 As a strategic planner I can determine the net energy yield of offshore wind farm clusters.
    - 1.3 As a strategic planner I can determine the optimum size, spacing and position offshore wind farm clusters.
    - 2.1 As a strategic planner I can determine the optimum strategic infrastructure to accommodate offshore wind farm clusters.
    - 3.1 As a developer I can determine the wake effects of neighbouring wind farm clusters on a single wind farm (meso and/or micro).
    - 3.2 As a developer I can determine the wake effects due to turbines within a wind farm.
    - 3.3 As a developer I can determine the net energy yield of a wind farm.
    - 3.4 As a developer I can determine the optimum spacing, position, turbine model and hub height of turbines within an offshore wind farm.
    - 3.5 As a developer, I want to use wind farm layout scenarios of my target wind farm with respect to nr of turbines, turbine types, power and thrust curves etc.
    - Other (Please described)

Deliverable 5.12 EERA DTOC calculation of scenarios

- 2 Codes
- 3 Input:
    - 3.1 Description of wind farm
    - 3.2 Description of turbines:
    - 3.3 Description of wind climate
    - 3.4 Remarks.
- 4. Output/results
- 5 Observations
    - 5.1 Observations on results.
    - 5.2 User experiences:
    - 5.3 Expert judgment

Deliverable 5.12 EERA DTOC calculation of scenarios

3. RESULTS

In the Appendices A to M the user reports from DTU, ECN, RES, CENER, Fraunhofer, CIEMAT, UPORTO, CRES, Sintef and Strathclyde are given.

The appendices A and B report DTU results from the first initial test runs. The observations made led to various improvements.

Appendic C reports results from ECN on the effect of different lay-outs on the net farm production using ECN's tool which were run off-line.

The appendices D, E and F give the user reports from RES, Uporto and Fraunhofer IWES, where Uporto makes a comparison between EERA-DTOC results and results from their in-house code VENTOS®/2.

In Appendix G the effect of variable tower height is reported by DTU. Appendix H reports a study of CRES showing the positive effect of a low induction rotor on the wake losses.

In Appendix I WaSP and Fuga results are run off-line and compared with the results from the EERA-DTOC tool.

In Appendices J and K the results from meso scale modelling are presented and the Appendices L and M show the results from the far future scenario which had to be run off-line

Appendices N and O report DTU results for the base and near future scenario where the impact of neighbouring wind farms is investigated and Appendix P include a scenario with lay-out for floating wind turbines.

Appendix Q reports DTU results regarding the comparisons of the WRF wind climates modelled by CENER, CIEMAT and DTU against 10 m winds derived from radar scatterometers on satellites.

Deliverable 5.12 EERA DTOC calculation of scenarios

4. CONCLUSIONS

Several parties carried out calculations with the software. Thereto a test matrix has been defined with which the the user stories and scenarios were divided over the partners.
All parties were asked to report the results of their calculations in a prescribed format so that a consistent and comparable set of user reports has been obtained. The progress of the tasks was discussed on a weekly basis through telcons which were attended by the participants involved in the testing.

One of the main obstacles for a thorough testing was formed by remote access problems, since firewall problems prevented many users to run the tool from their offices. These problems could sometimes be solved through workarounds, but this turned out to be a time consuming procedure. Together with the fact that testing of the tool started later than originally anticipated, this made that not all planned scenarios and user stories from the test matrix could be covered.

Generally speaking the users reported positive experiences, with easy installation (apart from the firewall problems) and a steep learning curve. The QGIS was sometimes mentioned to have long runtimes.

Most results which have been obtained were believed to be realistic. In many cases a comparison was made between Fuga and WAsP leading to a reasonable to good mutual agreement. Interfacing to other tools was however not possible yet from the EERA-DTOC tool by which the users who wanted to run other models than Fuga and WAsP had to run these cases off-line.

Very interesting was a study on the near future scenario in which the production was compared of a wind farm consisting of INNWIND.EU turbines and the production of the farm where the turbines were replaced by low induction (and higher diameter) AVATAR turbines. The farm with AVATAR turbines led to a higher gross energy production (as expected from the larger turbine) but also to lower wake losses which are attributed to the design concept (low induction) of the AVATAR turbine. The results of this study will be communicated to the AVATAR project.

Moreover a large number of observations were made which sometimes led to improvement of the tool, e.g.

- Too little detail in output results (largely solved)
- Expiry of licences without notice (solved)
- The use of an unconventional turbine tyoe (i.e. the AVATAR turbine) leads to unrealistic results (solved)
- The user story which investigates the effect of different turbine heights led to unrealistic cost variations, since the effect of tower height on turbine costs is not included yet.
- Some functionality didn't work on Unix, Mac (solved)
- Some puzzling results on the gross energy yield (still under investigation)
- It was found that the wind resource has to be changed at least once in the wind resource manager to get the correct wind resource even if other wind data are pre-selected in the GUI. This is an initialisation / misconfiguration problem. (users have been informed on this).

Deliverable 5.12 EERA DTOC calculation of scenarios

5. REFERENCES

1. Barthelmie, R. J., et al. *Flow and wakes in large wind farms: Final report for UpWind WP8.* Roskilde, Denmark: Risoe, 2011.

2. EERA. *EERA Design Tools for Offshore Wind Farm Cluster - Annex I - "Description of Work".* 13. September 2011.

3. Endegnanew, A. G., H. Svendsen, R. E. Torres-Olguin, und L. M. Faiella. *Design procedure for inter-array electric design (D2.2).* EERA-DTOC, 2013.

4. ENTSO-E. *Network Code for Requirements for Grid Connection Applicable to all Generators.* June 2012.

5. ENTSO-E. *Operational Reserve Ad Hoc Team Report - Final Version.* Brussels, 23. May 2012.

6. EURELECTRIC. *Ancillary Services. Unbundling Electricity Products – an Emerging Market.* Brussels, Belgium: EURELECTRIC Thermal Working Group, 2004.

7. Ferguson, Ana, Phil de Villiers, Brendan Fitzgerald, und Jan Matthiessen. *Benerfits in Moving the Inter-array Voltage from 33 kV to 66 kV AC for large offshore wind farms.* CarbonTrust, 2012.

8. Forewind. *Dogger Bank Teeside - Teesside Offshore Cable Corridor Selection Report.* Reading, UK: Forewind, 2012.

9. „Forewind - Dogger Bank." *Forewind Website.* 2011. http://www.forewind.co.uk/dogger-bank/overview.html (Zugriff am 29. 04 2013).

10. „Forewind Fact Sheet - April 2013." *Forewind.* 04 2013. http://www.forewind.co.uk/uploads/files/10898_FOR_Gen_Factsheet_v7_Hires.pdf (Zugriff am 29. 04 2013).

11. Margaris, I. D., A. D. Hansen, J. Bech, B. Andresen, und P. Sørensen. „Implementation of IEC Standard Models for Power System Stability Studies." *Proceedings of 11th International Workshop on Large-Scale Integration of Wind Power into Power Systems.* Lisbon, Portugal, 2012.

12. Stuart, P. *User Requirement workshop - EERA-DTOC Deliverable.* EERA, 2012.

13. Svendsen, H. G. „Planning Tool for Clustering and Optimised Grid Connection of O." *Energy Procedia*, 2013.

14. The Crown Estate. „The Crown Estate - About Us." *The Crown Estate.* 2013. http://www.thecrownestate.co.uk/about-us/ (Zugriff am 29. 4 2013).

15. „The Crown Estate - Round 3 wind farms." *The Crown Estate.* 2013. http://www.thecrownestate.co.uk/energy-infrastructure/offshore-wind-energy/our-portfolio/round-3-wind-farms/ (Zugriff am 29. 4 2013).

16. J. Badger et al: Benchmark report on wake models at cluster scale, EERA-DTOC deliverable D1.4, July 2013

17. P.E. Rethore et al: Benchmark report on wake models at wind farm scale, EERA-DTOC deliverable D1.3, July 2013

18. J.T.G. Pierik, U. Axelsson, E. Eriksson, D. Salomonsson, *EeFarm II Description, testing and application,* ECN-E--09-051, 2009.

19. **J.G, Schepers et al: How aerodynamic and electrical aspects come together in wind farm design, presented at EERA Deepwind conference, January 2014, http://www.sintef.no/project/Deepwind2014/Presentations/F/Schepers_G.pdf**

20. **Van Garrel et al EEFARM &Farmflow cabling demonstration ECN report. 2013**

21. **Jason Jonkman NREL reference turbine, February 15, 2007, NREL/NWTC**

Deliverable 5.12 EERA DTOC calculation of scenarios

A.1 Objective/user story

A1.1 Objective

Evaluate the impact of the combinations for the wind resource and wake models using the standard layout.

A1.2 User story and scenario

Base scenario (Race Bank)
User story
3.1 As a developer I can determine the wake effects of neighbouring wind farm clusters on a single wind farm (meso and/or micro).

A.2 Codes

Fuga, WAsP-Park and Levellised Cost Of Energy (LCOE) models

A.3 Input:

A.3.1 Description of wind farm

The Race Bank wind farm, located 27 km from the North Norfolk coast, has a planned capacity of 580 MW. Approximately 94 to 116 turbines in the range of 5-6.15 MW will be founded. The scenario assumes the farm to consist of 100 UPWIND 5MW reference turbines, since this type is well documented. The Race Bank wind farm is surrounded by several other wind farms which are either in operation already or they are in the planning phase. These surrounding farms are included in the scenario description.
The suggested layout of the farms (Figure 1) it based on the layout of the Horns Rev wind farm modified to 10x10 wind turbines. One main 'wind farm line' is oriented in the East-West direction and the other main wind farm line slightly skewed compared to the North-South direction. In Figure 1 the direction of the main wind farm lines is 5.1 rotor diameters but scenarios will be considered with different distances between the turbines ranging from 3.65 to 10 rotor diameters.
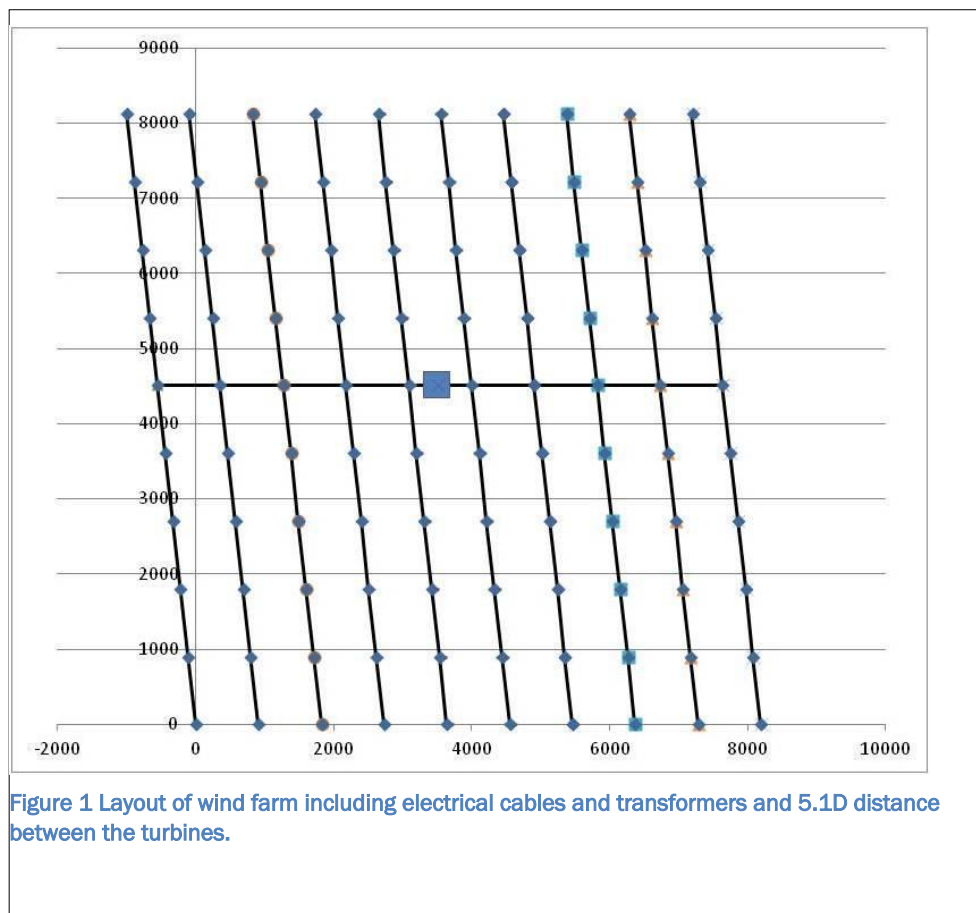
Deliverable 5.12 EERA DTOC calculation of scenarios

Figure 1 Layout of wind farm including electrical cables and transformers and 5.1D distance between the turbines.

A.3.2 Description of turbines:

The wind turbines from the base scenario have a rated power of 5 MW with a 14-rotor diameter of 126 m at a hub height of 90 m.

- Wind class: IEC class Ib

- Regulation: Variable speed, collective pitch

- Orientation of rotor: Upwind, overhang 5 meter

- Rated wind speed 11.4 m/s

- Cut-out wind speed 25 m/s

- Maximum rotor speed: 12.1 rpm (maximum tip speed: 80 m/s)

A.3.3 Description of wind climate

The WP5 Wind Resource file and the Fino-1 2004-2008 wind resource files, available from the DTOC Tool were used.

A.3.4 Remarks.

The different combinations of wind resource and wake model were used to estimate the various relevant quantities, such as the total gross and net annual energy production and costs of the investment and produced energy. The wind farm layout is the standard one presented in Figure 1. The DTOC tool uses the Race Bank as the active wind farm while all other neighboring farms are

Deliverable 5.12 EERA DTOC calculation of scenarios

selected with the Micro-scale wind impact. The different configurations used are presented in Table 1.

Table 1. Configuration of the different scenarios.

Configuration	Wind farm layout	Wind Resource	Wake Model
C1.	Standard (Fig 1.)	WP5	Fuga (+LCOE)
C2.	Standard (Fig 1.)	WP5	WAsP-Park (+LCOE)
C3.	Standard (Fig 1.)	F1 2004-2008	WAsP-Park (+LCOE)
C4.	Standard (Fig 1.)	F1 2004-2008	Fuga (+LCOE)

A.4 Output/results

The left panel of **Error! Reference source not found.** shows the ranking of the different onfigurations for increasing gross (solid line) and net (dashed line) annual energy production (AEP). Configuration 4 produces both the lowest gross and net AEP, increasing for C3 and C1, with C2 the highest.

The middle panel of **Error! Reference source not found.** shows the ranking of the configurations for ecreasing NPV costs. C2 produces the highest cost, decreasing for C1 and C3, while C4 produces the lowest costs. Similar are the results when looking at minimizing the levellised cost of energy (LCOE), shown in the right panel of **Error! Reference source not found.**.
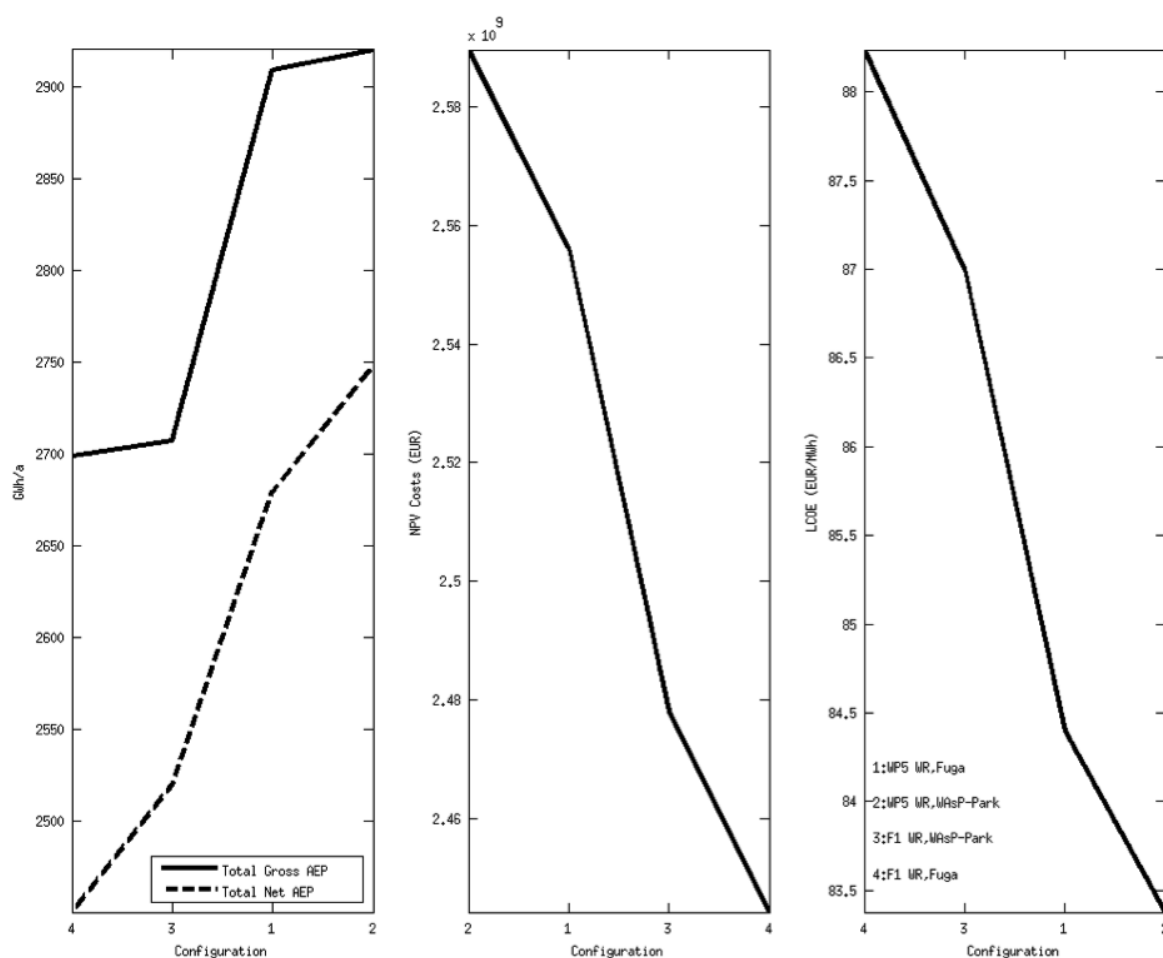

Figure 2. Results of the different configurations for the total gross and net annual energy production (left), the NPV costs (middle) and levellised cost of energy (right).

Deliverable 5.12 EERA DTOC calculation of scenarios

A.5 Observations

A.5.1 Observations on results.

From the configurations investigated, the WAsP-Park model with the WP5 wind resource produces the highest AEP (gross and net) while minimizing the LCOE.

A.5.2 User experiences:
When changing the wind climate from WP5 to F1, and vice versa, in order to use the LCOE model one should first run the scenario again using one of the 2 available wake models and then run the LCOE model.
While on the surrounding wind farms there is the option of Micro-, Meso- or No Impact when the Race Bank farm is active, selecting any of the options does not change the result. It is not clear if that should be the case, or what exactly that impact option is.
Unfortunately, editing the scenario in QGIS does not work in a Mac and a Linux (Ubuntu) machine, therefore it was not possible to evaluate the impact of modifying the layout of the surrounding wind farms.

A.5.3 Expert judgment
Regarding the results based on the different configurations, it seems that the WAsP-Park model estimates fewer wake losses, hence the higher net and gross AEP compared to Fuga. As far as the wind resource files are concerned, the WP5 resource also results in higher net and gross AEP compared to the Fino-1 2004-2008 resource.

Deliverable 5.12 EERA DTOC calculation of scenarios

7. APPENDIX B: DTU: NEAR FUTURE SCENARIO – STANDARD LAYOUT

B.1 Objective/user story

B.1.1 Objective

Evaluate the impact of the combinations for the wind resource and wake models using the standard layout.

B.1.2 User story and scenario

Near future scenario (Doggersbank)

User story
3.1 As a developer I can determine the wake effects of neighbouring wind farm clusters on a single wind farm (meso and/or micro).
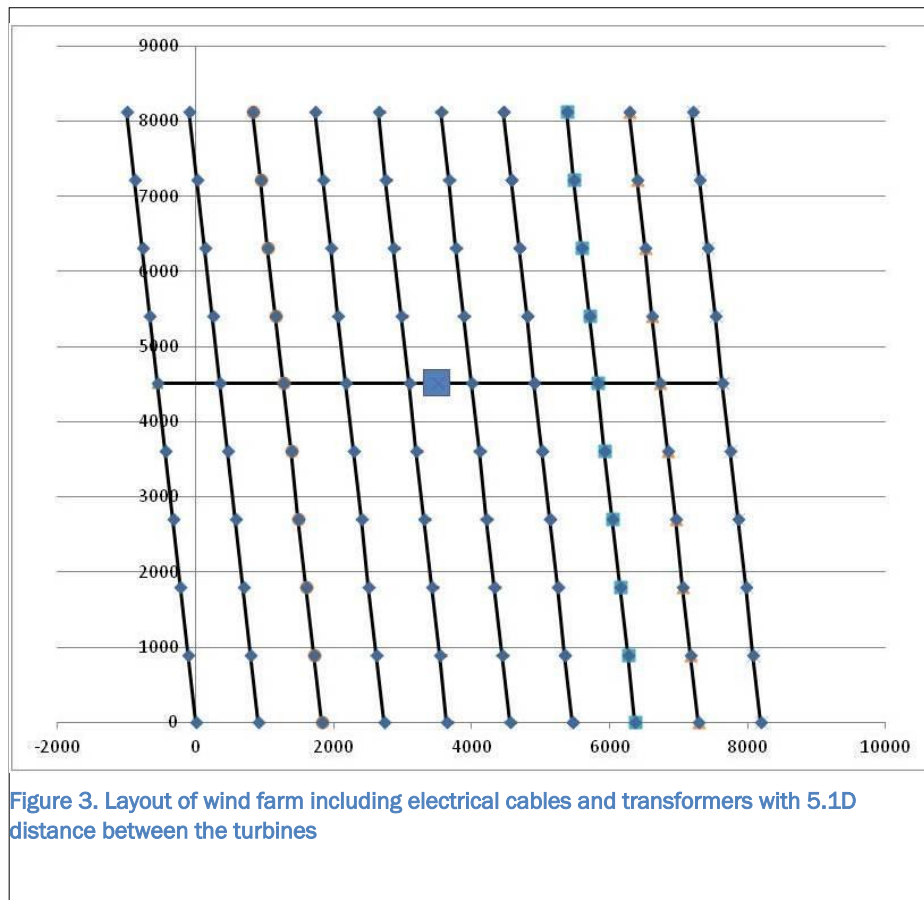
B.2 Codes

Fuga, WAsP-Park and Levellised Cost Of Energy (LCOE) models

B.3 Input:

B.3.1 Description of wind farm

This scenario is connected to the plan for an off-shore cluster at Dogger Bank. It starts with a 1GW wind farm consisting of 100 turbines with a rated power of 10 MW using the well documented INNWIND.EU reference turbine. The farm is assumed to be located at the southern part of the Doggersbank area and it is surrounded by other wind farms similar to the planned situation for Doggersbank.

The suggested layout of the farms (Figure 1) it based on the layout of the Horns Rev wind farm modified to 10x10 wind turbines. One main 'wind farm line' is oriented in the East-West direction and the other main wind farm line slightly skewed compared to the North-South direction. In Figure 1 the direction of the main wind farm lines is 5.1 rotor diameters but scenarios will be considered with different distances between the turbines ranging from 3.65 to 10 rotor diameters.

Deliverable 5.12 EERA DTOC calculation of scenarios

Figure 3. Layout of wind farm including electrical cables and transformers with 5.1D distance between the turbines

B.3.2 Description of turbines:

The wind turbines from the near-future scenario have a rated power of 10 MW with a 18rotor diameter of 178.3 m at a hub height of 119 m.

- Wind class: IEC class Ia

- Regulation: Variable speed, collective pitch

- Orientation of rotor: Upwind, overhang 7.1 meter

- Cut in wind speed: 4 m/s

- Rated wind speed 11.4 m/s

- Cut-out wind speed 25 m/s

- Minimum rotor speed 6 rpm

- Maximum rotor speed: 9.6 rpm (maximum tip speed: 90 m/s)

- Gearbox: Medium speed, Multiple stage generator

B.3.3 Description of wind climate

Deliverable 5.12 EERA DTOC calculation of scenarios

The WP5 Wind Resource file and the Fino-1 2004-2008 wind resource files, available from the DTOC Tool were used.

B.3.4 Remarks.

The different combinations of wind resource and wake model were used to estimate the various relevant quantities, such as the total gross and net annual energy production and costs of the investment and produced energy. The wind farm layout is the standard one presented in Table 1. The DTOC tool uses the Race Bank as the active wind farm while all other neighboring farms are selected with the Micro-scale wind impact. The different configurations used are presented in Table 1.

Table 2. Configuration of the different scenarios.

Configuration	Wind farm layout	Wind Resource	Wake Model
C1.	Standard (Fig 1.)	WP5	Fuga (+LCOE)
C2.	Standard (Fig 1.)	WP5	WAsP-Park (+LCOE)
C3.	Standard (Fig 1.)	F1 2004-2008	WAsP-Park (+LCOE)
C4.	Standard (Fig 1.)	F1 2004-2008	Fuga (+LCOE)

B.4 Output/results

The left panel of Figure 4 shows the ranking of the different configurations for increasing gross (solid line) and net (dashed line) annual energy production (AEP). Configuration 4 produces both the lowest gross and net AEP, increasing for C3 and C1, with C2 the highest.

The middle panel of Figure 4 shows the ranking of the configurations for decreasing NPV costs. C2 produces the highest cost, decreasing for C1 and C3, while C4 produces the lowest costs. Similar are the results when looking at minimizing the levellised cost of energy (LCOE), shown in the right panel of Figure 4.
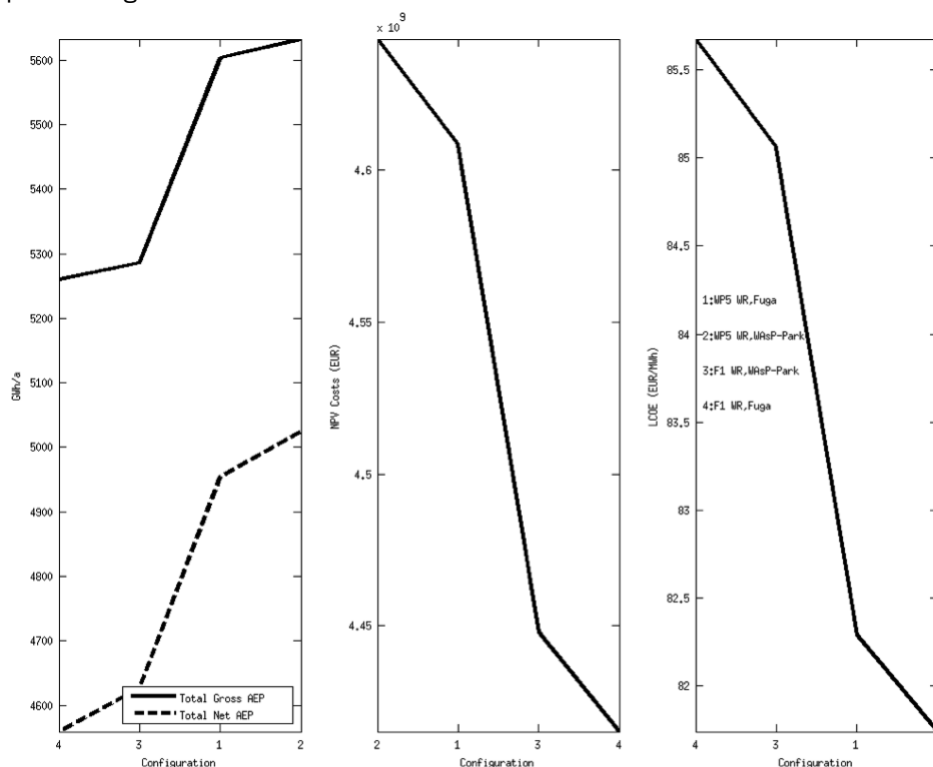

Figure 4. Results of the different configurations for the total gross and net annual energy production (left), the NPV costs (middle) and the Levellised Cost Of Energy (right).

Deliverable 5.12 EERA DTOC calculation of scenarios

B.5 Observations

B.5.1 Observations on results.

From the configurations investigated, the WAsP-Park model with the WP5 wind resource produces the highest AEP (gross and net) while minimizing the LCOE.

B.5.2 User experiences:
When changing the wind climate from WP5 to F1, and vice versa, in order to use the LCOE model one should first run the scenario again using one of the 2 available wake models and then run the LCOE model.
While on the surrounding wind farms there is the option of Micro-, Meso- or No Impact when the Race Bank farm is active, selecting any of the options does not change the result. It is not clear if that should be the case, or what exactly that impact option is.
Unfortunately, editing the scenario in QGIS does not work in a Mac and a Linux (Ubuntu) machine, therefore it was not possible to evaluate the impact of modifying the layout of the surrounding wind farms.

B.5.3 Expert judgment
Regarding the results based on the different configurations, it seems that the WAsP-Park model estimates fewer wake losses, hence the higher net and gross AEP compared to Fuga. As far as the wind resource files are concerned, the WP5 resource also results in higher net and gross AEP compared to the Fino-1 2004-2008 resource.

Deliverable 5.12 EERA DTOC calculation of scenarios

C.1 Objective/user story

C.1.1 Objective

To determine the net energy yield of a wind farm taking into account both aerodynamic and electrical losses from ECN codes using WRF input data.

C.1.2 User story and scenario

Near future scenario

User story
3.2 As a developer I can determine the wake effects due to turbines within a wind farm.
3.3 As a developer I can determine the net energy yield of a wind farm.

C.2 Codes

Farmflow and EEFARM (off-line)

Deliverable 5.12 EERA DTOC calculation of scenarios

C.3 Input

C.3.1 Description of wind farm

The near future scenario is connected to (aspects of) the plans for an off-shore cluster at Dogger Bank. As explained in D5.2 it starts with a 1GW wind farm consisting of 100 turbines with a rated power of 10 MW using the well documented INNWIND.EU reference turbine. The farm is assumed to be located at the southern part of the Dogger Bank area and it is surrounded by other wind farms similar to the planned situation for Dogger Bank of figure 3.

The wind farm layout is given in Figure 1. It is based on the layout of the Horns Rev wind farm the only difference lies in the fact that Horns-Rev considers 10x8 wind farms where the present wind farm lay-out has been modified to 10x10 wind turbines. One main 'wind farm line' is oriented in the East-West direction and the other main wind farm line slightly skewed compared to the North-South direction. Distances between the turbines along the main wind farm lines are 5.6 rotor diameters.
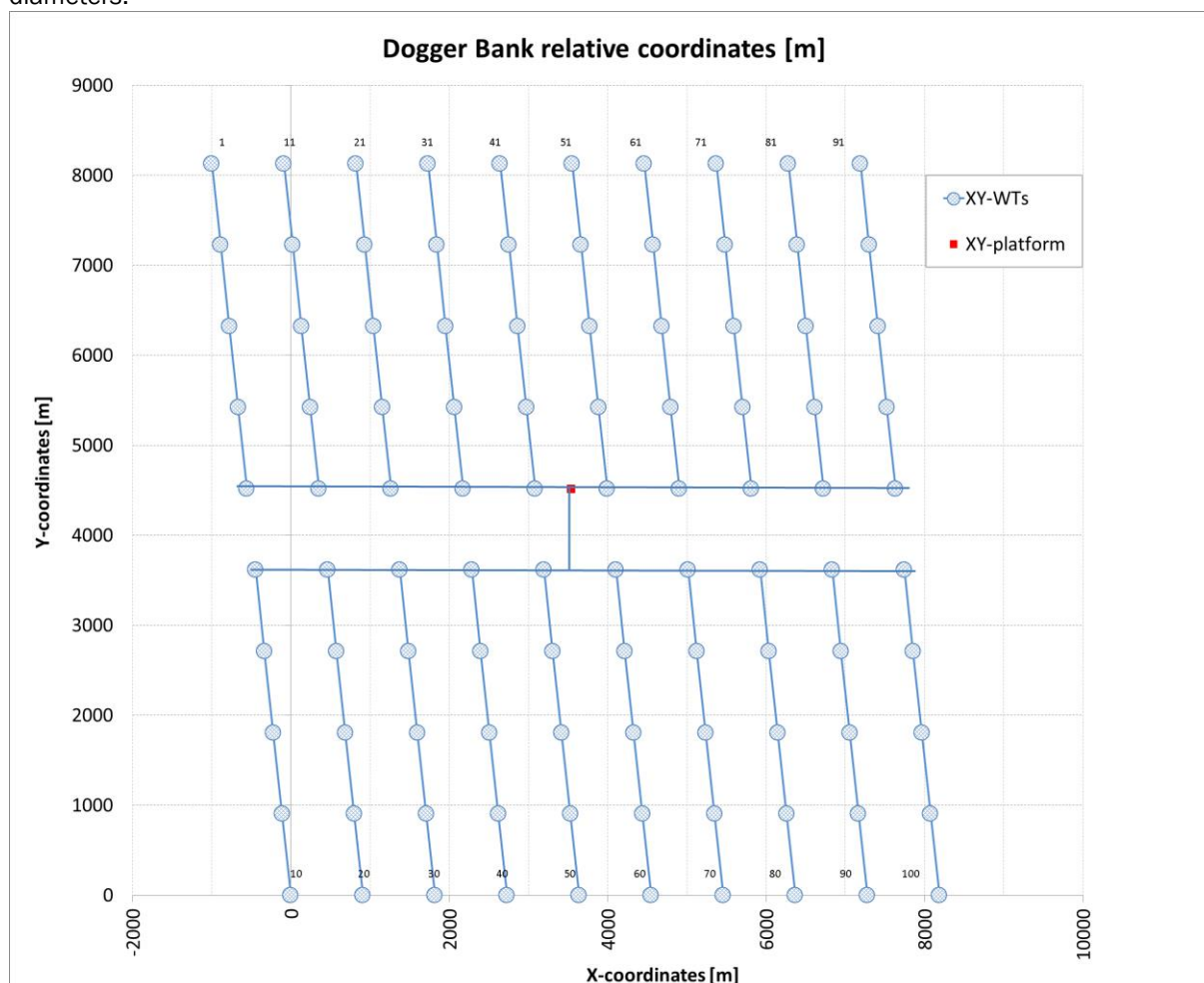

Figure 5: Layout of wind farm

3.2 Description of turbines:

For the near future scenario a 10 MW turbine is selected. Such turbines are not on the market yet. As explained in D5.2 the INNWIND.EU reference turbine is proposed since the data of this turbine are already made publicly available by DTU. The main characteristics of this turbine are:

Deliverable 5.12 EERA DTOC calculation of scenarios

- Rated power: 10 MW
- Rotor diameter: 178.3 m
- Hub height: 119 m
- Wind class: IEC class Ia
- Regulation: Variable speed, collective pitch
- Orientation of rotor: Upwind, overhang 7.1 meter
- Cut in wind speed: 4 m/s
- Rated wind speed 11.4 m/s
- Cut-out wind speed 25 m/s
- Minimum rotor speed 6 rpm
- Maximum rotor speed: 9.6 rpm (maximum tip speed: 90 m/s)
- Gearbox: Medium speed, Multiple stage generator

A detailed description on the turbine including a power curve and C Dax curve as needed in many wake models can be found at: http://dtu-10mw-rwt.vindenergi.dtu.dk/

From the electrical point of view, for the purpose of AC grid stability simulations, wind turbine models are described by wind conversion technology according to the new IEC standard, the IEC 61400-27-1 4 , in four categories: type 1, 2, 3 and 4, were types 3 and 4 are the most relevant including (DFIG, SCIG, WRSG and PMSG). Technical capabilities are presented to analyze the possible available Ancillary Services provided by wind turbines, e.g. reactive power provision capabilities. Note that for the present purpose, the electrical design of the turbine can be considered independent of the aerodynamic design as long as the correct tip speed ratios (and the resulting rotor characteristics) are obtained.

C.3.3 Description of wind climate

The near future farm is located at the Dogger Bank East of North England in relatively shallow waters (18 to 63 meters), see figure 3. Dogger Bank is part of the UK Crown Estate Round 3 area (8,660 km 2 , the largest of the Round 3 zones) with distances between 125 and 290 kilometers off the east coast of Yorkshire, UK.

The development consortium Forewind has defined several projects, each divided in phases of 1.2 MW: Creyke Beck A and B, Teesside A and B (where Teesside C and D are planned for a later stage). The whole estimated capacity of Dogger Bank could add up to 9GW,

Figure 3 shows approximate locations of Creyke Beck A and B and Teesside A and B projects. The 1GW wind farm under consideration is be located at the Creyke Beck A site, which is the most Southerly project from figure 3, 131 km from the shore at its closest point. The surrounding farms are given by the above mentioned projects: Creyke Beck B is located in North from the Creyke Beck A site, also 131 km from the shore at its closest point. Teesside A is furthest away from the shore with a closest point from shore at 196km and Teesside B is 165 km from shore. These farms have a 1GW capacity as well with a similar layout as suggested for the Creyke Beck A farm.

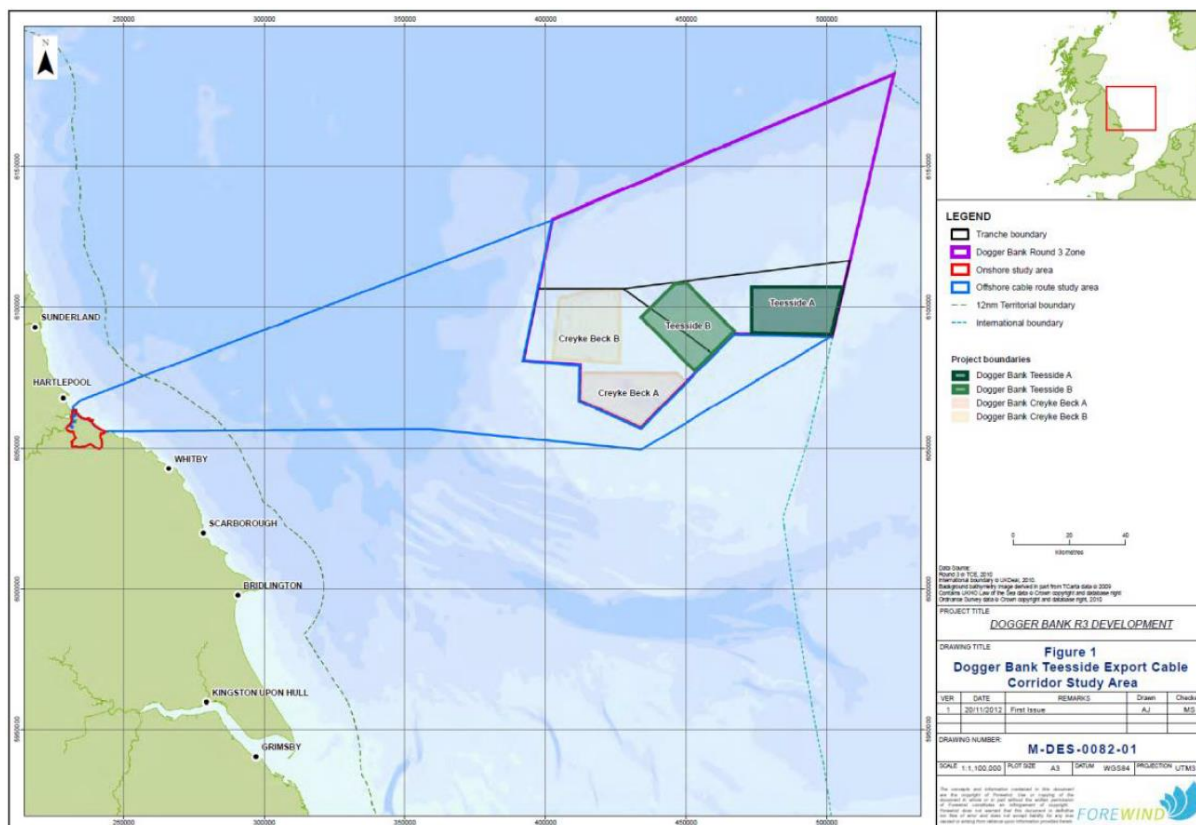*Deliverable 5.12 EERA DTOC calculation of scenarios*

Figure 6: Location of Dogger Bank projects

Wind input has been provided by DTU in the form of WRF calculations. Thereto the data as supplied without surrounding wind farms have been used. Some problem occurred in the determination of the ambient turbulence intensity as needed in the Farmflow calculations. This turbulence intensity is not straightforwardly available from the WRF data but from the WRF results a wind shear has been determined which together with the provided z0 data yields a turbulence intensity at hub height of 8% at nearly neutral conditions. This value of 8% was considered rather high and therefore the turbulence intensity was reduced to 6%.

C.3.4 Collection grid

For the inter-array cabling a radial topology is used, starting from each of the numbered WTs towards the substation, positioned at the center of the wind farm. The medium voltage level is chosen as 66kV.
The cable type is a 66/69kV 240mm² 3-core XLPE cable, rated at 58MVA, as specified in Annex B. No optimization has been performed on alternative topologies or different cable ratings along the strings. The cable lengths have been calculated as the distances between the turbines times a slack of 10% plus a vertical distance of 50m between the sea bed and the platform for each cable feed-in. The connections to the platform positioned are along the main directions in the wind farm, as shown in Figure 5.The total array cable length is 140km. Further, the turbine transformers are included, although the losses ae set to zereo while the output power is measured at the HV side. Note that no separate AC-collection platform is considered and also no interconnections to neighboring wind farms. So the inter-array cables directly feed in the HVDC converter platform that directly connects to the terrestrial grid through the onshore HVDC converter substation.

3.5 Transmission grid
The modeled transmission grid consists of the following components:

Deliverable 5.12 EERA DTOC calculation of scenarios

- An onshore and an onshore multilevel Voltage Source Converter (VSC), each rated 1216MW, at +/-320kV DC-voltage.
- An Offshore platform costs, taken from the NSCOGI Offshore technology report, 'ENTSOE 1000MW VSC +/-500kV, 8000 tonnes', which fits most with the converter specifications.
- A pair of 3-winding transformers 66/66/ 375 kV, 590MVA and Gas Insulated Switchgear.
- Onshore substation, with two transformers of 600MVA and Switchgear.
- A pair of HVDC XLPE cables, bipolar configuration, +/-320kV, 1200mm^2, 1146MW.

C.3.6 Economic assumptions

Quantity	Value	Unit
Economic lifetime	20	Years
Interest rate	7	%
Depreciation rate	2	%

C.3.7 Remarks

Deliverable 5.12 EERA DTOC calculation of scenarios
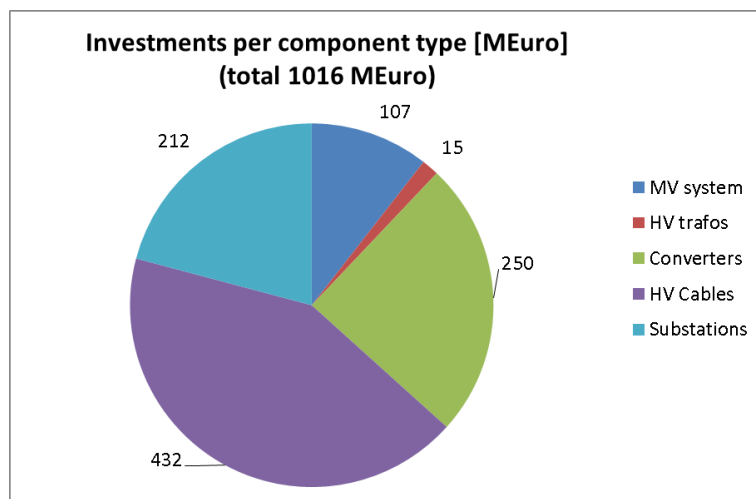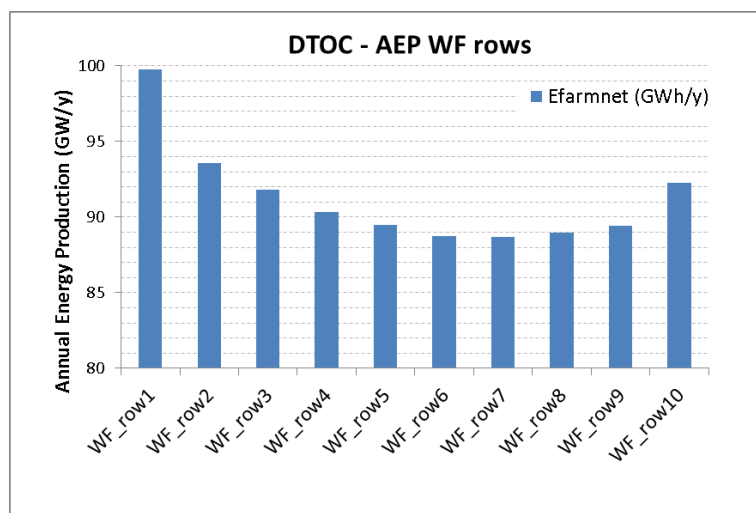
C.4. Output/results

C.4.1 General

Below, the investments, annual energy output, losses and levelized costs are given, followed by the results per component type.

	InvTot	Efarmnet	ElossCu	Eloss	Efail	Efail Rel	LTC
	(ME)	(GWh/y)	(GWh/y)	(-)	(GWh/y)	(-)	(Eur/kWh)
MV system	107,2	913,0	5,23	0,6%	1,61	0,2%	0,0093
HV system	908,9	824,1	46,54	5,1%	40,87	4,5%	0,0878
Total	1016,1	824,1	51,77	5,6%	42,48	4,6%	0,0972

C.4.2 Investments

Investments per component type [MEuro]
(total 1016 MEuro)

107
15
212
250
432

- MV system
- HV trafos
- Converters
- HV Cables
- Substations

C.4.2 Energy output

DTOC - AEP WF rows

Annual Energy Production (GW/y)

■ Efarmnet (GWh/y)

WF_row1 WF_row2 WF_row3 WF_row4 WF_row5 WF_row6 WF_row7 WF_row8 WF_row9 WF_row10

C.4.3 Electrical losses

Deliverable 5.12 EERA DTOC calculation of scenarios

Transmission losses per component type [%]
(total 5,1%)

0,6%

0,4%

2,3%

2,6%

- MV system
- HV trafos
- Converters
- HV Cables

Lost energy due to failure, per component type [%]
(total 4.5%)

0,2%

0,2%

2,4%

2,0%

- MV system
- HV trafos
- Converters
- HV Cables

Deliverable 5.12 EERA DTOC calculation of scenarios

C.5 Observations

C.5.1 Observations on results

HVDC cables dominate the total investment costs, because of the connection distance of 300km. MV cable losses only have a small contribution to the wind farm losses, compared to the wake deficits. The proper distribution of the arrays over the different HV transformers and transformer windings leads to some reduction of the HV transformer loading.

The transmission losses of 5.1% are mainly determined by the HVDC converter stations (2.6%) and the HVDC cables (2.3%). Loss reduction in the HVDC system will therefore directly reduce the total losses and will also lead to cost reductions of the HVDC system itself, e.g. because of a reduced need for cooling.

Not-produced energy due to component failure adds up to 4.5% and is therefore as significant as the transmission losses. For the HVDC cables the failure losses are even a little higher than the transmission losses.

Notes:

- For the HVDC cable losses a constant cable core temperature (worst case approach) has been assumed.

- In contrary to the transmission losses, which are well defined (and also well predictable in time), the failure lost energy is an estimate that includes a large uncertainty.

- Please note that that the transmission losses are determined over the so-called net energy amount, i.e. after subtraction of the failure losses.

C.5.2 User experiences

N.r. the calculations are run off-line

C. 5.3 Expert judgment

Results look feasible.

Deliverable 5.12 EERA DTOC calculation of scenarios

D.1 Objective/user story

D.1.1 Objective

Evaluate the usefulness and ease of use of the DTOC software. This report focuses on user experience, rather than results and observations.

D.1.2 User story and scenario

Base scenario (Race Bank).

3.2 As a developer I can determine the wake effects due to turbines within a wind farm.
3.3 As a developer I can determine the net energy yield of a wind farm.

D.2 Codes

WAsP-Park, FUGA

D.3 Input:

D.3.1 Description of wind farm

The planned Race Bank wind farm will be located 27 km from the North Norfolk coast. The planned capacity is 580 MW, provided by 94-116 turbines in the range of 5-6.15 MW. The present scenario assumes the farm to consist of 100 UPWIND 5MW reference turbines. Race Bank wind farm is surrounded by several other wind farms which are either operational or in the planning phase.

The suggested layout of the farms (Figure 1) it based on the layout of the Horns Rev wind farm modified to 10x10 wind turbines. One main 'wind farm line' is oriented in the East-West direction and the other main wind farm line slightly skewed compared to the North-South direction. In Figure 1 the direction of the main wind farm lines is 5.1 rotor diameters but scenarios will be considered with different distances between the turbines ranging from 3.65 to 10 rotor diameters.
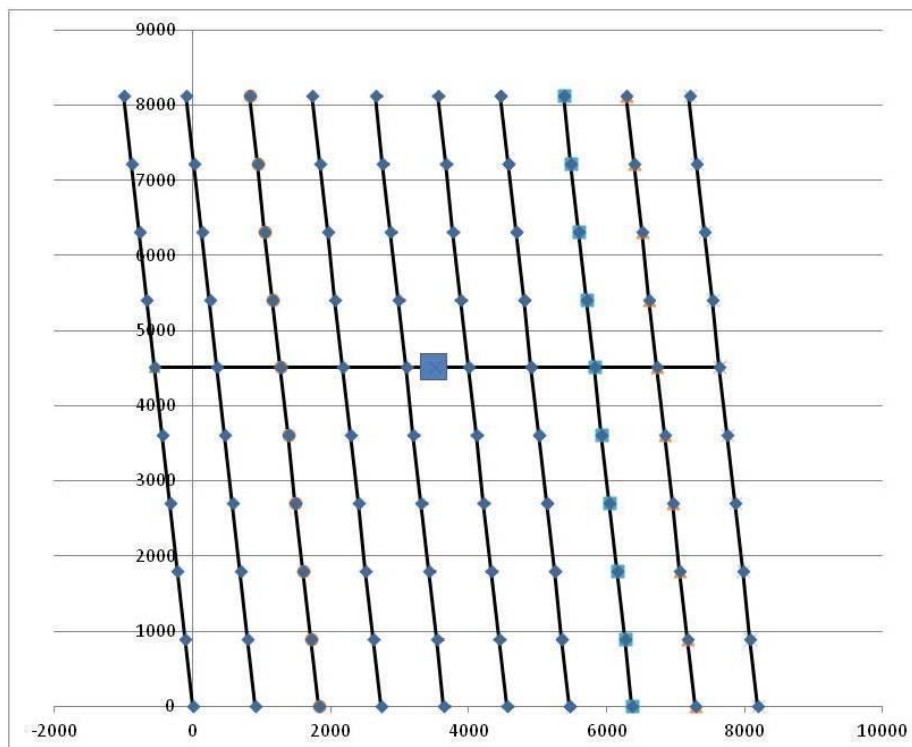
Deliverable 5.12 EERA DTOC calculation of scenarios

Figure 7 Layout of wind farm including electrical cables and transformers and 5.1D distance between the turbines.

D.3.2 Description of turbines:

Details of the wind turbines used for the base scenario (Race Bank):

- Rated power: 5 MW
- Rotor diameter: 126 m
- Hub height: 90 m
- Wind class: IEC class Ib
- Regulation: Variable speed, collective pitch
- Orientation of rotor: Upwind, overhang 5 meter
- Rated wind speed 11.4 m/s
- Cut-out wind speed 25 m/s
- Maximum rotor speed: 12.1 rpm (maximum tip speed: 80 m/s)

D.3.3 Description of wind climate

The Race Bank WP5 Base Scenario Wind Resource file (as per the provided tutorial) was used.

D.4 Output/Results

Deliverable 5.12 EERA DTOC calculation of scenarios

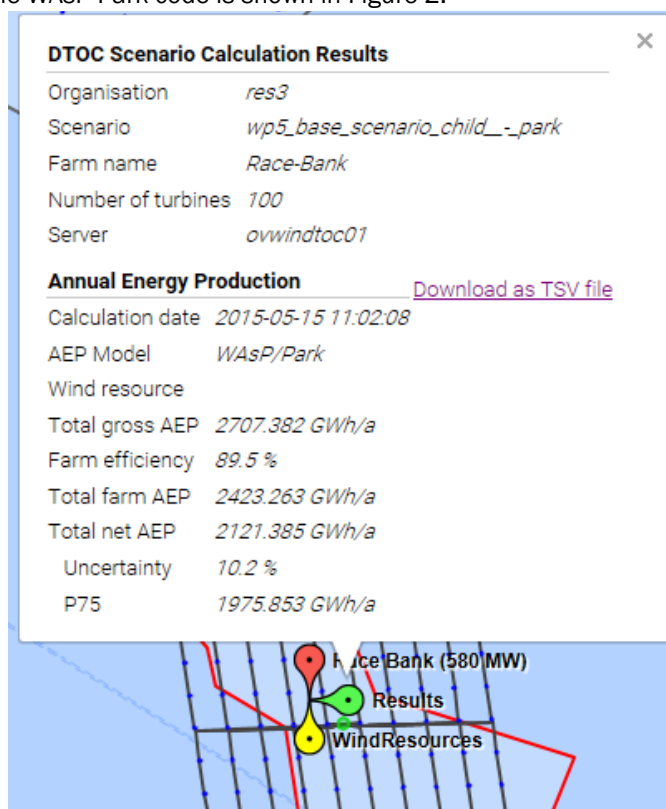The output from using the WAsP-Park code is shown in Figure 2.

Figure 2 DTOC output when using the WAsP-Park code to calculate results for the base scenario (Race Bank)

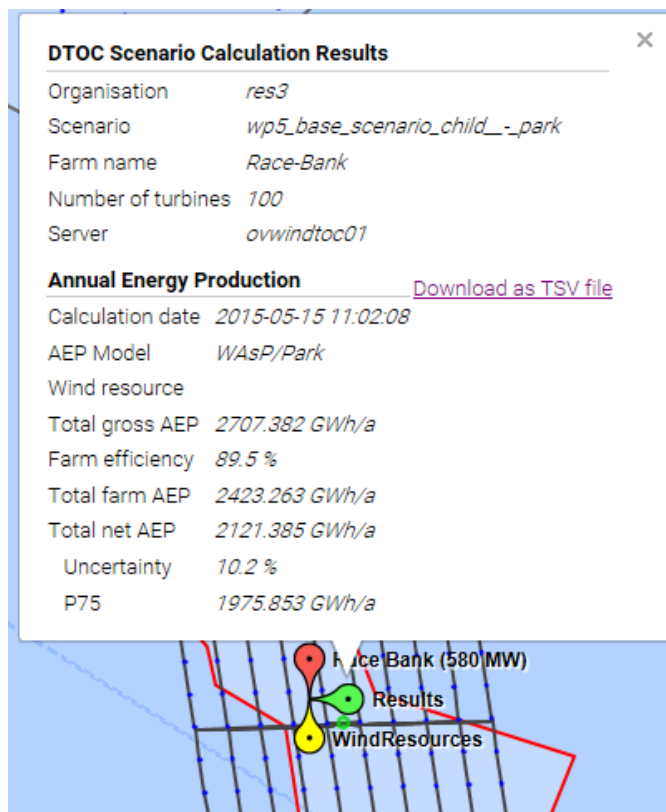The output from using the FUGA code is shown in Figure 3.

Deliverable 5.12 EERA DTOC calculation of scenarios

Figure 3 DTOC output when using the FUGA code to calculate results for the base scenario (Race Bank)

D.5 Observations

D.5.1 User experiences:

Scenario 3.2: As a developer I can determine the wake effects due to turbines within a wind farm

It is possible to compare the net yields of the different models, but as the wake losses are not reported as a separate loss factor it is not easy to see the direct impact of wakes.

Only a static comparison report is provided (Figure 4), so it is not possible to compare scenarios and test that they perform as expected. There are no instructions on how to set up a scenario comparison report so this may have been done incorrectly.

Deliverable 5.12 EERA DTOC calculation of scenarios

DTOC Energy Production Report (Static Example) 23.04.2014
EON, 2014 Reference LCOE: 13.5 ct/kWh
Reference Scenario: BWII - WAsP

	Scenario Shortname	BWII - WAsP *	BWII - FLaP	BWII - WAsP 100m
Comment		Calculations with WAsP	Calculations with FLaP	Calculations with WAsP, hub height: 100m
	Last Update	2014.04.22 14:30	2014.04.22 16:30	2014.04.23 11:05
Turbines				
	Turbine Manufacturer	Areva	Areva	Areva
	Turbine Type	M5000	M5000	M5000
	Nominal Power [kW]	5000	5000	5000
	Rotor Diameter [m]	116	116	116
	Hub Height [m]	90	90	100
Farm				
	Number of Turbines	80	80	80
	Nominal Power Wind Farm [MW]	400	400	400
Results				
	AEP Gross [GWh/a]	1'758.2	1'747.6	1'846.1
	AEP Farm [GWh/a]	1'613.8	1'600.9	1'702.6
	AEP Net [GWh/a]	1'495.0	1'483.1	1'577.1
	Capacity Factor [%]	46.1%	45.7%	48.6%
	Wind Farm Efficiency	91.8%	91.6%	92.2%
	Availability	96.0%	96.0%	96.0%
	Electrical Losses	3.50%	3.50%	3.51%
	LCOE [Cent/kWh]	13.5	13.4	14.2
	LCOE [%]	+100.00%	+99.20%	+105.50%
	delta LCOE [%]	+0.00%	-0.80%	+5.50%

Figure 4 Example static comparison report

A blank page is returned when attempting to view the "Single Farm Report" (Figure 5). Again, there are no instructions on how to set up a Single Farm Report so this may have been done incorrectly.
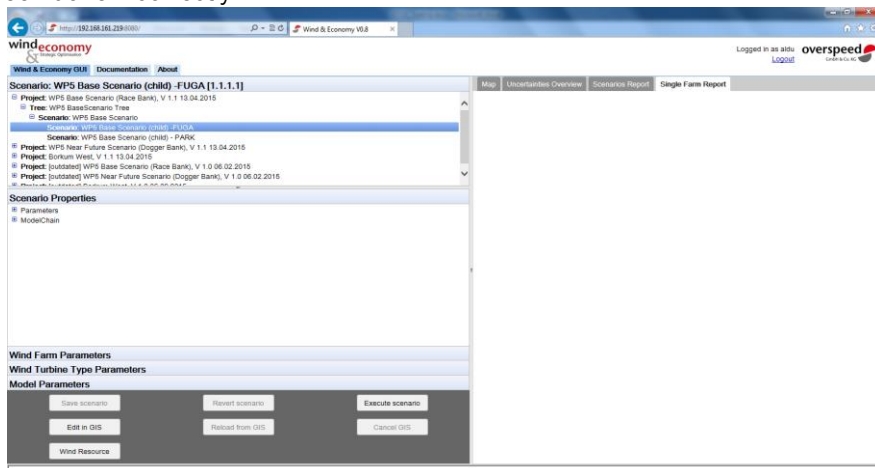

Figure 5 Blank page resulting when attempting to view a "Single Farm Report"

The yield and the breakdown of losses for individual turbines are not visible. This would be required to identify which turbines are being most affected by wake losses.

Scenario 3.3: As a developer I can determine the net energy yield of a wind farm
This is very clear from the results summary window. More detail, showing per turbine results would be useful.

Deliverable 5.12 EERA DTOC calculation of scenarios

E.1 Objective/user story

E.1.1 Objective

As a wind turbine wake modeller, determining total and sector-wise Wind Farm wake losses, to evaluate overall efficiency and minimize prejudicial conditions in Wind Farm operation. A large number of variables and conditions affect this, so variations on the base scenario will be studied, including different wake models and wind resources, different turbine spacing, wind turbine power and thrust curves and surrounding wind farm wake effects. The base scenario is also reproduced with an off-line CFD wake modelling tool [1][2], to evaluate its results versus the state-of-the-art linear wake models present on the on-line platform.

E.1.2 User story and scenario

Base scenario (Race Bank)

User stories:
3.1 As a developer I can determine the wake effects of neighbouring wind farm clusters on a single wind farm (meso and/or micro).
3.2 As a developer I can determine the wake effects due to turbines within a wind farm.
3.4 As a developer I can determine the optimum spacing, position, turbine model and hub height of turbines within an offshore wind farm.
3.5 As a developer, I want to use wind farm layout scenarios of my target wind farm with respect to nr of turbines, turbine types, power and thrust curves etc.

E.2 Codes

WAsP/Park and Fuga (on-line)
VENTOS®/2 (off-line)

E.3 Input

E.3.1 Description of wind farm

The wind farm layout is as supplied on the base scenario configuration supplied on the Wind&Economy platform. Based on the layout of the Horns Rev wind farm, it was expanded to 10x10 wind turbines and has a row/column wind turbine spacing of 7.22 D. The inclination of the columns relative to North-South direction is of 7°. **Error! Reference source not found.** shows the coordinates of the corner WTs, in both global and local coordinates.

Corner WTs	Easting [m]	Northing [m]	X (local) [m]	Y (local) [m]
WT 001	354841.26	5912914.06	-997.98	8128.97
WT 010	355839.24	5904785.09	0.00	0.00
WT 091	363031.26	5912914.06	7192.02	8128.97
WT 100	364029.24	5904785.09	8190.00	0.00

Table 3 - Base scenario layout's corner wind turbine coordinates

A variation of the above layout - named "compact" layout - was also used, with a row/column wind turbine spacing reduced by 10%, to 6.5 D.

The scenario also included several neighboring wind farms in the cluster: Inner Dowsing, Lincs, Lynn, and Sheringham Shoal, all already in production, and Dudgeon, Triton Knoll 1 & 2 and Race Bank, in planning phase. The Wind&Economy platform supplied the actual layout and wind turbine models for the former, as well as hypothetical layouts and turbine selections for the latter. These were used by the platform on on-line calculations where necessary.

E.3.2 Description of turbines

The NREL Upwind 5MW reference wind turbine [3] assumed on the base scenario was used, with the power and thrust coefficient curves as supplied on the Wind&Economy platform:

- Rated power: 5 MW;
- Rotor diameter: 126 m;
- Power curve (as supplied): 3819.6 kw (@10 m/s);
- Thrust coefficient (as supplied): 0.7920 (@10 m/s);
- Hub height: 90 m.

A variation on the NREL Upwind 5MW reference wind turbine was also used, named NREL HiPower 6MW, with up-scaled (+10%) power and thrust-coefficient curve but otherwise exactly as described above:

- Rated power: 5 MW;
- Rotor diameter: 126 m;
- Power curve (user modified): 4201.6 kw @ 10 m/s;
- Thrust coefficient (user modified): 0.8712 @ 10 m/s;
- Hub height: 90 m.

E.3.3 Description of wind climate

The "WP5 Wind Resource", "Fino-1 2004-2008, 103.5m" and "Cener-WRF-RaceBank" wind resource files were used, available from the Wind&Economy platform were used for the on-line calculations.

When using the off-line CFD wake model, static inflow conditions calibrated to the wind speed levels similar to those seen on the available wind resources (~10 m/s) and typical off-shore turbulence intensity levels (~5%). The need for "wind tunnel" type boundary conditions of the CFD code implies a series of runs with static wind direction, simulating a full wind rose with a resolution of 5°. Neutral stability regime is assumed.

E.3.4 Remarks

The results from the off-line CFD runs were later combined with the "Cener-WRF-RaceBank" wind resource files, supplied via-email by Overspeed, to produce comparable wind farm efficiency values.

E.4. Output/results

The key output we are tracking on all off-line calculations is the overall wind farm efficiency, measuring the aerodynamic production losses due to internal wake effects. The Gross AEP is also tracked, as it gives a good indication of the average free-stream velocities at the site.

All scenarios are variations on the base scenario, which follows the default configuration, with the standard 10x10 layout with 7.22D internal spacing, populated with the NREL Upwind 5MW wind turbine.

Deliverable 5.12 EERA DTOC calculation of scenarios

	WAsP/Park		Fuga	
Wind Resource	Efficiency [%]	Gross AEP [GWh/a]	Efficiency [%]	Gross AEP [GWh/a]
FINO1	89.5	2707.382	90.8	2698.683
WP5	91.0	2919.866	92.1	2908.604
CENER	89.0	2476.641	90.3	2468.258

Table 4 Wind farm performance as function of wind resource and wake model, on default Base scenarion configuration

All combinations of the wind resource and wake model were tested on the default scenario configuration, study for which the results are presented on **Error! Reference source not found.**. All scenario calculations, from this point forward, were executed using the "CENER-WRF-RaceBank" wind resource and the WAsP/Park wake model.

Wind Impact	Efficiency [%]	Gross AEP [GWh/a]
None	89.0	2476.641
Meso	89.0	2476.641
Micro	89.0	2476.641

Table 5 - Neighbouring wind farm's wind impact configuration has no effect on target farms performance

The user is given the choice of taking into consideration the wake effect of neighboring wind farms into the target wind farm's calculations, either through Meso-scale wake modelling or through micro-scale wake modelling (WAsP/Park and Fuga models, included elsewhere in this study). **Error! Reference source not found.** shows the results from studying the impact of activating either option on all (in production or in planning phase) neighbor wind farms included in the scenario.

Scenario	Efficiency [%]	Gross AEP [GWh/a]
Base	89.0	2476.641
HiPower WT	87.2	2724.315
Compact layout	87.8	2475.629

Table 6 - Impact on wind farm performance of changing internal spacing and turbine model

Considering a fixed geometry for the layout, the internal spacing and the wind turbine thrust are the two main variables affecting the wind farm efficiency. The base scenario was compared with two variations: one with the HiPower wind turbine, with 10% stronger power and thrust curves, and one with a more compact layout, with 10% reduced row/column wind turbine spacing. The results are present in **Error! Reference source not found.**.

Using the off-line CFD calculations with the wake model, a wind farm efficiency rose was produced. The off-line VENTOS®/2 model was run for every 5°, meaning each run represents a ±2.5° sector. Wind farm efficiency (for each sector) was calculated using the average calculated wind turbine power (over the whole wind farm), relative to the average calculated wind turbine power for unaffected front row/column (excluding row/column ends). This efficiency rose is presented in **Error! Reference source not found.**.

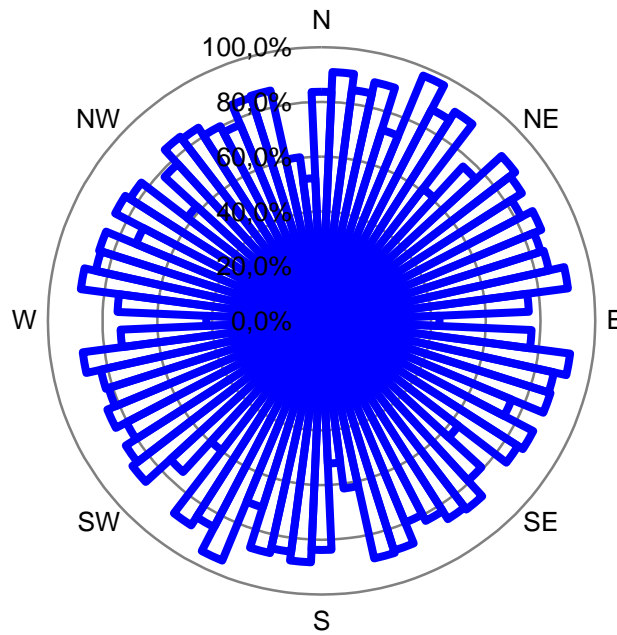*Deliverable 5.12 EERA DTOC calculation of scenarios*

Figure 8 - Wind farm efficiency rose, 5° sectors (as per off-line simulations)

The 5° sector efficiency rose results were re-calculated by weighted averages into a 22.5° sector efficiency rose (see **Error! Reference source not found.**), for compatibility with the CENER wind resource files.
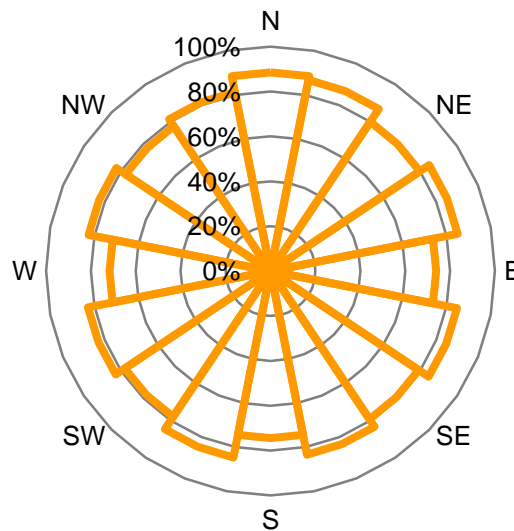

Figure 9 - Wind farm efficiency rose, 22.5° sectors (to match CENER wind resource sector size)

The product of the efficiency wind rose with the average (over all wind turbines) frequency rose from the CENER wind resource is 78.0%, the overall, sector-weighted, wind farm efficiency from the off-line VENTOS®/2 and comparable with those from the on-line models (see **Error! Reference source not found.**).

E.5 Observations

Deliverable 5.12 EERA DTOC calculation of scenarios

E.5.1 Observations on results

Wind resource and wake models are, as expected, combining non-linearly: both are having an effect on the overall wind farm efficiency, as shown in **Error! Reference source not found.**. However, while the wind resource is naturally having an effect on the gross AEP, the wake model is unexpectedly having one as well, even if a small one.

The wind resources with higher gross AEPs are the ones with higher free-stream velocities. In a wind speed range where the thrust coefficient curve is dropping with speed, this explains that wind farm efficiencies increase with the gross AEP. **Error! Reference source not found.** shows that changing the wind impact of the neighbouring wind farms yielded no effect on the target wind farm performance, either with micro or meso impact. The absence of meso-scale wake effect can explain the latter, while the former is probably due to the neighbouring wind farms being out of range of the presently implemented micro-scale models. A quick test on the Lincs/Lynn/Inner Dowsing cluster to the SW (very closely spaced) shows that at that range, micro wind impact affects WF performance, which probably confirms that assumption.

The variations introduced to the wind farm configuration had the expected impact on wind farm efficiency. **Error! Reference source not found.** shows that reducing wind turbine spacing by 10% and increasing the machine's power and thrust coefficient curves by that same amount has an impact on the efficiency value that is very similar, which is to be expected for linear wake models such as WAsP/Park and Fuga. The gross AEP calculations also behave predictably: they increase by 10% in the HiPower WT case (consequence of the 10% increase in the power curve) but suffer nearly no change in the compact layout case (reduced layout footprint leads to minute changes in wind resource data being used).

There is a large gap between wind farm efficiency values calculated by on-line models and through our off-line calculations. Though the method to arrive upon these values is very different, they should be somewhat comparable. The VENTOS®/2 wake model tends to over-estimate wake deficit, both in the case of an isolated wind turbine [**Error! Reference source not found.**] and inside a wind farm [**Error! Reference source not found.**], particularly in cases where the run perfectly captures the row/column alignment, which it does in this case - see wind from East and West in **Error! Reference source not found.**, capturing the wind turbine rows (efficiency drops nearly to 40%). Missing this alignment (by less than 2.5º, half the sector width), like in the case of the columns (approximately N-S), the efficiency drop (to nearly 50%) is significantly lower. The diagonals (NE-SW and NW-SE) are also narrowly missed, and this combined with larger spacing means an even smaller efficiency drop (to about 60%). This goes some way in explaining between the off-line calculated efficiency (78.0%) and the on-line calculation results (around 90% for all cases). **Error! Reference source not found.** shows that compounding individual run results into wider sectors dilutes these effect to an extent where they are only marginally distinguishable the overall trend. The on-line calculations, using such wide sectors, are unable to capture this.

G.5.2 User experiences

Given the potential capabilities of the tool, it seems very intuitive and comprehensive. Integration with google maps with overlays is very well achieved.

While creating variations to the wind farm configuration, downloading and re-uploading modified wind farm layout and wind turbine model list was very simple and quick. When working on a wind farm layout, this process can be a good alternative to going through Qgis for those who are not familiar with the software or prefer other ways of manipulating wind turbine positions.

Scenario tree management could be helped by additional "copy" options. "Duplicate scenario" and "Clone scenario" are useful, but perhaps there should be the option to duplicate (or even clone) a whole branch of a scenario tree. I was also unable to clone the scenario at the root of the tree, this should be possible if the user wants to create a new tree going in a direction yet unexplored by any of the existing branches.

Copying a previously executed scenario seems to yield a "bugged" scenario, where the platform does not load the map and overlays, leaving only a white screen in the "Map" tab. By creating a "Child scenario" from the "parent" I was able to work around the issue.

G.5.3 Expert judgment

For a wind turbine wake modeler, the wind farm performance reporting, without being too extensive, has to be more detailed, breaking down the AEP and efficiency calculation with frequency, energy and efficiency roses, at least an average for the wind farm, if not necessarily for

Deliverable 5.12 EERA DTOC calculation of scenarios

each wind turbine. Maybe this is intended for the "Single Farm Report" tab, which is for now empty?

Implementing some form of meso-scale wake modelling should be a priority. Without it, it is only possible to take into account the presence of neighboring wind farms at a really short range (through micro-scale wake modelling) or using a wind resource with the impact built into it. If the wind resource relies on WRF calculations, considering different cluster configurations can be very computationally expensive.

E.6 References

1. Castro, F. and Palma, J. and Silva Lopes, A. *Simulation of the Askervein Flow. Part 1: Reynolds Average Navier-Stokes Equations (k-ε Turbulence Model)*, Boundary-Layer Meteorology, 2003, 107, 501-530

2. Gomes, V M. M. G. C. and Palma, J. M. L. M. and Lopes, A. S. *Improving Actuator Disk Wake Model*, Journal of Physics: Conference Series, 2014, 524, 012170

3. Jonkman, J. *NREL reference turbine*, February 15, 2007, NREL/NWTC

4. *Hansen, K. Wind farm wake verification*, EWEA Offshore 2015 Event, 10-12 March 2015, Copenhagen, Denmark

Deliverable 5.12 EERA DTOC calculation of scenarios

F.1 Objective/user story

F.1.1 Objective

The standard layout of the base and the near future scenario were used to compare different configurations regarding the assessed model and chosen wind climate which are available in the DTOC tool. Besides, the effect of a different design of the wind park Borkum West has been evaluated. For all configurations the results of AEP were compared.

F.1.2 User story and scenario

- Base scenario (Race Bank)
- Near future scenario (Doggersbank)
- Borkum West base scenario

User story
1.1 As strategic planner or developer I can determine the wake impact of individual wind farms within a cluster on each other (just meso)
1.3 As a strategic planner I can determine the optimum size, spacing and position of offshore wind farm clusters.
3.3 As a developer I can determine the net energy yield of a wind farm.

F.2 Codes

The WAsP/Park model and the Fuga model were used for the test calculations.

F.3 Input

F.3.1 Description of wind farm

The standard layout of the base as well as the near future scenario and the available layout of Borkum West base scenario were used for the calculations.
For one calculation the layout of the wind farm Borkum West was changed. The spacing between some rows of wind turbines was increased as it is shown in **Error! Reference source not found.**.
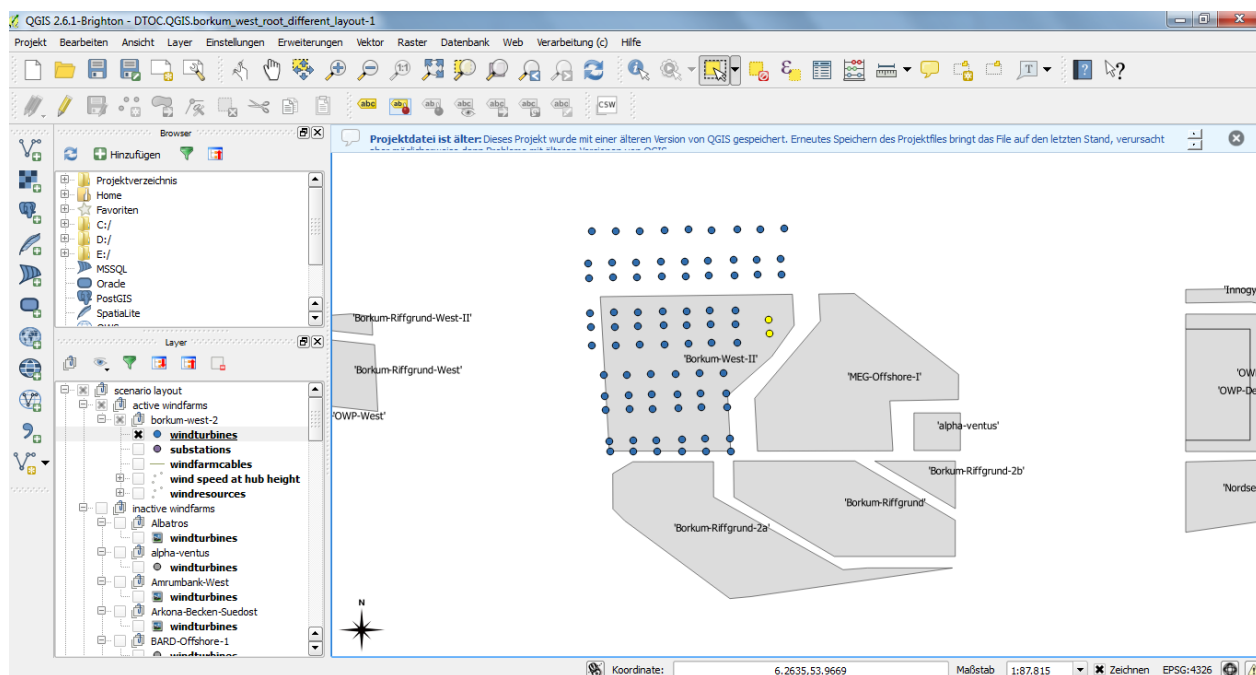
Deliverable 5.12 EERA DTOC calculation of scenarios

Figure 10: Changed layout of the wind farm Borkum West Base scenario.

F.3.2 Description of turbines

The standard turbines available in the DTOC tool for each scenario were used.

F.3.3 Description of wind climate

The calculations were done with different wind resources available in the DTOC tool:
- Cener Race Bank, 100 m, with wake effects of surrounding farms
- Cener Race Bank, 100 m, no wake effects of surrounding farms
- Cener WRF Race Bank, 90 m
- DTU DoggerBank, 100 m, with wake effects of surrounding farms
- FINO1 (2004-2008), 103.5 m

F.3.4 Remarks

Table 1 shows the different calculations which were done. The A-configurations investigate the effect of different wind resources on the results. The effect of the use of different models is shown by the B-configurations. For the C-configurations the layout of the wind farm was changed and the results can be compared with the outcome of the calculation with the original layout.

Table 7: Configuration of the different scenarios.

Configuration	Wind farm layout	Wind Resource	Wake Model
A.1	Base scenario	Cener Race Bank, 100 m, with wake effects of surrounding farms	WAsP/Park
A.2	Base scenario	Cener Race Bank, 100 m, no wake effects of surrounding farms	WAsP/Park
A.3	Base scenario	Cener WRF Race Bank, 90 m	WAsP/Park
B.1	Near future scenario	DTU DoggerBank, 100 m, with wake effects of surrounding farms	WAsP/Park
B.2	Near future scenario	DTU DoggerBank, 100 m, with	Fuga

Deliverable 5.12 EERA DTOC calculation of scenarios

		wake effects of surrounding farms	
C.1	Borkum West base scenario	FINO1 (2004-2008), 103.5 m	WAsP/Park
C.2	Borkum West, changed layout (**Error! Reference source not found.**)	FINO1 (2004-2008), 103.5 m	WAsP/Park

F.4. Output/results

The results for the AEP calculations for the different configurations shown in Table 1 are presented in the following. **Error! Reference source not found.** plots the results of net AEP for the configurations.

A.1
```
AEP Model    WAsP/Park
Wind resource     Cener Race Bank at 100m level
Total gross AEP   2476.641 GWh/a
Farm efficiency   89.0 %
Total farm AEP    2205.088 GWh/a
Total net AEP     1930.389 GWh/a
Total net AEP uncertainty    10.2 %
Total net AEP P75 1797.960 GWh/a
```

A.2
```
AEP Model    WAsP/Park
Wind resource     Cener Race Bank reference at 100m level
Total gross AEP   2664.505 GWh/a
Farm efficiency   90.0 %
Total farm AEP    2398.102 GWh/a
Total net AEP     2099.358 GWh/a
Total net AEP uncertainty    10.2 %
Total net AEP P75 1955.338 GWh/a
```

A.3
```
AEP Model    WAsP/Park
Wind resource     Cener-WRF-RaceBank
Total gross AEP   2476.641 GWh/a
Farm efficiency   89.0 %
Total farm AEP    2205.088 GWh/a
Total net AEP     1930.389 GWh/a
Total net AEP uncertainty    10.2 %
Total net AEP P75 1797.960 GWh/a
```

B.1
```
AEP Model    WAsP/Park
Wind resource     DTU DoggerBank at 100m level
Total gross AEP   5087.284 GWh/a
Farm efficiency   82.6 %
Total farm AEP    4201.570 GWh/a
Total net AEP     3678.159 GWh/a
Total net AEP uncertainty    10.2 %
Total net AEP P75 3425.830 GWh/a
```

B.2

Deliverable 5.12 EERA DTOC calculation of scenarios

```
AEP Model    Fuga
Wind resource      DTU DoggerBank at 100m level
Total gross AEP   5058.980 GWh/a
Farm efficiency    87.0 %
Total farm AEP    4403.794 GWh/a
Total net AEP     3855.191 GWh/a
Total net AEP uncertainty     10.2 %
Total net AEP P75 3590.717 GWh/a
```

C.1
```
AEP Model    WAsP/Park
Wind resource      Fino1 2004-2008, 103.5m
Total gross AEP   1799.872 GWh/a
Farm efficiency    91.1 %
Total farm AEP    1639.178 GWh/a
Total net AEP     1434.977 GWh/a
Total net AEP uncertainty     10.2 %
Total net AEP P75 1336.535 GWh/a
```

C.2
```
AEP Model    WAsP/Park
Wind resource      Fino1 2004-2008, 103.5m
Total gross AEP   1799.865 GWh/a
Farm efficiency    93.0 %
Total farm AEP    1674.271 GWh/a
Total net AEP     1465.699 GWh/a
Total net AEP uncertainty     10.2 %
Total net AEP P75 1365.149 GWh/a
```
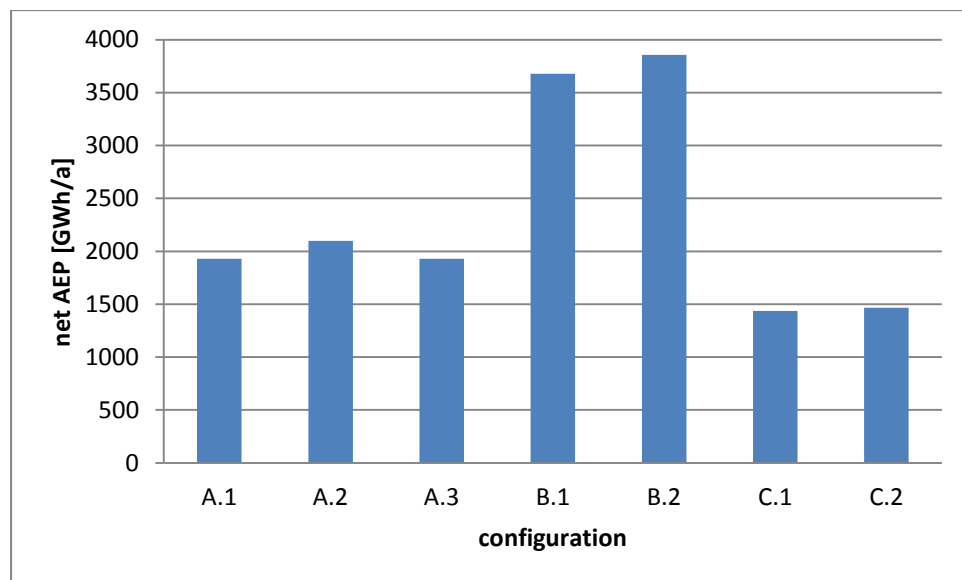

Figure 11: Results of net AEP for the different configurations.

F. 5 Observations

F.5.1 Observations on results

Deliverable 5.12 EERA DTOC calculation of scenarios

The results of the calculations of the A-configurations show that the use of the wind resource with wakes effects of surrounding wind farms (A.1) causes a decrease in the net AEP in comparison to the results of the wind resource without wake effects (A.2) -as expected. A decrease of 8 % is calculated by the WAsP model. Using the wind resource of the WRF model (A.3) exactly the same results as for the configuration A.1 are obtained. This has to be checked if it's correct.

The B-configurations demonstrate the difference by using the WAsP/Park (B.1) and the Fuga (B.2) model. A deviation of 177 Gwh/a for the net AEP of DoggerBank is calculated. The WAsP/Park model produces in this case less AEP than the Fuga model.

The change in the layout (C.2) of the wind farm Borkum West results in an increase of the net AEP in comparison with the original layout (C.1). The results of both C-configurations show a difference of 31 Gwh/a for the net AEP.

F.5.2 User experiences

The installation of the required software was no problem on a Windows-PC. But the firewall of our institute prohibits the VPN-connection to the DTOC server. For the calculations another internet connection outside of the institute had to be used.

The tool runs without problems during the tests. The QGIS has a very long runtime (after an action everything is frozen for a while) which is slightly inefficient and time consuming.

F.5.3 Expert judgment

The DTOC tool can be understood easily and the documentation and tutorials are very helpful. The connection to QGIS for changes in the layout of the wind farm is very nice. It would be great if the problems with the long runtimes of QGIS can be avoided.

The tool can be very helpful to calculate different scenarios/ configurations and compare them very easily. In addition to the results for a wind farm, the user can get a feeling about the performance of different configurations and possible uncertainties of the results. At the moment no results for each single wind turbine can be reached which would be nice in the future.

Judgement regarding the tested user stories:

- **User story 1.1: As strategic planner or developer I can determine the wake impact of individual wind farms within a cluster on each other (just meso). It's difficult to understand if it's sufficient to select a wind resource which includes wake effects of surrounding wind farms or if I have to activate other wind farms in the surrounding.**
- **User story 1.3: As a strategic planner I can determine the optimum size, spacing and position of offshore wind farm clusters. There is no optimisation by the tool, so I have to do it by myself step by step. This is time consuming.**
- **User story 3.3: As a developer I can determine the net energy yield of a wind farm very easily.**

Deliverable 5.12 EERA DTOC calculation of scenarios

G.1 Objective/user story

G.1.1 Objective

Trying the tool to yield multiple scenarios with many different hub heights and based on different inputs.

G.1.2 User story and scenario

Base scenario (Race Bank).
User stories:
3.2 As a developer I can determine the wake effects due to turbines within a wind farm.
3.3 As a developer I can determine the net energy yield of a wind farm.
3.4 As a developer I can determine the optimum spacing, position, turbine model and **hub height** *of turbines within an offshore wind farm.*

G.2 Codes

Used: The latest (v1.1, 13.4.2015) scenario trees with WAsP/PARK and the LCOE tool v1.1.

G.3 Input:

G.3.1 Description of wind farm

Race Bank in standard configuration, 100 turbines in a Horns Rev layout.

G.3.2 Description of turbines:

NREL-Upwind5MW-5000-126-90-theo-1225.

G3.3 Description of wind climate

Used the CENER runs including the surrounding wind farms, for 80m, 100m and 120m levels.

G.3.4 Remarks.

I tried to change as little as possible from the standard configured by Overspeed.

G.4. Output/results

Three variations of the CENER dataset with all surrounding wind farms were chosen for the calculations, representative for 80m a.g.l., 100m and 120m. For those three resource data sets, four different hub heights were calculated: 80m, 90m, 100m and 110m.

Deliverable 5.12 EERA DTOC calculation of scenarios

Gross AEP

CENER 80m
CENER 100m
CENER 120m

Farm AEP

CENER 80m
CENER 100m
CENER 120m

Farm Eff

CENER 80m
CENER 100m
CENER 120m

Deliverable 5.12 EERA DTOC calculation of scenarios
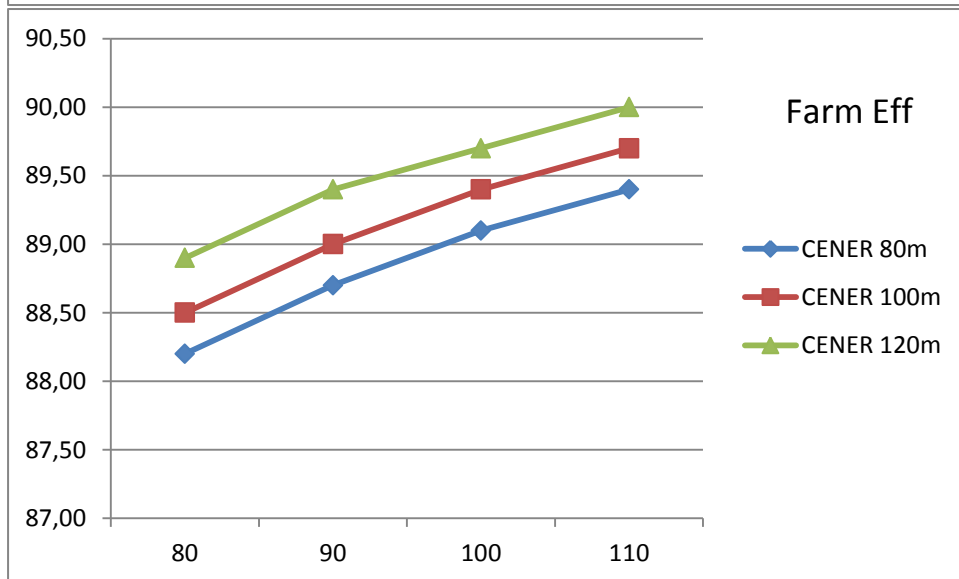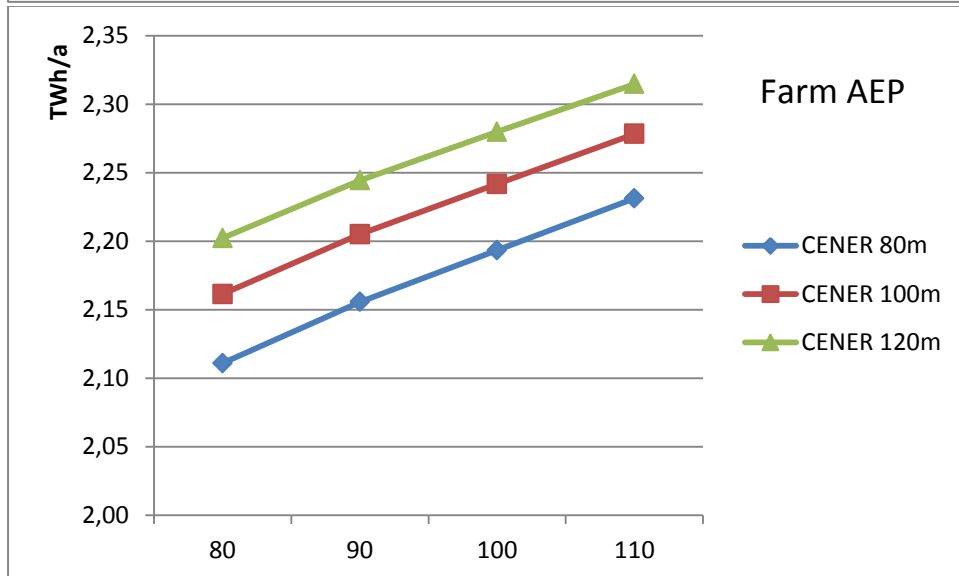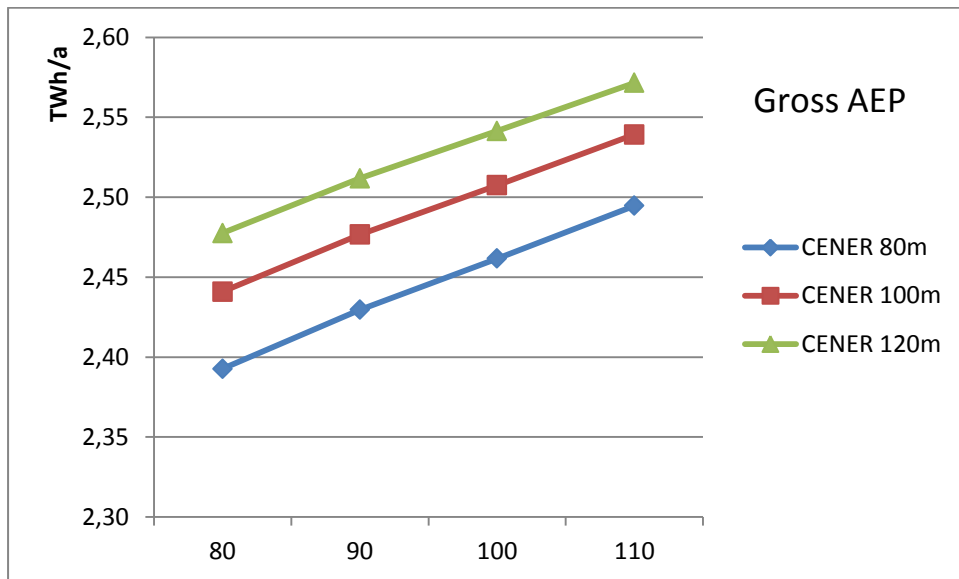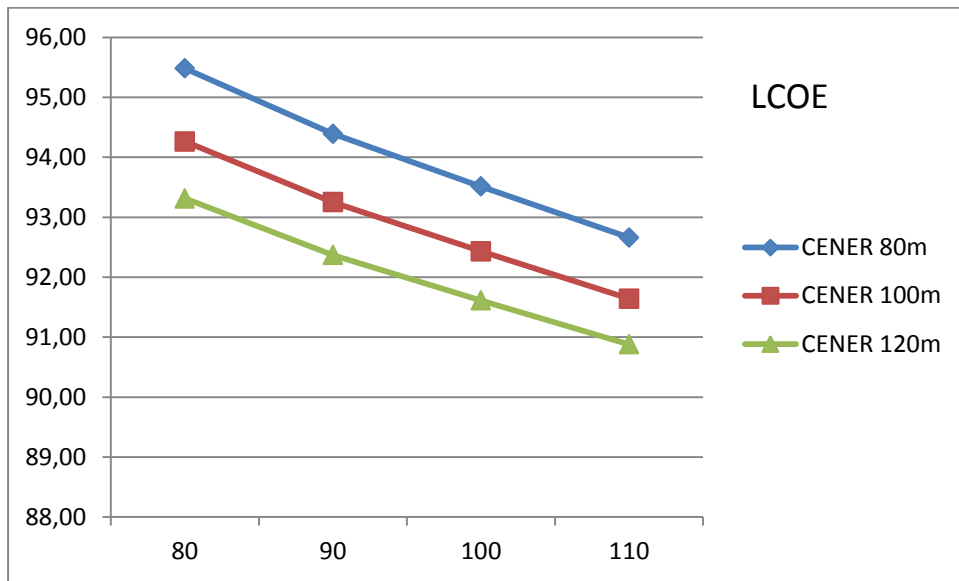
G.5 Observations

G.5.1 Observations on results.

As the CAPEX does not seem to take the length of the tower into account, it is not surprising that the LCOE decreases (lowest plot) when more wind is caught (first plot). On first glance, it is more surprising that the farm efficiency increases, i.e. the wake losses decrease, when the hub height increases. But that can be explained by the higher amount of rated power at higher wind speeds. Above rated power, the wake losses decrease as there is more than enough wind anyway to run the turbines.

It is clear that the system does not try to convert the height of the modelled wind climate to the hub height, otherwise the three lines should be much closer to each other.

G.5.2 User experiences:

Deliverable 5.12 EERA DTOC calculation of scenarios

Building the scenario tree took some time, as there was quite some reloading involved. However, running the scenarios took much longer, as there is no "run all calculations" command on the top scenario level the way it is implemented in WAsP. Also every single model run had to be invoked by hand - at least an automatic run of the LCOE model after updating the WAsP or FUGA results should be possible.

The analysis of the results was done by exporting the .tsv files and importing them in Excel. This involved a lot of manipulation of numbers and files, before all was integrated in a single plot. Here, the comparative reporting facility is sorely missing.

G.5.3 Expert judgment

The drop of LCOE with increased hub height seems right, though the LCOE model does not take a price change with hub height into account. This would make the decrease less steep.

Deliverable 5.12 EERA DTOC calculation of scenarios

H.1 Objective/user story

H.1.1 Objective

Evaluate the impact of different wind turbine models and wind farm layouts on the energy yield. As a secondary goal an evaluation of different wake models is also performed.

H.1.2 User story and scenario

Near future scenario (Doggersbank)
User story

- As a developer I can determine the optimum spacing, turbine model and hub height of turbines within off-shore farms

- As a developer I want to use wind farm lay-out scenarios of my target wind farm with respect to nr of turbines, turbine types, thrust curves etc

H.2 Codes

Fuga, WAsP-Park and Levellised Cost Of Energy (LCOE) models from the DTOC tool. Additional results from in-house CRESFarm tool. The latter tool uses the GCL model for wake losses estimation, calibrated based on the findings of the EERA-DTOC project for densely packed wind farms.

H.3 Input:

H.3.1 Description of wind farm

This scenario is connected to the plan for an off-shore cluster at Dogger Bank. It starts with a 1GW wind farm consisting of 100 turbines with a rated power of 10 MW using the INNWIND.EU reference turbine. The farm is assumed to be located at the southern part of the Doggersbank area and it is surrounded by other wind farms similar to the planned situation for Doggersbank.
The suggested layout of the farms is described in other parts of the report and will not be repeated here. In addition to the "standard" layout, layouts with increased / decreased distances and rotated wind turbines were considered for evaluation purposes.

H.3.2 Description of turbines:

Deliverable 5.12 EERA DTOC calculation of scenarios

The initial wind turbines from the near-future scenario have a rated power of 10 MW with a rotor diameter of 178.3 m at a hub height of 119 m. The modified AVATAR wind turbine that is also considered has a hub height of 127m and a diameter of 205m. There is a substantial difference in the power and thrust curves between the two as shown in Figure 12
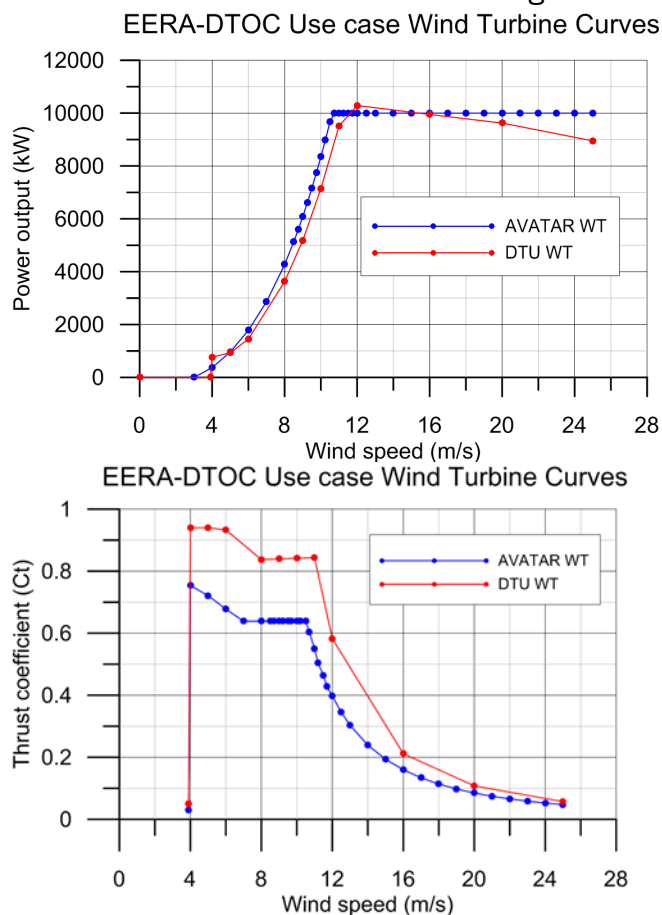

Figure 12. Power and Thrust curves for the AVATAR and DTU wind turbines

The AVATAR wind turbine was designed to have lower thrust for the same rated power, resulting in potential benefits for application in large offshore wind farms.

H.3.3 Description of wind climate

The Doggerbank-wrf-20150210 Wind Resource file was used for most comparisons. For the effect of neighbouring wind farms, the DTU Doggerbank files at 119m with and without wake effects were used. In all cases tabulated data at 12 wind directions were available. The raw data was provided by OverSpeed and was also used for the in-house tool computations.
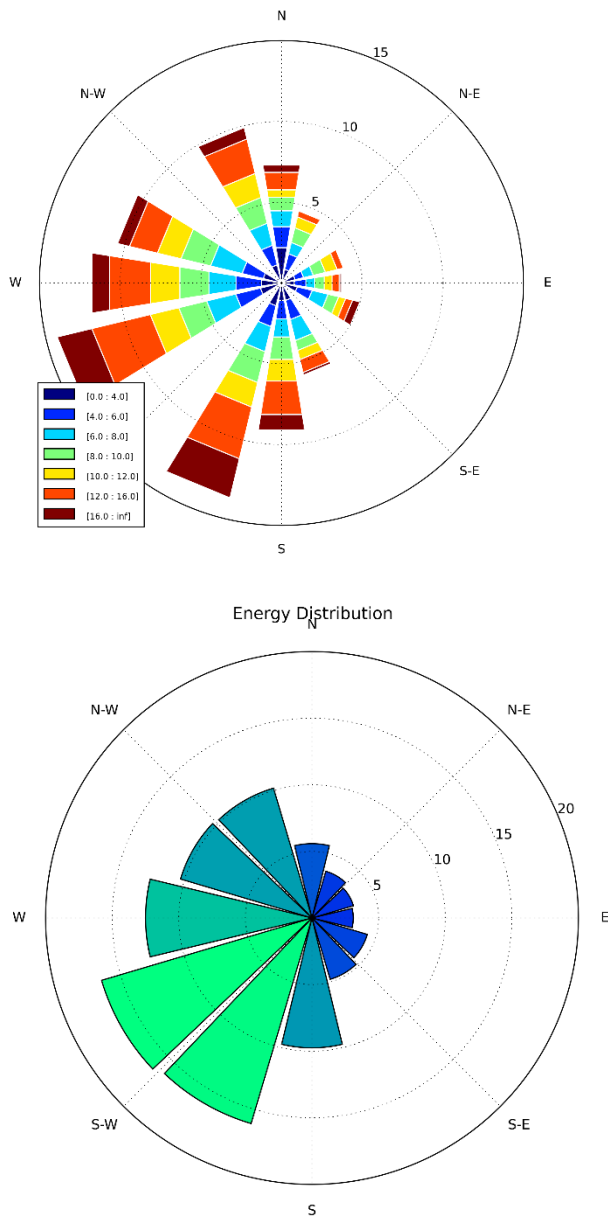
Deliverable 5.12 EERA DTOC calculation of scenarios

Figure 13. Wind roses at the Doggersbank site

H.3.4 Remarks.

Different combinations of wake models and layouts were used to estimate the various relevant quantities, such as the total gross and net annual energy production and costs of the investment and produced energy. In all cases the reference layout is the 10x10 provided in the tool.

Table 8. Configuration of the different scenarios.

WT Type	Wind farm layout	Wind Resource	Wake Model
DTU	Standard	Doggerbank-wrf-20150210	WAsP, Fuga, CRESFarm
AVATAR	Standard	Doggerbank-wrf-	WAsP, Fuga,

Deliverable 5.12 EERA DTOC calculation of scenarios

		20150210	CRESFarm
DTU	Spacing from 85%-110%	Doggerbank-wrf-20150210	WAsP, Fuga
AVATAR	Spacing from 85%-100%	Doggerbank-wrf-20150210	WAsP, Fuga
DTU	Rotated +/- 10 degs	Doggerbank-wrf-20150210	WAsP, Fuga
AVATAR	Standard	DTU WRF at 119m without neighbouring farm wake effects	WAsP/Park
AVATAR	Standard	DTU WRF at 119m *with* neighbouring farm wake effects	WAsP/Park

H.4. Output/results

In order to study the effect of the WT type, the AVATAR and DTU wind turbines were evaluated using the WAsP/Park and Fuga wake models. As shown in Figure 14 a 2-4% increase in yield is estimated using the low-induction AVATAR rotor. The results are reproducible with both wake models, though the wake effects predicted by the WAsP model are larger in both cases.
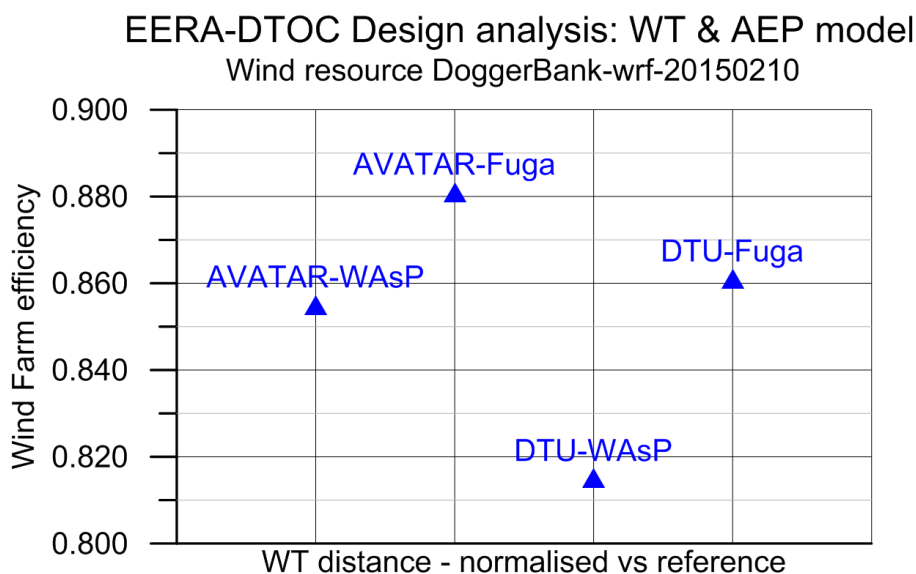

Figure 14. Results from the WT comparison

The next set of calculations was intended to examine the tool's ability to predict the effects of the layout on AEP. To this end, changes in spacing and orientation were performed, as shown in Figure 15.
For the spacing it seems that for every 5% decrease in inter-turbine distance there is a ~1% decrease in the wind farm efficiency (Figure 16). The use of the AVATAR rotor results in higher wind farm efficiency, so that one could use a distance reduced by 15% and get the same efficiency as the original WT.

Deliverable 5.12 EERA DTOC calculation of scenarios

EERA-DTOC Design analysis: Layout
Wind Turbine distance change

EERA-DTOC Design analysis: Layout
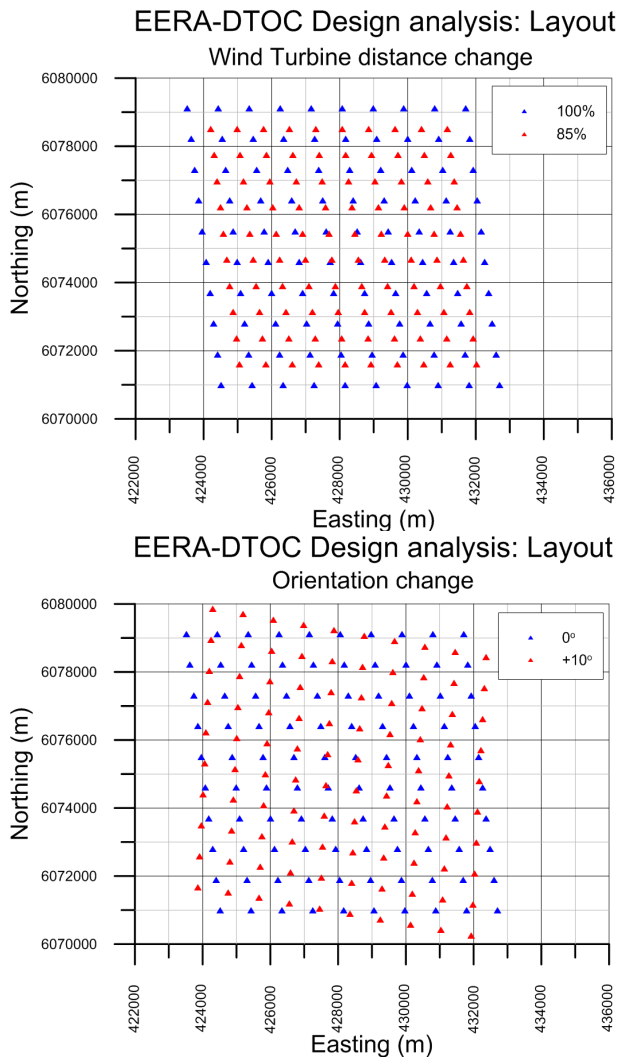### Orientation change

Figure 15. Changes in spacing and orientation for the standard layout

As far as the wind farm orientation is concerned, the results are show in
. It is obvious that the chosen orientation is near-optimum, with relatively small variations within a 10deg sector. Deviating further results in a substantial increase in wake losses, as expected.

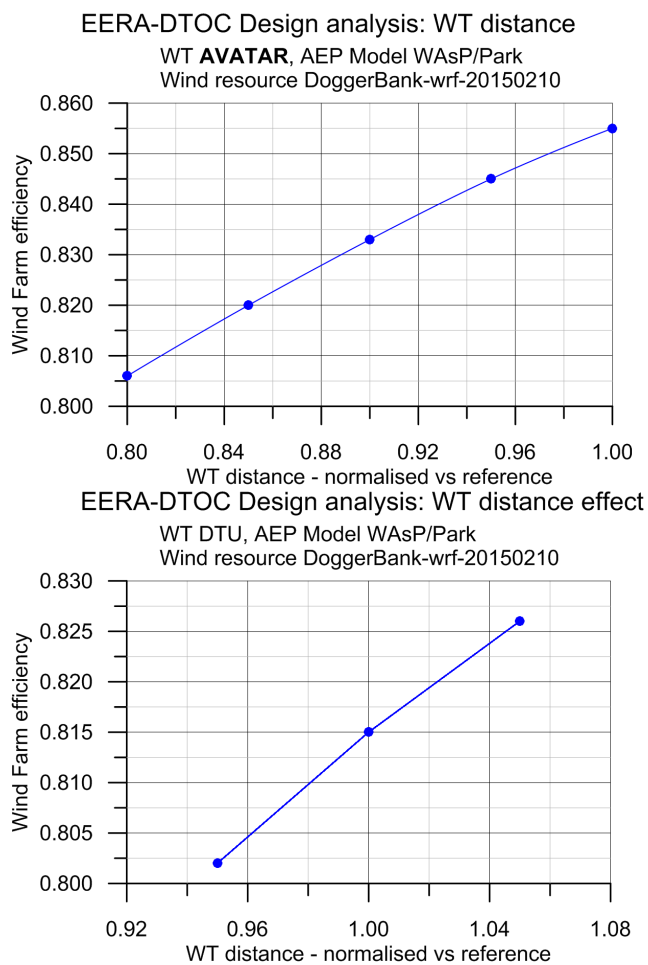*Deliverable 5.12 EERA DTOC calculation of scenarios*

Figure 16. Change of wind farm efficiency with spacing

For comparison purposes an in-house tool was also used for the reference layout, using a different wake model. The comparison of the predicted losses is shown in Figure 17. The distribution of the losses within the wind farm are given in Figure 19 (using CRESFarm), showing that the reduce thrust coefficient of the AVATAR rotor results in more of the turbines working with smaller wake losses compared to the original layout.

A more detailed comparison of gross and net yield for the three models is given in Figure 20. It should be noted that the gross yield should be the same for all models, as it is only dependent on the power curve and wind resources, but as the wind resources are incorporated in a slightly different manner in the in-house tool (using weights for the different available locations instead of the nearest node) there is a difference in that. The overall difference (combination of increased hub height, increase energy capture at low speeds and reduced wake effects) is shown in Figure 21.

A final test was related to the effect of surrounding wind farms in energy yield. These are incorporated through the use of modified resource files, that take into acccount the reduced wind potential because of the energy extraction from other wind farms. A single test was used for this comparison, using two different wind resource files, as listed in Table 8. The results show a ~3% decrease as a result of the operation of neighbouring wind farms.

Deliverable 5.12 EERA DTOC calculation of scenarios
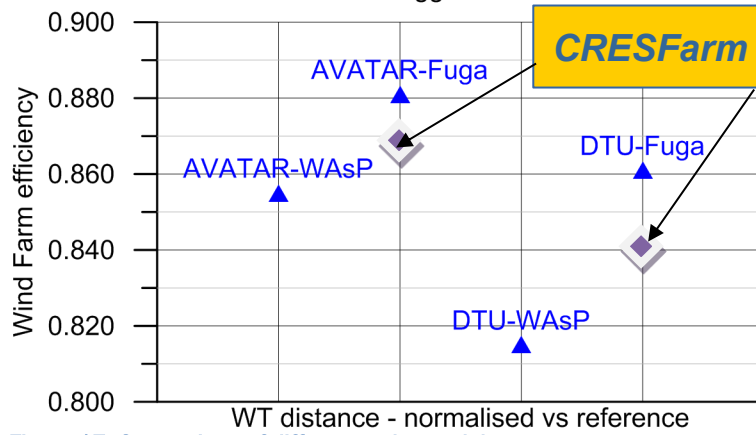
Figure 17. Comparison of different wake models
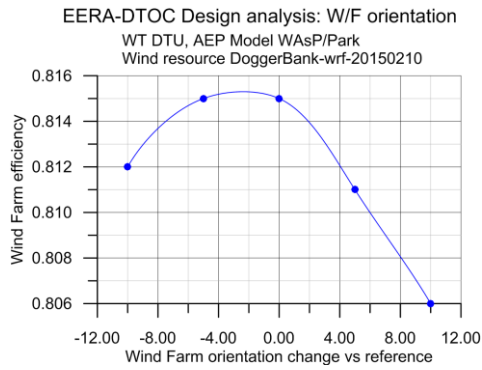
Figure 18. Effect of wind farm orientation on efficiency

Deliverable 5.12 EERA DTOC calculation of scenarios
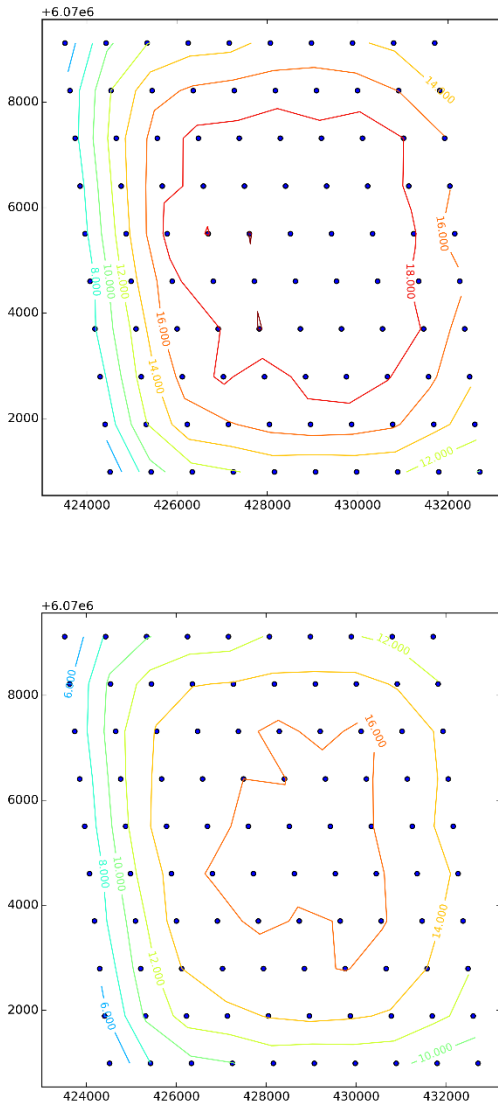
Figure 19. Distribution of wake losses using different wind turbine models
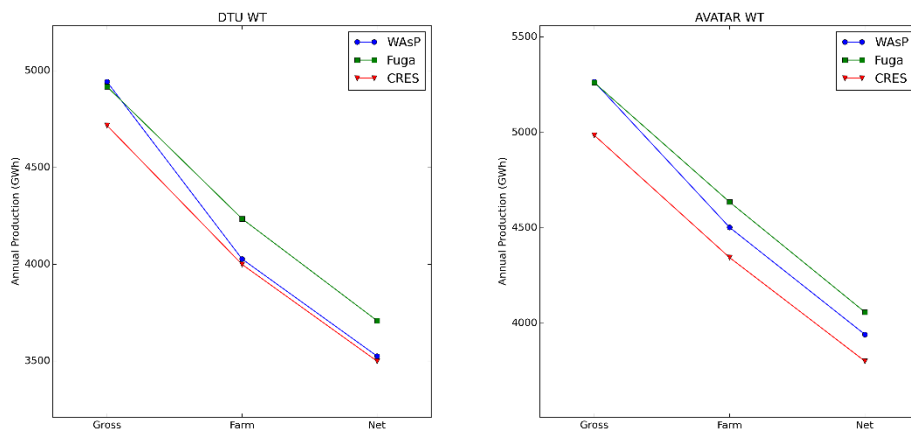
Figure 20. Estimate of annual energy yield for both WT types

Deliverable 5.12 EERA DTOC calculation of scenarios
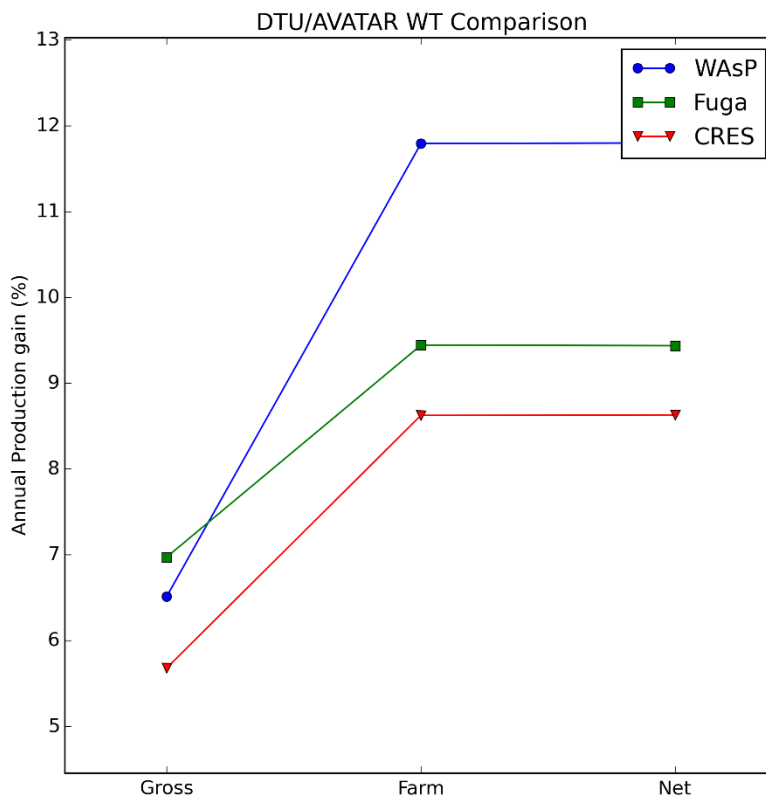
Figure 21. Gains from the low-induction rotor

Table 9: Effect of neighbouring wind farms

	Gross	Farm	Net
Without Wakes	5514	4780	4185
With Wakes	5376	4641	4063
Difference	-2.5%	-2.9%	-2.9%

H.5 Observations

H.5.1 Observations on results.

The WAsP/Park model seems to predict larger wake losses than the Fuga model, with the in-house model being between the two. The changes (depending on layout, WT type etc) are consistent for all wake models.
The effect of spacing and orientation on AEP is evaluated consistently, though there was no time to perform more detailed investigations of optimized (non-regular) layouts, to check their effect on the results.
The use of a low-induction rotor results in a 3-4% gain in wind farm efficiency. In addition to that there is a 4-6% gain in gross energy yield, giving an overall gain that can be ~10%.

H.5.2 User experiences:

Deliverable 5.12 EERA DTOC calculation of scenarios

Downloading the used wind resources is currently not available, though in practical use one would probably upload measured wind resources in the prescribed format.

Edits of the scenarios were performed directly on the input xml files, as the QGIS integration was largely dependent on the QGIS version used, and was not always easy to perform.

The effect of neighbouring wind farms is currently included through a change in the wind resources. A simpler method with a modification of the available wind resource file (to account for different future development scenarios) would be beneficial.

H.5.3 Expert judgment

The relative differences between different calculation methods are within the accuracy generally expected from wake loss engineering models (where uncertainties can be quite large). At the moment the abilities for a more detailed analysis, in the form of seasonal and diurnal variations, effect of stability, etc. are not incorporated in the model.

Deliverable 5.12 EERA DTOC calculation of scenarios

14. APPENDIX I: VALIDATION OF WASP AND FUGA AEP CALCULATIONS IN THE EERA-DTOC TOOL

I.1 Objective/user story

I.1.1 Objective

Validation of annual energy production (AEP) estimates performed with the FUGA and WAsP models, which are integrated in the current version of the EERA-DTOC tool v1.1.1, against `offline' AEP estimations using the WAsP v11.2 and FUGA v2.8.2.1 software are here performed for both the base scenario at the Race-Bank wind farm and the near-future scenario at the Dogger-Bank Creyke Beck A wind farm. In WAsP and FUGA the AEP estimates reflect both the gross and net energy yields, i.e. those without and with consideration of the wake effects, respectively. In the DTOC tool the net AEP estimate not only includes the wake loss but also the farm efficiency (from other losses) and a farm AEP estimate will be the equivalent to the WAsP-FUGA net one.
Mimics of these scenarios made on the DTOC tool were exported as WAsP projects. The WAsP projects can be opened in the WAsP and FUGA software and so the AEP of the wind farms were re-computed and compared to the results using the DTOC tool.

I.1.2 User story and scenario

Base scenario (Race Bank)
Near future scenario (Doggersbank)

User story	Yes/no	Remarks
3.2 As a developer I can determine the wake effects due to turbines within a wind farm.	Yes	
3.3 As a developer I can determine the net energy yield of a wind farm.	Yes	

I.2 Codes

The following table lists the codes used and the way how the codes are operated (i.e. within the EERA-DTOC user interface or off-line)

Code	Operation
WAsP	Offline
FUGA	Offline
WAsP	Online
FUGA	Online

Deliverable 5.12 EERA DTOC calculation of scenarios

I.3 Input:

I.3.1 Description of wind farm

The default based scenario at the Race-Bank wind farm and the default near-future scenario at the Dogger-Bank wind farm are used.

I.3.2 Description of turbines:

For the Race-Bank wind farm the NREL-Upwind 5MW-5000-126-90-theo-1225 wind turbine is used and for the Dogger-Bank wind farm the DTU 10 MW RWT-10000-178.3-120-theo-1225 wind turbine

I.3.3 Description of wind climate

Observed wind climate (OWC) files on each turbine position are used for both wind farms. For Race-Bank the OWC is at 90 m AMSL and for Dogger-Bank at 100 m AMSL

I.3.4 Remarks.

The OWC files were extracted from the default scenarios in the DTOC tool

I.4 Output/results

Base scenario – Race-Bank wind farm
Figure 1 shows the base scenario in WAsP. As illustrated the gross AEP is 2479.42 GWh and the net AEP is 2207.80 GWh. The estimations of the DTOC tool using the WAsP model are 2476.64 GWh and 2205.10 GWh for the gross and farm AEPs, respectively.
Figure 2 shows the base scenario in FUGA. As illustrated the gross AEP is 2471.00 GW h and the net AEP is 2231.60 GWh, being both results very similar to those using WAsP. The estimations of the DTOC tool using the FUGA model are 2468.26 GWh and 2228.92 GWh for the gross and farm AEPs, respectively.

Near-future scenario – Dogger-Bank wind farm
Figure 3 shows the base scenario in WAsP. As illustrated the gross AEP is 4945.76 GWh and the net AEP is 4029.37 GWh. The estimations of the DTOC tool using the WAsP model are 5285.63 GWh and 4342.21 GWh for the gross and farm AEPs.

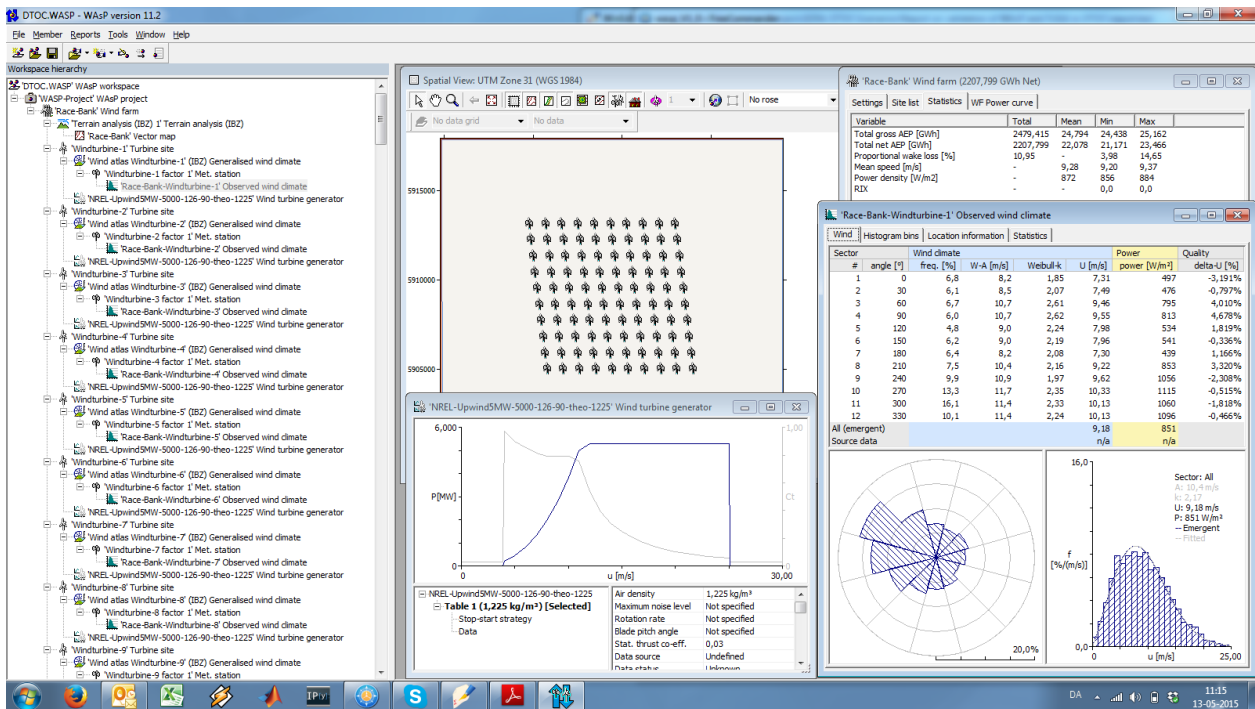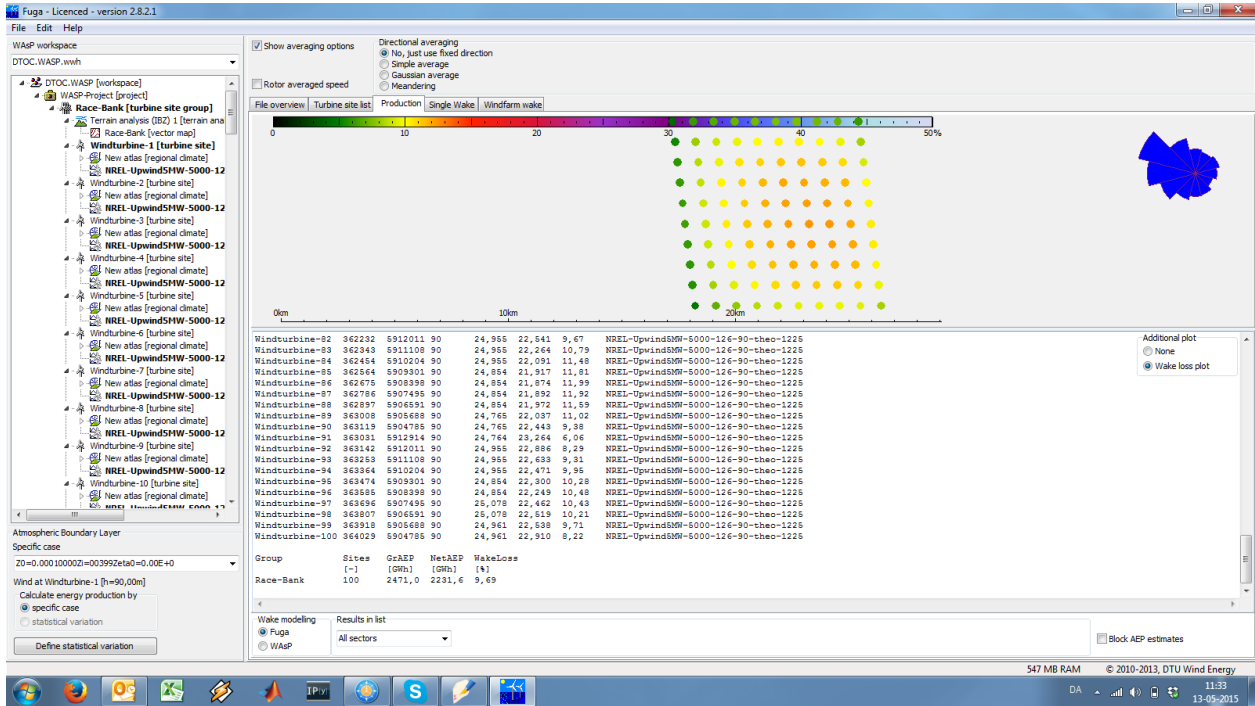*Deliverable 5.12 EERA DTOC calculation of scenarios*

Figure 22 WAsP computations of the base scenario at the Race-Bank wind farm

Figure 23 FUGA computations of the base scenario at the Race-Bank wind farm

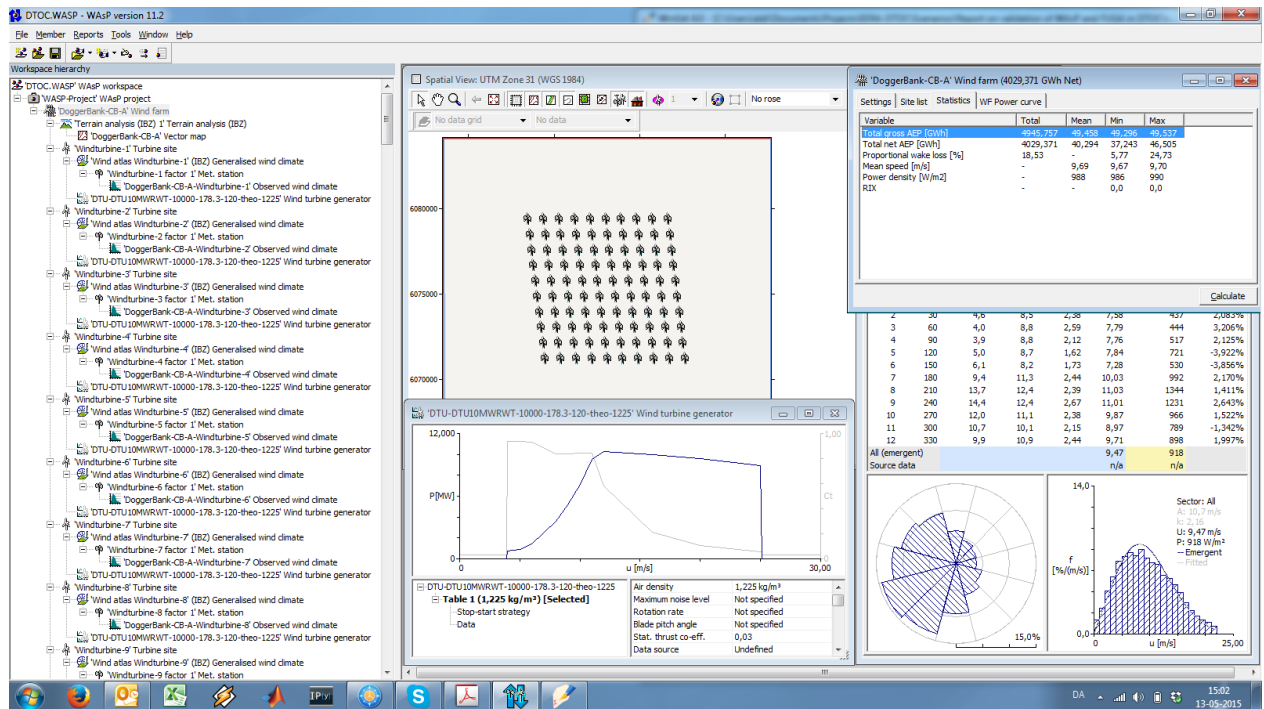*Deliverable 5.12 EERA DTOC calculation of scenarios*

Figure 24 WAsP computations of the near-future scenario at the Dogger-Bank wind farm

Figure 4 shows the base scenario in FUGA. As illustrated the gross AEP is 4920.60 GWh and the net AEP is 4238.50 GWh, the gross AEP value being very similar to that using WAsP with a much lower wake loss (for FUGA it is 13.86\% and for WAsP 18.53\%). The estimations of the DTOC tool using the FUGA model are 5260.46 GWh and 4559.07 GWh for the gross and net AEPs, respectively.

I.5 Observations

I.5.1 Observations on results.

`Offline' AEP estimations of the base scenario using WAsP and FUGA show nearly identical results as those from the EERA-DTOC tool v1.1.1 using the WAsP and FUGA models. For the near-future scenario there is a difference of ~7\% in both the WAsP and FUGA calculations for both the gross and net/farm AEPs. This suggests that the wind climate used in the tool and in the `offline' calculations for the near-future scenario is most probably different. This needs to be checked by Overspeed.
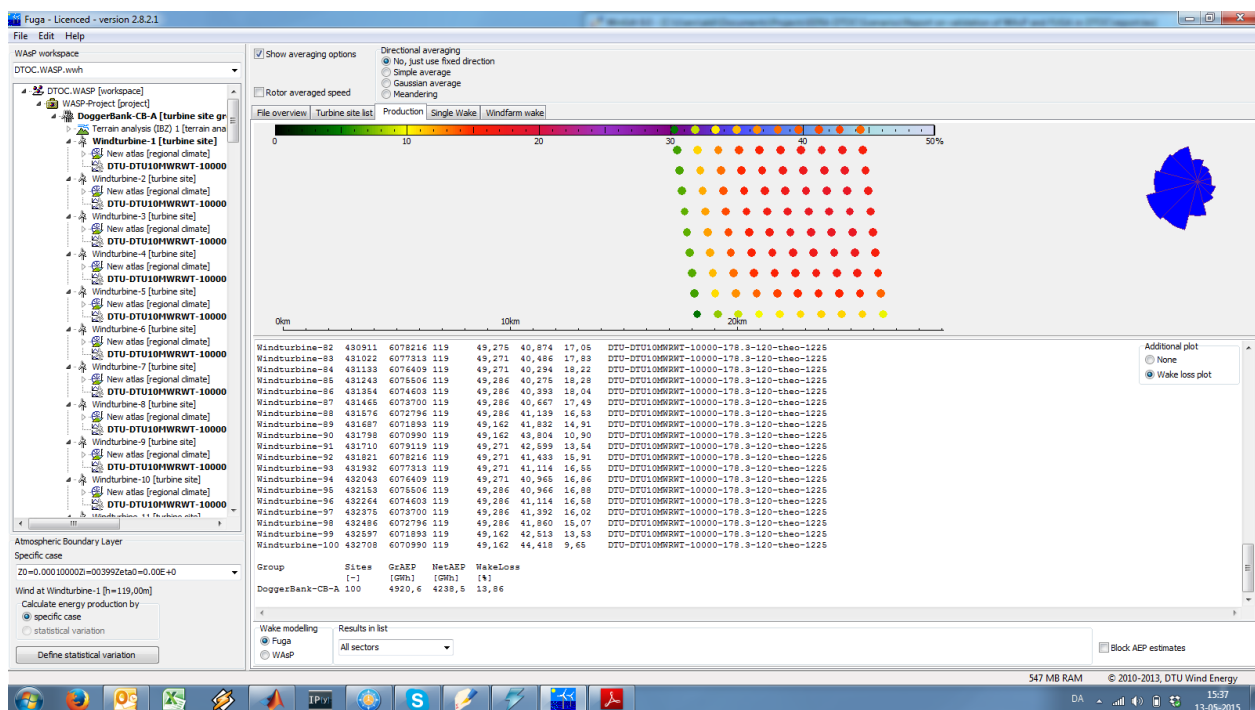
Deliverable 5.12 EERA DTOC calculation of scenarios

Figure 25 FUGA computations of the near-future scenario at the Dogger-Bank wind farm

Deliverable 5.12 EERA DTOC calculation of scenarios

J.1 Objective/user story

J.1.1 Objective

As the size and concentration of offshore wind farms increase, the study of potential wake losses produced by the presence of neighbor wind farms on an area of interest could be a relevant aspect to take into account.

Strong wind speeds with low variations on wind direction and a relatively flat surface, like the ocean, constitute the ideal conditions for the formation of wakes due to the presence of offshore wind farms. These wakes effects can spread for dozens or even hundreds of kilometers and affect the meteorological conditions within a large area surrounding a given wind farm or cluster of wind farms.

When analyzing regions with a high concentration of wind farms, it is necessary to evaluate large areas surrounding the area of interest. This translates into the necessity of simulating very large domains, which sometimes include multiple wind farms with different sizes and wind turbine characteristics.

Current microscale wake models focus on wakes effects created by individual wind turbines and the subsequent deficits inside the wind farm, using high resolution numerical grids that have to be limited based on each computational constraints. For that reason, the simulation of very large areas is a lengthy and delicate process.

If the main goal is to determine a suitable location to the construction of a new wind farm, or evaluate the wind speed deficits resulting from the presence of wind farms on the neighborhood of an area of interest, a lower resolution simulation, covering a larger area and focusing mainly on far wakes could be a useful tool. In those situations current mesoscale models could be an important tool in the wind farm planning. State of the art mesoscale models, such as the *Weather Research and Forecasting* model (WRF), have already implemented a wind farm parameterization (Fitch scheme (Fitch 2012)) that allows the estimation of wake losses created by individual or clusters of wind farms.

A demonstration of mesoscale capability is carried out in this study. A suitable area was identified and a complete study of the wind conditions in that region was performed using the WRF model. The study pretends to focus on the expected wake losses at the future Race Bank location, resulting from the presence of multiple wind farms in its proximity.

J.1.2 User story and scenario

Base scenario (Race Bank)

User Story	Yes/No
1.1 As strategic planner or developer I can determine the wake impact of individual wind farms within a cluster on each other (just meso)	Yes
1.2 As a strategic planner I can determine the net energy yield of offshore wind farm clusters.	No
1.3 As a strategic planner I can determine the optimum size, spacing and position offshore wind farm clusters.	No
2.1 As a strategic planner I can determine the optimum strategic infrastructure to accommodate offshore wind farm clusters.	No
3.1 As a developer I can determine the wake effects of neighbouring wind farm clusters on a single wind farm (meso and/or micro).	Yes
3.2 As a developer I can determine the wake effects due to turbines within a wind farm.	No

Deliverable 5.12 EERA DTOC calculation of scenarios

3.3 As a developer I can determine the net energy yield of a wind farm.	No
3.4 As a developer I can determine the optimum spacing, position, turbine model and hub height of turbines within an offshore wind farm.	No
3.5 As a developer, I want to use wind farm layout scenarios of my target wind farm with respect to nr of turbines, turbine types, power and thrust curves etc.	Yes

J.2 Codes

Using the state of the art *Weather Research and Forecasting* (WRF) (Skamarock 2008) mesoscale model, that includes a wind farm parameterization scheme (Fitch scheme (Fitch 2012)), it is possible to simulate the far wake effects of a single or cluster of wind farms.

WRF ARW model, version (3.6) is used and three, two-way nested domains centered in the area of interest, are defined. The domains have horizontal resolutions of 27km, 9km and 3km as shown in *Figure 26*.
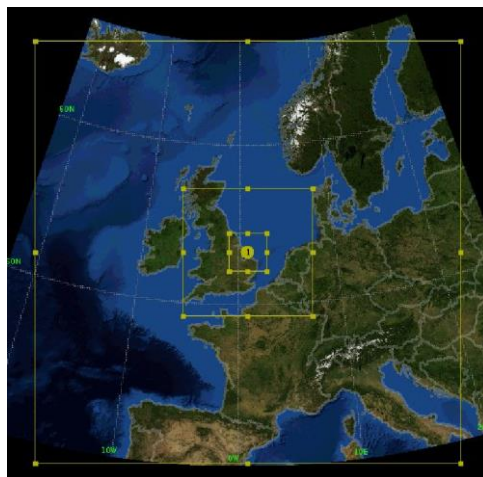

Figure 26: Base scenario WRF domain

All simulations used the following parameterizations: WRF Single-Moment (WSM) 3-class simple ice scheme (Hong 2004) as microphysics, Rapid Radiative Transfer Model scheme (Mlawer 1997) to long wave radiation, Dudhia scheme (J. Dudhia 1989) to the short wave radiation, MYNN (Nakanishi 2004) as surface layer option, Noah Land-Surface model (F. C. Dudhia 2001) as surface physics, MYNN 2.5 level TKE scheme in the boundary layer and Kain-Fritsch (new Eta) scheme (Fritsch 1990) as cumulus option.

J.3 Input:

J.3.1 Description of wind farm

The Greater Wash area (*Figure 27*) in the UK was designated as a potential offshore wind farm development region in 2002, leading to the construction/planning of several offshore wind farms. Lynn, Lincs, Inner Dowsing, Sheringham Shoal, Triton Knoll A and B, Dudgeon and Race Bank wind farms are considered in this study. The first four wind farms are already operating, while the last three are planned to be built in a relatively near future.
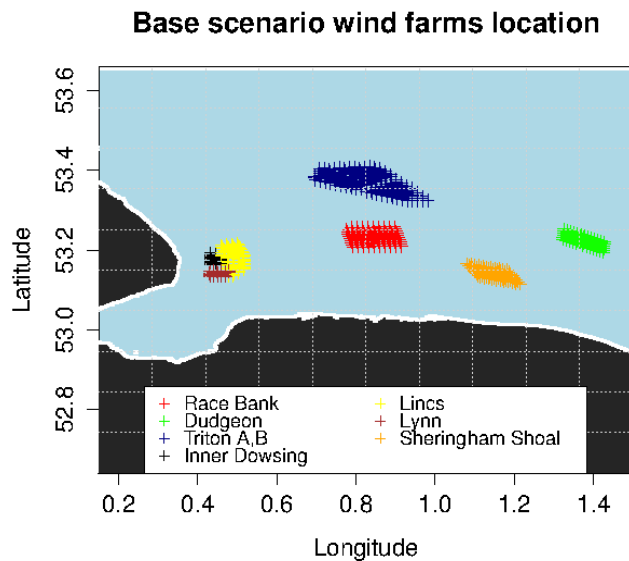
Deliverable 5.12 EERA DTOC calculation of scenarios

Base scenario wind farms location

Figure 27: Great Wash turbines positions

The Race Bank wind farm will be located at 27 km from the North Norfolk coast at the Eastern part of England and centered at 53.276oN; 0.841oE and it is surrounded by several other offshore wind farms. Since no official wind turbine type or positions are defined for the Race Bank and Triton Knoll wind farms at this point, two layouts are proposed (*Figure 28*) in order to carry out the study in the area. A 500MW wind farm, constituted by 100 turbines with a rated power of 5MW is considered for Race Bank, while the Triton Knoll wind farm is constituted by 200 wind turbines with rated powers of 6MW.
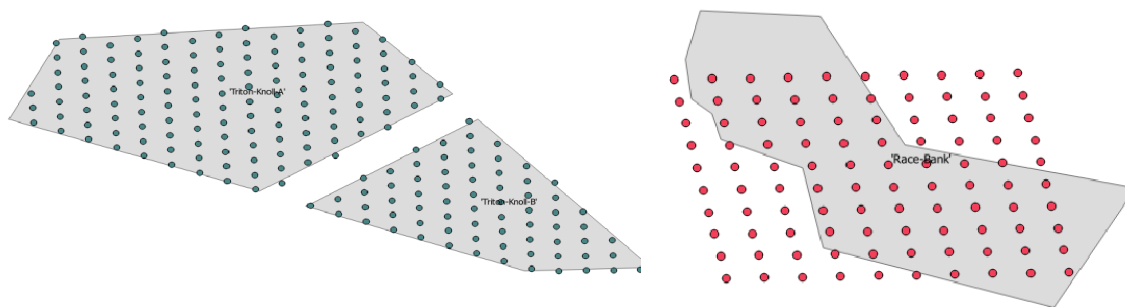

Figure 28: Triton Knoll and Race Bank proposed layouts

 Lynn, Lincs and Sheringham Shoal offshore wind farms are already operating in the Great Wash area while Triton Knoll, Dudgeon and Race Bank are planned to be built in the near future (*Figure 27*). Three simulations are performed:

1. **Control Run:** Without wind farms. Will constitute the reference wind climate at the area.
2. **Sim. 3:** Run with operating and planned wind farms, without Race Bank(Lynn, Lincs, Inner Dowsing, Sheringham Shoal, Dudgeon and Triton Knoll)
3. **Sim. 4:** Run with operating, planned wind farms and Race Bank(Lynn, Lincs, Inner Dowsing, Sheringham Shoal, Dudgeon, Triton Knoll and Race Bank)

Deliverable 5.12 EERA DTOC calculation of scenarios

J.3.2 Description of turbines:

Real turbine characteristics and positions are hard to find, so some adjustments had to be made in order to obtain the required input data. Four different types of turbines were used.

Below are the descriptions of the turbine characteristics of each machine type:

1. Race Bank:
    a. Type of machine: PHATAS-4 5.0MW-126
    b. Rated Power: 5MW
    c. Diameter: 126m
    d. Hub Height: 90m
    e. Power Curve: Available
    f. Ct Curve: Available

2. Inner Dowsing, Lincs and Lynn:
    a. Type of machine: Siemens SWT3.6-120
    b. Rated Power: 3.6MW
    c. Diameter: 120m
    d. Hub Height: 90m
    e. Power Curve: Obtained from graphic observation
    f. Ct Curve: Same as PHATAS-4 5.0MW-126

3. Sheringham Shoal:
    a. Type of machine: Siemens SWT6.0-120
    b. Rated Power: 6MW
    c. Diameter: 120m
    d. Hub Height: 90m
    e. Power Curve: Scaled up from Siemens SWT3.6-120
    f. Ct Curve: Same as PHATAS-4 5.0MW-126

4. Triton Knoll and Dudgeon:
    a. Type of machine: Siemens SWT6.0-154
    b. Rated Power: 3.6MW
    c. Diameter: 154m
    d. Hub Height: 90m
    e. Power Curve: Scaled up from Siemens SWT3.6-120
    f. Ct Curve: Same as PHATAS-4 5.0MW-126

J.3.3 Description of wind climate

Due to the multiple scenarios to take into account, a typical year, based on the Best Annual Means methodology (Chavez-Arroyo 2015), representative of a 10 years period (2002-2011), is calculated. This methodology provides a viable alternative, in which the simulation of 365 days within the 10 years period, should result in an equivalent wind climate to the one obtained by simulating the entire 10 years. This way it is possible to save computational resources and deliver

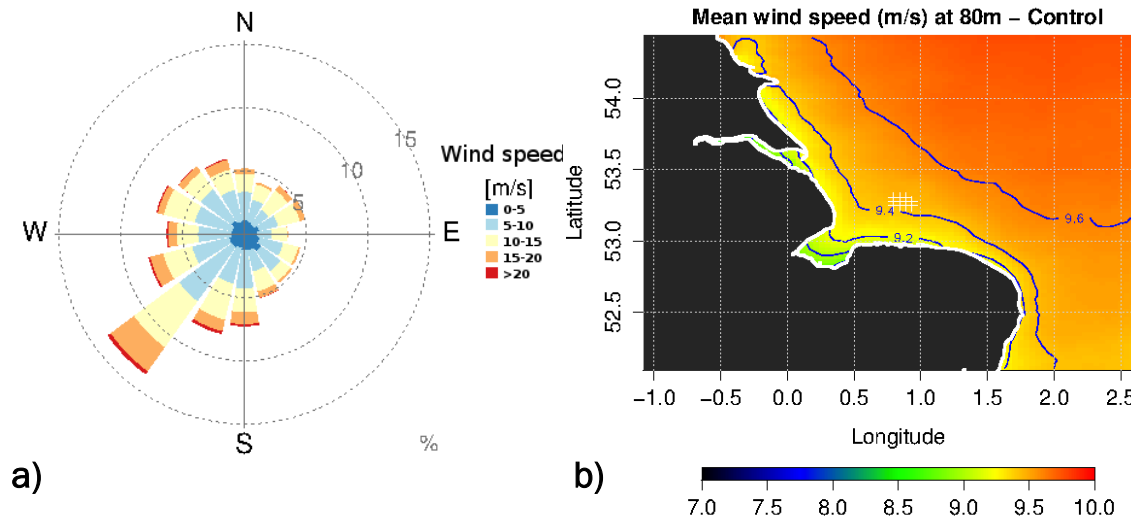*Deliverable 5.12 EERA DTOC calculation of scenarios*

the final results in a much faster way. The wind climates from all the simulations are calculated by averaging the hourly outputs from the entire simulated period.

J.4. Output/results

J.3.4 Mean wind speed

The average wind speed at the future Race Bank location is affected by the number of wind farms considered in each run. The unperturbed average wind speed at Race Bank wind farm is around 9.5 m/s with a slightly predominance of south westerly winds, illustrated by the wind rose at the center of the Race Bank wind farm (*Figure 29 a)*). The Race Bank wind farm is almost entirely surrounded by other wind farms and consequently, the average wind speed in its location is approximately 0.5 m/s lower when compared to the reference run.

Simulation 3 shows a decrease in the average wind speed created by the presence of neighbor wind farms at the Race Bank location. The sheer size of Dudgeon and Triton Knoll wind farms contributes to more pronounced wake effects in the future Race Bank wind farm location, but since the predominant wind sector is relatively free of wind farms the average wind speed deficits at the area of interest are lower than expected.
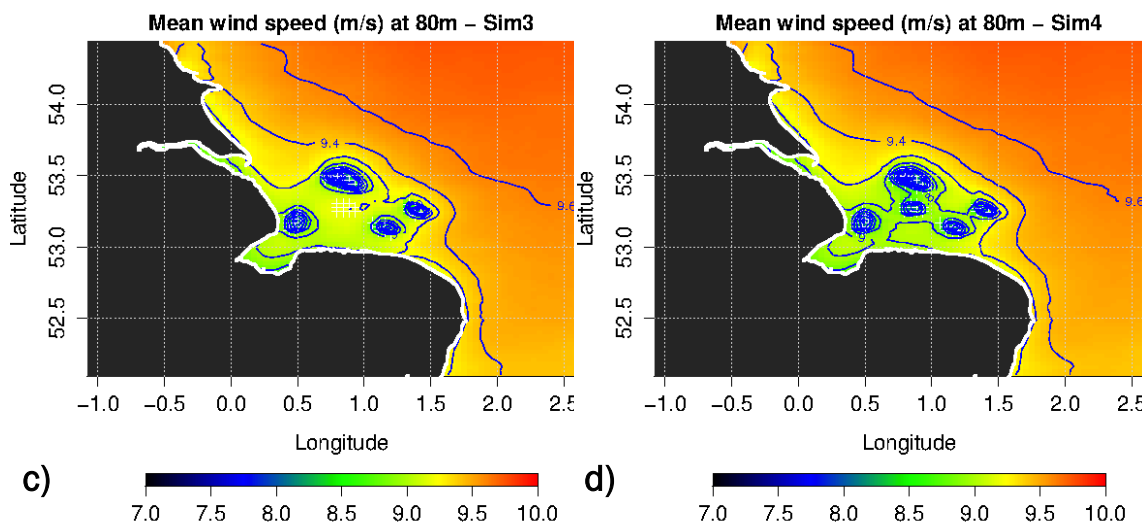
Deliverable 5.12 EERA DTOC calculation of scenarios

Mean wind speed (m/s) at 80m – Sim3 c)

Mean wind speed (m/s) at 80m – Sim4 d)

Figure 29: Control run wind rose (a) and mean wind speed: Control run (b), Sim 3 (c) and Sim 4 (d)

J.3.5 Mean wind speed deficit

An easier way to ascertain the impact of the far wake effects is to calculate the mean wind speed deficit percentage at the region of interest. The mean wind speed deficit is calculated by comparing the unperturbed state of the atmosphere with each of the WRF simulations.

$$Mean_{WsD} = \left(\frac{Ws_{Control} - Ws_{Wakes}}{Ws_{Control}} \right) * 100$$

Where $Ws_{Control}$ is the wind speed from the control run and Ws_{Wakes} is the wind speed from the WRF simulations using real wind turbine positions and specifications.

Figure 30 which could be a relatively accurate representation of the near future scenario, indicates that the impact from all the neighbor wind farms is noticeable and contributes to wind speed deficits around 2-4%.

One of the main reasons for the wind speed deficits not being more elevated is the absence of wind farms on the predominant wind direction sector. For the exactly same reason, in Sim.4 the wind speed deficit at Triton Knoll, originated by the presence of the Race Bank wind Farm could go up to 8%.
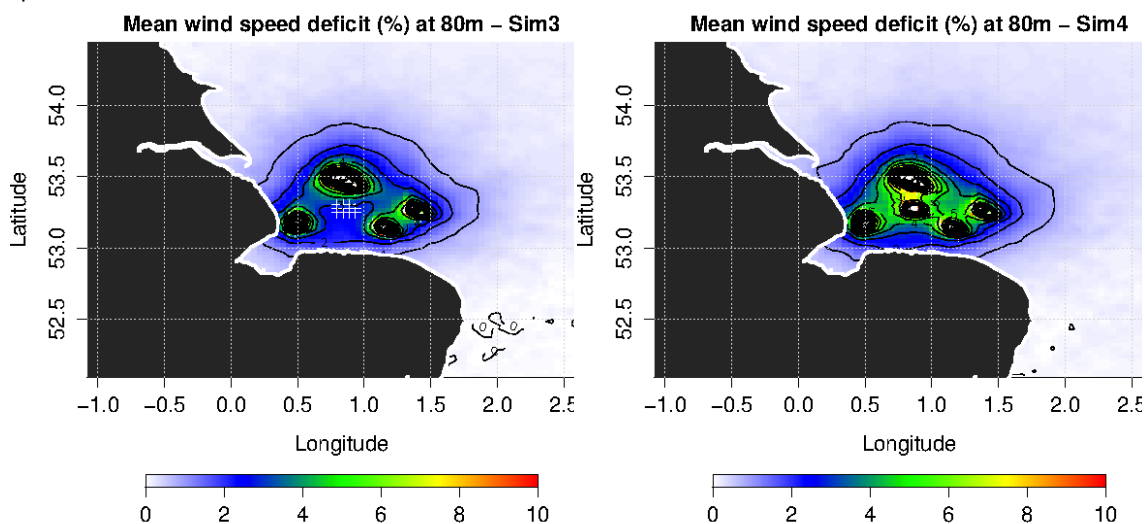

Mean wind speed deficit (%) at 80m – Sim3

Mean wind speed deficit (%) at 80m – Sim4

Figure 30: Mean wind speed deficit percentage: Sim 3 (left) and Sim 4 (right)

Deliverable 5.12 EERA DTOC calculation of scenarios

Depending on wind direction, wake losses at Race Bank could be very different. The outputs are divided in 16 sectors and analyzed in higher detail.

In Sim 3, the highest wake losses are created by Northerly winds. The Triton Knoll wind farm has a big impact on downstream wind speeds, contributing to wake losses around 10% (*Figure 31 a)*). Expected wakes losses around 3-6% are registered from the East (E), East-southeast (ESE) and West-southwest (WSW) sectors.
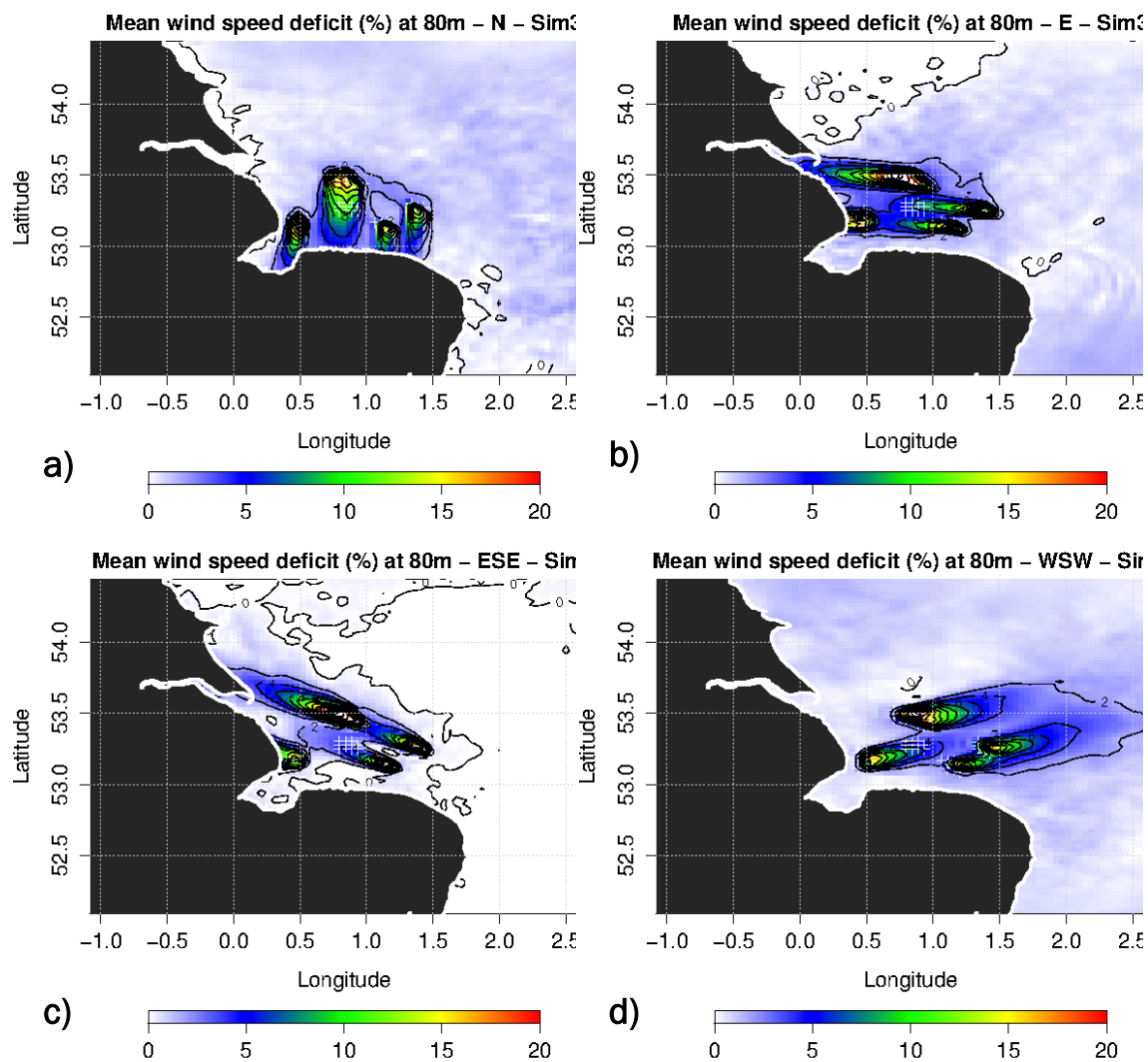

Figure 31: Mean wind speed deficit in selected sectors from Sim 3: N (a), E (b), ESE (c) and WSW (d).

J.5 Observations

J.5.1 Observations on results.

The work focused on the study of far war wake effects produced by neighbor wind farms in a given area of interest. The wake effects are simulated with the mesoscale model WRF, activating the wind farm parameterization included in its later versions. The parameterization, based on the Fitch scheme, is able to interpret real turbine positions, characteristics, power and thrust curves

Deliverable 5.12 EERA DTOC calculation of scenarios

and treat each turbine individually. It is a powerful tool when analyzing large areas with a high concentration of wind farms since it is possible to simulate the major interactions between single wind farms or clusters of wind farms.

Sim.3 shows that considering both Triton Knoll and Dudgeon wind farms will result in higher wake losses (4%) in the Race Bank wind farm. These losses are not higher due to the south West sector being free of wind farms, as was described before. Even thou, 4% average losses could translate into significant money losses.

After analyzing the results in each sector of direction, it was possible to see that, as expected, the sheer size of the Triton Knoll and Dudgeon wind farms are the main reason behind the expected wake losses at the Race Bank wind farm. Northerly winds originate wake losses of around 10% while Easterly wind wind could originate wake losses around 6%.

As a final conclusion, it seems that the mesoscale model provides a useful tool when studying far wake effects produced by single or clusters of wind farms. The main advantage is the capacity of the model to simulate the meteorological conditions of large areas and the possibility of including multiple wind farms with individual turbine information.

J.5.2 User experiences:

It is still very difficult to find real data (turbine positions and characteristics) from offshore wind farms. When analyzing large areas with several wind farms, owned by different clients, probably some assumptions will have to be made in order to generate all the necessary inputs to the mesoscale simulations. Due to the low resolutions used in this configuration, it is not expected that the final results would be greatly affected, but when possible it is highly recommended to use real turbine positions and characteristics.

Another difficulty is the lack of offshore measurements. In order to validate this methodology it would be extremely important to have wind measurements from a region affected by the construction of new wind farms in the vicinity. Time series of the unperturbed (previous to the construction) and perturbed (after construction) would be an invaluable asset in the model validation.

J.5.3 Expert judgment

This tool can be very helpful on predicting wind speed deficits provoked by existing or planned wind farms in the proximity of an area of interest. Due to the growing number and concentration of offshore wind farms in some areas, this aspect becomes extremely important.

By using mesoscale models to estimate possible wake losses, it is possible to simulate large areas and at the same time, obtain useful meteorological information that cannot be calculated by current microscale models (mesoscale phenomena, seasonal tendencies, low level sea breezes, etc). The output from the mesoscale simulation can also be used as an input to current microscale models, providing more detailed and robust wind characteristics in the region.

At this point, this configuration does not replace the use of current microscale wake models to obtain the wake effects inside a wind farm or to calculate the AEP of the wind farm. It should be used as a complement to current microscale wake models.

Bibliography

Barthelmie, R. J., et al. *Flow and wakes in large wind farms: Final report for UpWind WP8.* Roskilde, Denmark: Risoe, 2011.

Chavez-Arroyo, R., Amezcua, J., Fernandes-Correia, P., Lozano-Galiana, S., Probst, O., Sanz-Rodrigo, J. "A novel approach to statistical dynamical downscaling for long-term wind resource predictions." *Applied Thermal Engineering*, no. In Press (2015).

Dudhia, F. Chen and J. "Coupling and advanced land surface-hydrology model with the Penn State-NCAR MM5 modeling system. Part I: model implementation and sensitivity." *Monthly Weather Review* 129 (2001): 569–585.

Dudhia, J. "Numerical study of convection observed during the winter monsoon experiment using a mesoscale two-dimensional model." *Journal of the atmospheric sciences* 46, no. 3077-3107 (1989).

Deliverable 5.12 EERA DTOC calculation of scenarios

EERA. EERA Design Tools for Offshore Wind Farm Cluster - Annex I - "Description of Work". September 13, 2011.

Endegnanew, A. G., H. Svendsen, R. E. Torres-Olguin, and L. M. Faiella. *Design procedure for inter-array electric design (D2.2).* EERA-DTOC, 2013.

ENTSO-E. Network Code for Requirements for Grid Connection Applicable to all Generators. June 2012.

ENTSO-E. Operational Reserve Ad Hoc Team Report - Final Version. Brussels, May 23, 2012.

EURELECTRIC. *Ancillary Services. Unbundling Electricity Products – an Emerging Market.* Brussels, Belgium: EURELECTRIC Thermal Working Group, 2004.

Ferguson, Ana, Phil de Villiers, Brendan Fitzgerald, and Jan Matthiessen. Benerfits in Moving the Inter-array Voltage from 33 kV to 66 kV AC for large offshore wind farms. CarbonTrust, 2012.

Fitch, A. C. et al. "Local Mesoscale Impacts of Wind Farms as Parameterized in a Mesoscale NWP model." *Monthly Weather Review*, 2012.

Forewind. Dogger Bank Teeside - Teesside Offshore Cable Corridor Selection Report. Reading, UK: Forewind, 2012.

—. "Forewind - Dogger Bank." *Forewind Website.* 2011. http://www.forewind.co.uk/dogger-bank/overview.html (accessed 04 29, 2013).

—. "Forewind Fact Sheet - April 2013." *Forewind.* 04 2013. http://www.forewind.co.uk/uploads/files/10898_FOR_Gen_Factsheet_v7_Hires.pdf (accessed 04 29, 2013).

Fritsch, J. S. Kain and J. M. "A one-dimensional entraining/detraining plume model and its application in convective parameterization." *Journal of the Atmospheric Sciences* 47 (1990): 2784–2802.

Hong, S.-Y., Dudhia, J. and Chen, S.-H. "A revised approach to ice microphysical processes for the bulk parameterization of clouds and precipitation." *Monthly Weather Review* 132 (2004): 103-120.

Margaris, I. D., A. D. Hansen, J. Bech, B. Andresen, and P. Sørensen. "Implementation of IEC Standard Models for Power System Stability Studies." *Proceedings of 11th International Workshop on Large-Scale Integration of Wind Power into Power Systems.* Lisbon, Portugal, 2012.

Mlawer, E. J., Taubman, S. J., Brown, P. D., Iacono, M. J. and Clough, S. A. "Radiative transfer for inhomogeneous atmospheres: RRTM, a validated correlated-k model for the." *Journal of Geophysical Research* 102, no. 16663-16682. (1997).

Nakanishi, M. and Niino, H. "An improved Mellor-Yamada level- 3 model with condensation physics: its design and verification." *Boundary-Layer Meteorology* 112 (2004): 1-31.

Skamarock, W. C., Klemp, J.B., Dudhia, J., Gill, D. O. , Barker, D. M., Duda, M. G., Huang, X. Y., Wang, W., Powers, J. G. "A description of the advanced research WRF version 3." *NCAR technical note TN-475+STR*, 2008: 113pp.

Stuart, P. User Requirement workshop - EERA-DTOC Deliverable. EERA, 2012.

Svendsen, H. G. "Planning Tool for Clustering and Optimised Grid Connection of O." *Energy Procedia*, 2013.

The Crown Estate. "The Crown Estate - About Us." *The Crown Estate.* 2013. http://www.thecrownestate.co.uk/about-us/ (accessed 4 29, 2013).

—. "The Crown Estate - Round 3 wind farms." *The Crown Estate.* 2013. http://www.thecrownestate.co.uk/energy-infrastructure/offshore-wind-energy/our-portfolio/round-3-wind-farms/ (accessed 4 29, 2013).

Deliverable 5.12 EERA DTOC calculation of scenarios

16. APPENDIX K: CIEMAT: NEAR FUTURE SCENARIO – NET ENERGY YIELD (OFF-LINE)

K.1 Objective/user story

K.1.1 Objective
The increase in computational power reached during the last decades allows for the use of mesoscale models to reach very high horizontal resolutions. The advantage of using mesoscale models is that the simulation of the wind farm conditions can be accomplished in a real environment using initial and boundary conditions from data bases such as the reanalysis ones, for example. In addition, the large size of the area over which the atmospheric evolution is simulated, allows for the inspection of the characteristics of the wind farm wakes.

The use of mesoscale modeling to reproduce the power deficits associated with wind turbine wakes in an offshore environment has already been analyzed in different cases. In particular, CIEMAT has been working with the Weather Research and Forecasting (WRF) mesoscale model (1) for many years and presented a comprehensive evaluation of this mesoscale model ability to reproduce the effects of wind turbine wakes at the wind farm scale (2).

The effects of the wind farm in the atmosphere are simulated assuming that the turbines constitute an elevated momentum sink and a source of turbulent kinetic energy (3, 4).

In this particular case, the main objective is to show the performance of the WRF model to simulate the average power and the annual net energy yield at each point of the cluster constituting the Near Future Scenario (Dogger Bank projects) as well as the total net energy yield of the reference wind farm (Creyke Beck A), for different layouts, varying the spacing between the wind turbines.

K.1.2 User story and scenario
Near future scenario

User Story	Yes/No
1.1 As strategic planner or developer I can determine the wake impact of individual wind farms within a cluster on each other (just meso)	Yes
1.2 As a strategic planner I can determine the net energy yield of offshore wind farm clusters.	No *
1.3 As a strategic planner I can determine the optimum size, spacing and position offshore wind farm clusters.	No
2.1 As a strategic planner I can determine the optimum strategic infrastructure to accommodate offshore wind farm clusters.	No
3.1 As a developer I can determine the wake effects of neighbouring wind farm clusters on a single wind farm (meso and/or micro).	Yes
3.2 As a developer I can determine the wake effects due to turbines within a wind farm.	Yes
3.3 As a developer I can determine the net energy yield of a wind farm.	Yes
3.4 As a developer I can determine the optimum spacing, position, turbine model and hub height of turbines within an offshore wind farm.	No
3.5 As a developer, I want to use wind farm layout scenarios of my target wind farm with respect to nr of turbines, turbine types, power and thrust curves etc.	No

Deliverable 5.12 EERA DTOC calculation of scenarios

*In this case the net energy yield for the cluster was not determined, but it could be determined using this method

K.2 Codes

The model used is the Weather Research and Forecasting model (WRF; 1). It is a numerical weather prediction (NWP) and atmospheric simulation system designed for both research and operational applications.

This model has been used to downscale the outputs (ERA-Interim reanalysis data, http://www.ecmwf.int/en/research/climate-reanalysis/era-interim) provided by the ECMWF (the European Center for Medium-Range Weather Forecasts, http://www.ecmwf.int/) in a domain that covers a large area, centered at the North Sea (fig.1).

The WRF model (version 3.4) (1) has been configured using a total of four two-way domains interacting with a three to one spatial refinement in order to reach a horizontal resolution of 1km in the innermost domain that comprises the Dogger Bank area (Figure 1). A total of 36 vertical levels were prescribed, five of them within the first 200 m of the atmosphere.

A number of subgrid scale processes are parameterized by WRF. The shortwave and longwave radiation schemes follow the works by Dudhia (5) and Mlawer *et al.*(6) respectively. Microphysical processes are represented with the WRF singlemoment six class scheme (7), whereas the cumulus effects are parameterized only in the outermost three domains (8 y 9). The air–sea momentum flux is parameterized following the work by Charnock (10). The effects of the turbulent vertical mixing within the planetary boundary layer are parameterized using a 1.5 order scheme that predicts the turbulent kinetic energy (11) and advects it with the wind. The scheme is based on the work by Mellor and Yamada (12) but includes a better formulation of buoyancy effects and a master length scale that depends on atmospheric stability.

The effects of the wind turbines over the atmospheric flow are parameterized following the work by Fitch *et al*. (3&4). The wind turbines are represented as an elevated sink of momentum and a source of turbulent kinetic energy that responds to the wind speed according to a specified function approximating the effects of the turning rotors on the flow.

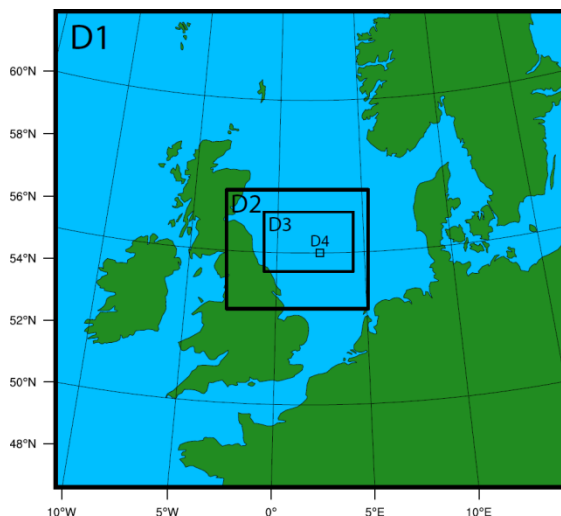The outputs are hourly data for the whole year 2013.

Figure 32: The four domains used in the WRF simulation with 27, 9, 3 and 1km of horizontal resolution. The number of points of each domain (west-east by north-south) is 70x65, 58x49, 19x19, and 100x67, respectively.

Deliverable 5.12 EERA DTOC calculation of scenarios

K.3 Input

K.3.1 Description of wind farm

The near future scenario is connected to (aspects of) the plans for an off-shore cluster at Dogger Bank. As explained in D5.2 it starts with a 1GW wind farm consisting of 100 turbines with a rated power of 10 MW using the well documented INNWIND.EU reference turbine. The farm is assumed to be located at the southern part of the Dogger Bank area and it is surrounded by other wind farms similar to the planned situation for Dogger Bank of figure 2.

The wind farm layout is given in Figure 1. It is based on the layout of the Horns Rev wind farm the only difference lies in the fact that Horns-Rev considers 10x8 wind farms where the present wind farm lay-out has been modified to 10x10 wind turbines. One main 'wind farm line' is oriented in the East-West direction and the other main wind farm line slightly skewed compared to the North-South direction. Distances between the turbines along the main wind farm lines are 5.1 rotor diameters.
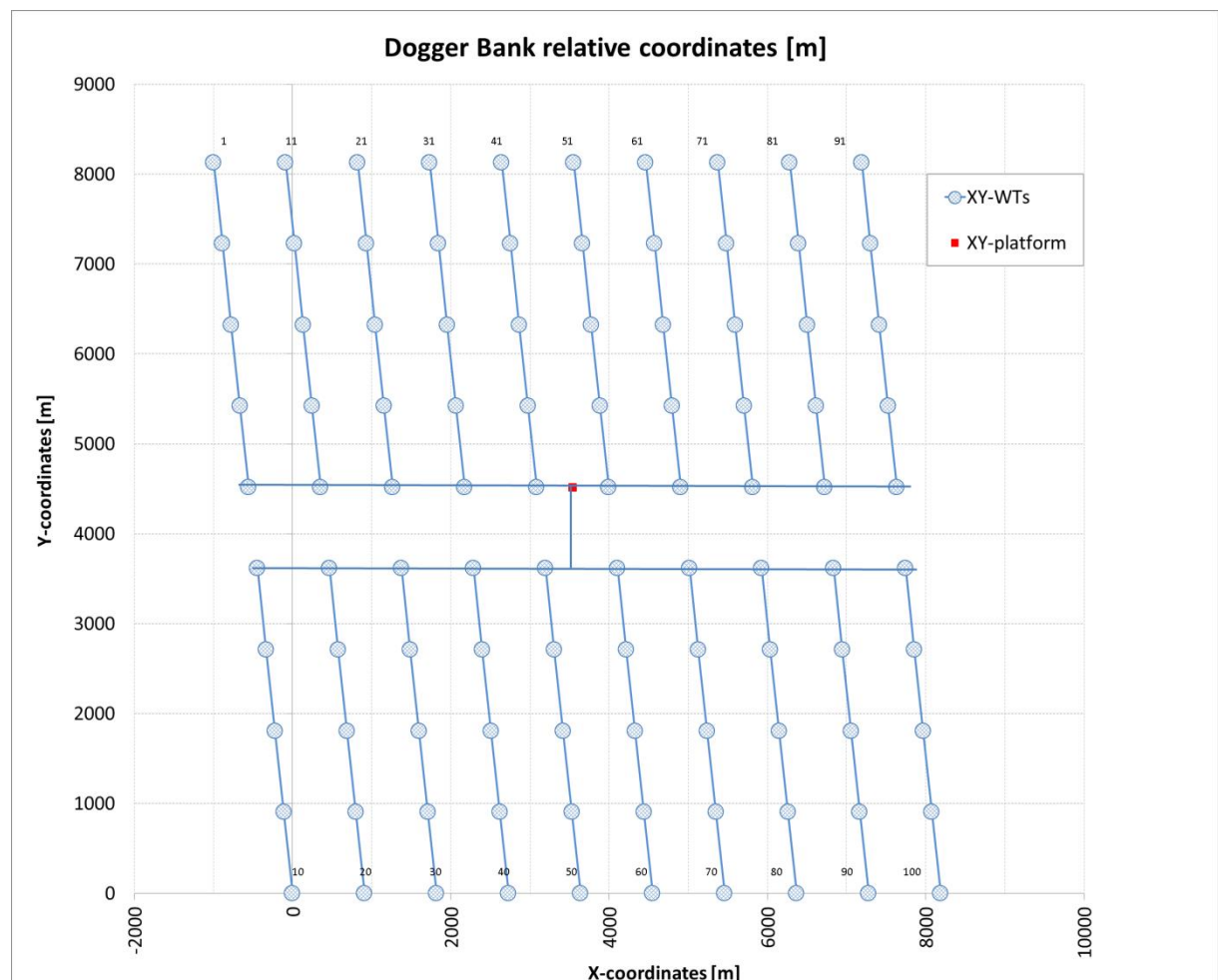

Figure 33: Layout of wind farm

K.3.2 Description of turbines:

Deliverable 5.12 EERA DTOC calculation of scenarios

For the near future scenario a 10 MW turbine is selected. Such turbines are not on the market yet. As explained in D5.2 the INNWIND.EU reference turbine is proposed since the data of this turbine are already made publicly available by DTU. The main characteristics of this turbine are:

- Rated power: 10 MW
- Rotor diameter: 178.3 m
- Hub height: 119 m
- Wind class: IEC class Ia
- Regulation: Variable speed, collective pitch
- Orientation of rotor: Upwind, overhang 7.1 meter
- Cut in wind speed: 4 m/s
- Rated wind speed 11.4 m/s
- Cut-out wind speed 25 m/s
- Minimum rotor speed 6 rpm
- Maximum rotor speed: 9.6 rpm (maximum tip speed: 90 m/s)
- Gearbox: Medium speed, Multiple stage generator

A detailed description on the turbine including a power curve and C Dax curve as needed in many wake models can be found at: http://dtu-10mw-rwt.vindenergi.dtu.dk/

K.3.3 Description of the Dogger Bank projects
The near future farm is located at the Dogger Bank East of North England in relatively shallow waters (18 to 63 meters), see figure 3. Dogger Bank is part of the UK Crown Estate Round 3 area (8,660 km 2 , the largest of the Round 3 zones) with distances between 125 and 290 kilometers off the east coast of Yorkshire, UK.
The development consortium Forewind has defined several projects, each divided in phases of 1.2 MW: Creyke Beck A and B, Teesside A and B (where Teesside C and D are planned for a later stage). The whole estimated capacity of Dogger Bank could add up to 9GW,
Figure 3 shows approximate locations of Creyke Beck A and B and Teesside A and B projects. The 1GW wind farm under consideration is be located at the Creyke Beck A site, which is the most Southerly project from figure 3, 131 km from the shore at its closest point. The surrounding farms are given by the above mentioned projects: Creyke Beck B is located in North from the Creyke Beck A site, also 131 km from the shore at its closest point. Teesside A is furthest away from the shore with a closest point from shore at 196km and Teesside B is 165 km from shore. These farms have a 1GW capacity as well with a similar layout as suggested for the Creyke Beck A farm.
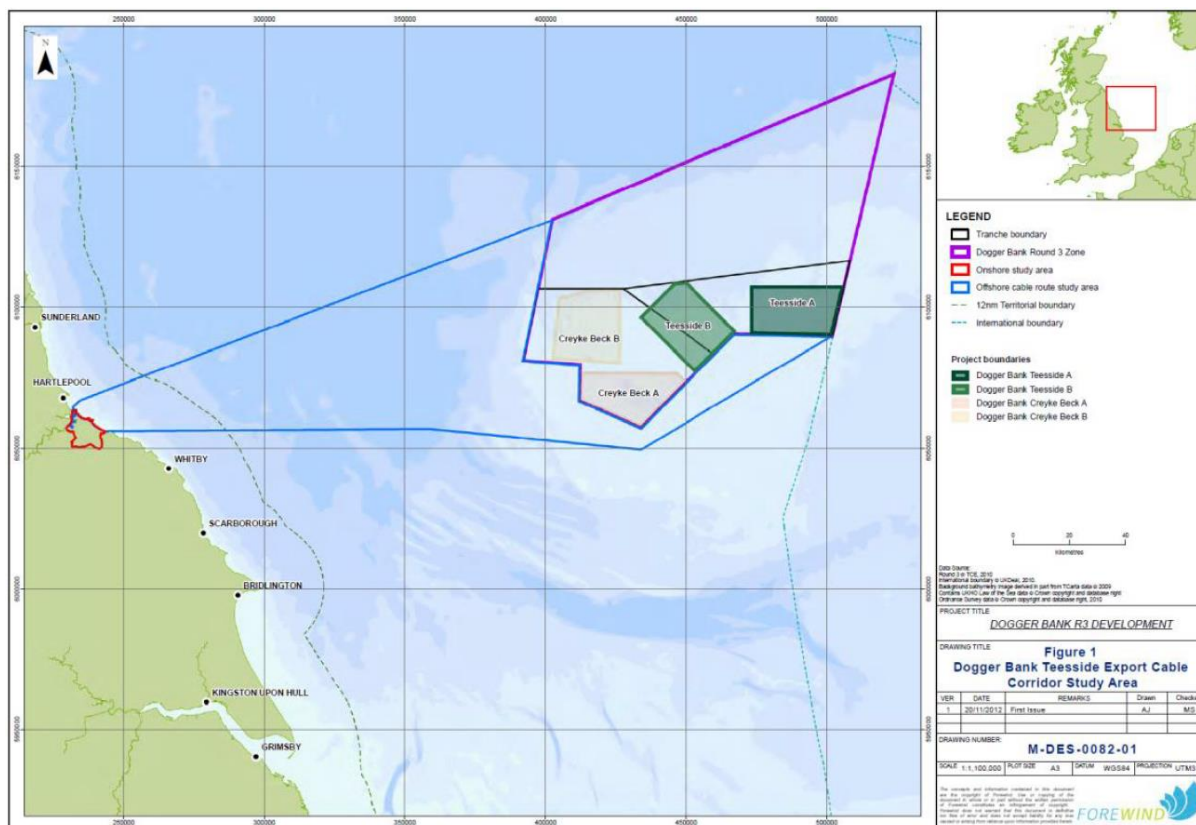
Deliverable 5.12 EERA DTOC calculation of scenarios

Figure 34: Location of Dogger Bank projects

K.4 Output/results

Since the main goal is to determine the net energy yield for the reference wind farm (Creyke Beck A) within the Dogger Bank Projects, for different spacing between the wind turbines (10, 7.3, 5.1 and 3.85 diameters) , the WRF model has been run for the year 2013, using the information about the wind turbine description (section F.3).

The WRF model (version 3.4) (1) has been configured using a total of four two-way domains interacting with a three to one spatial refinement in order to reach a horizontal resolution of 1km in the innermost domain that comprises the Dogger Bank area (Figure 1). A total of 36 vertical levels were prescribed, five of them within the first 200 m of the atmosphere.

The WRF outputs give the hourly average wind power (among many other variables) for each cell of the different domains, for the complete year 2013. With these values, the annual net energy yield was calculated for every cell.

Figures 4 to 6 are an example to see the refinement in the calculations of the energy per cell when downscaling from the domain 2 (9km resolution) to the domain 4 (1km resolution). The case for inter-turbine spacing of 5.1 rotor diameters has been chosen because it corresponds to the layout showed in figure 2. The "x" in the figures show the wind turbines position.
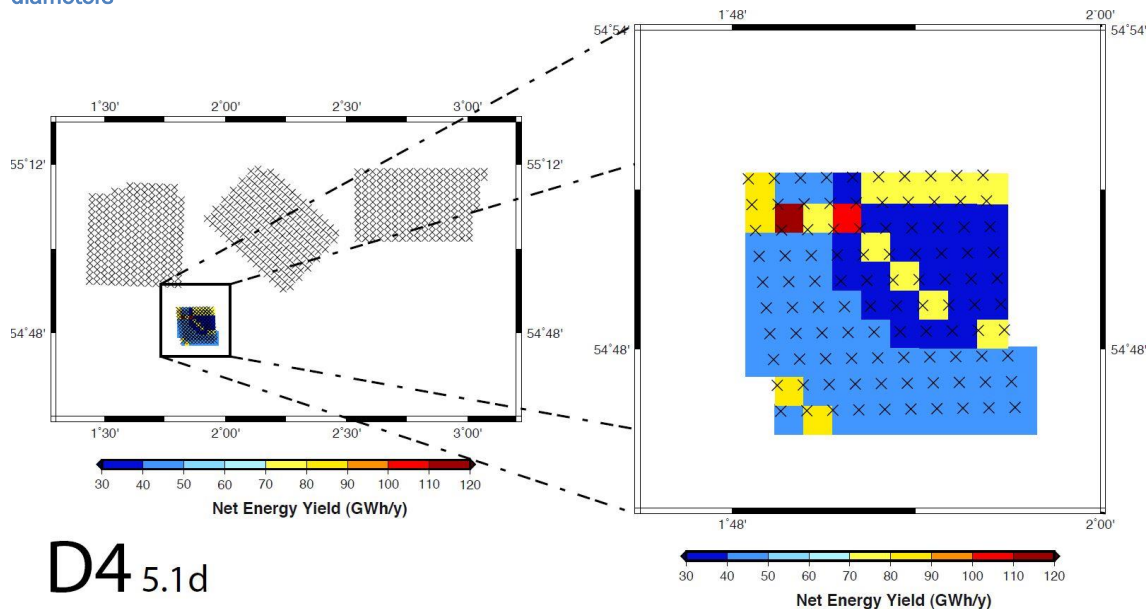
Deliverable 5.12 EERA DTOC calculation of scenarios
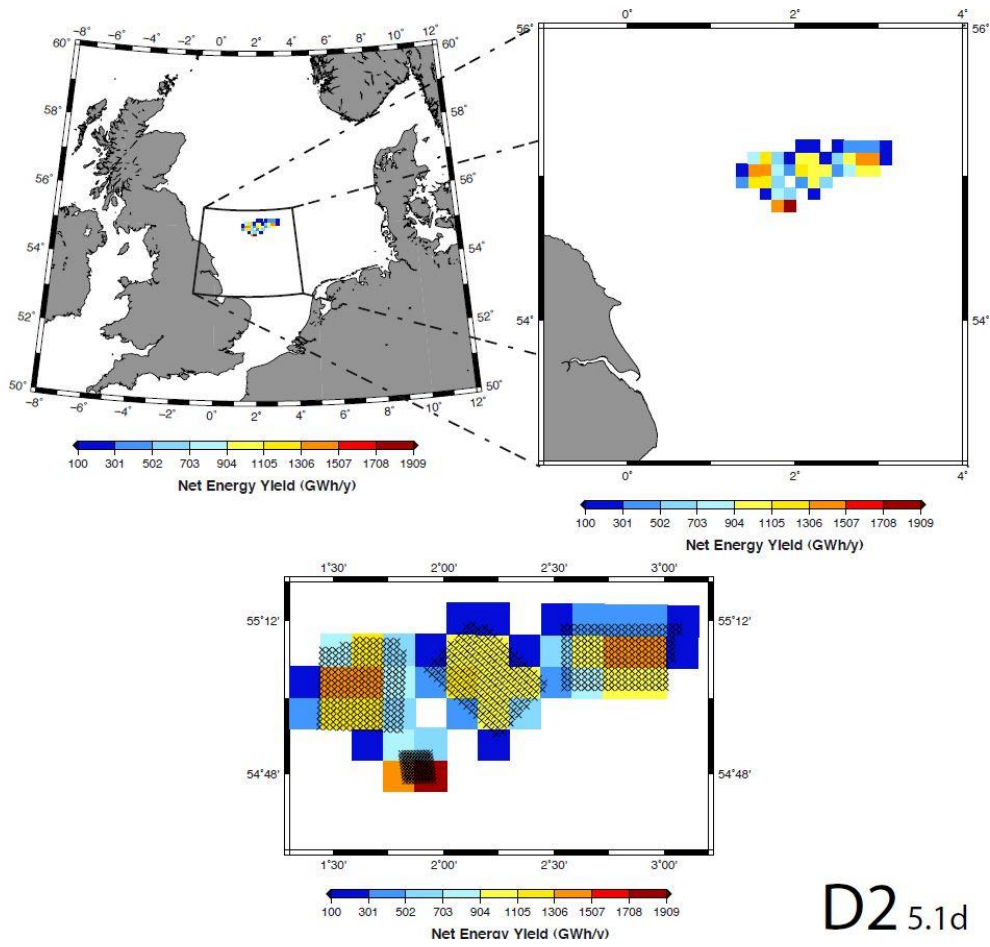
Figure 4: WRF output for the domain 2 (9km resolution) for the case with inter-turbine spacing of 5.1 rotor diameters

Deliverable 5.12 EERA DTOC calculation of scenarios
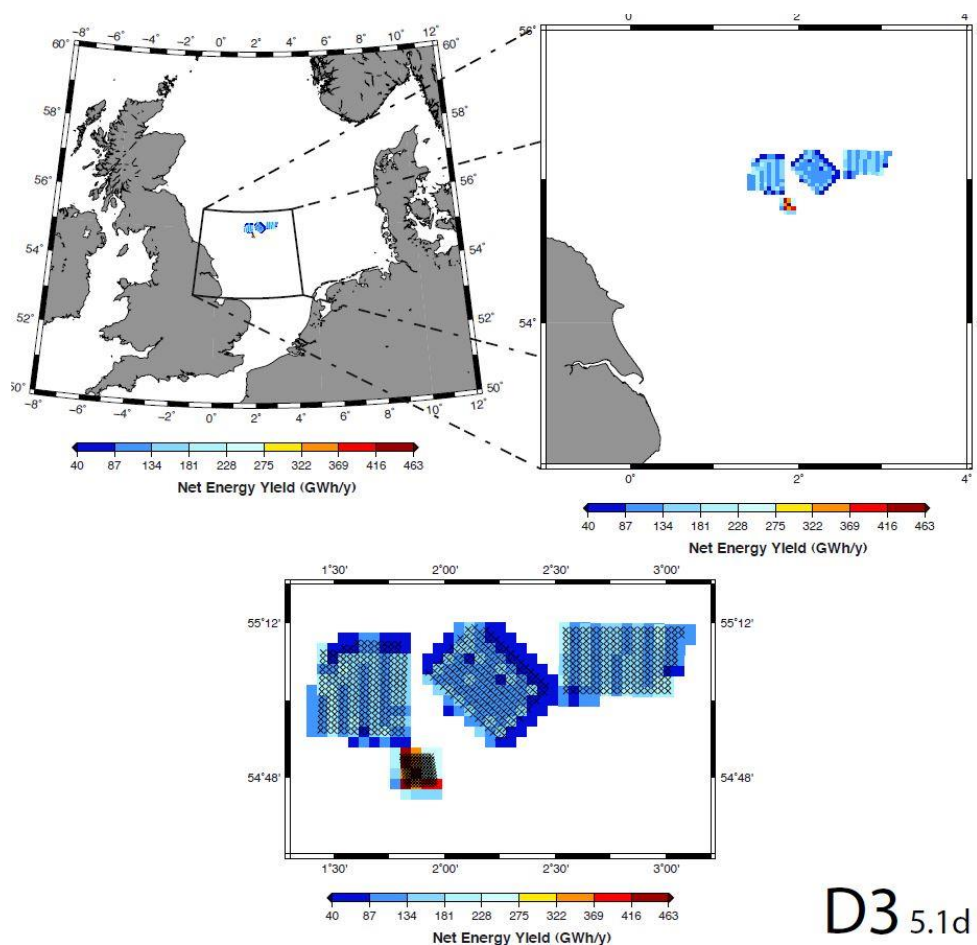
Figure 4: WRF output for the domain 3 (3km resolution) for the case with inter-turbine spacing of 5.1 rotor diameters
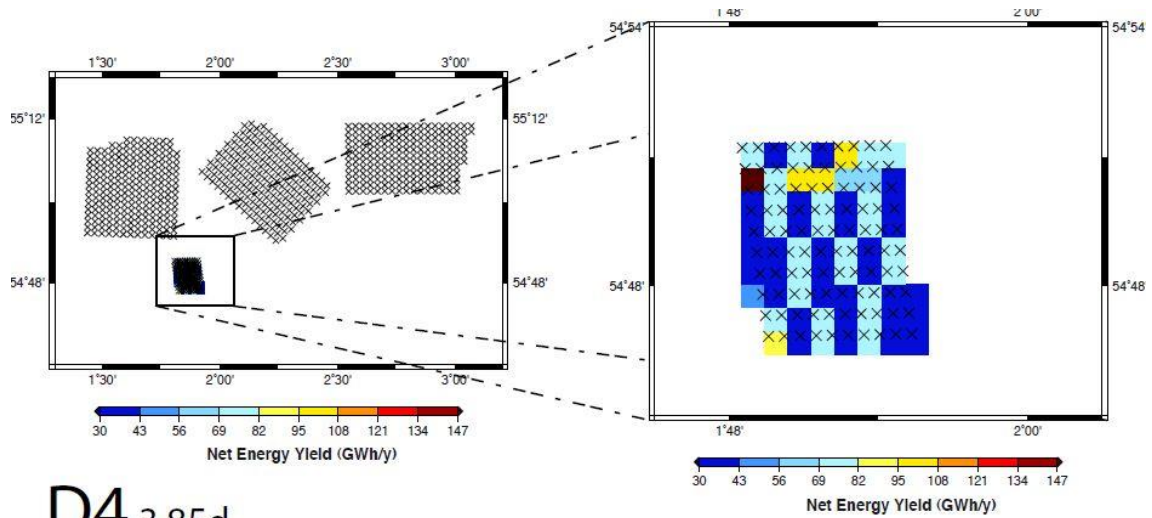

Figure 4: WRF output for the domain 4 (1km resolution) for the case with inter-turbine spacing of 5.1 rotor diameters

The outputs for other inter-turbine spacing (7.3 and 3.85 rotor diameters) are shown in figures 5 and 6.

Deliverable 5.12 EERA DTOC calculation of scenarios
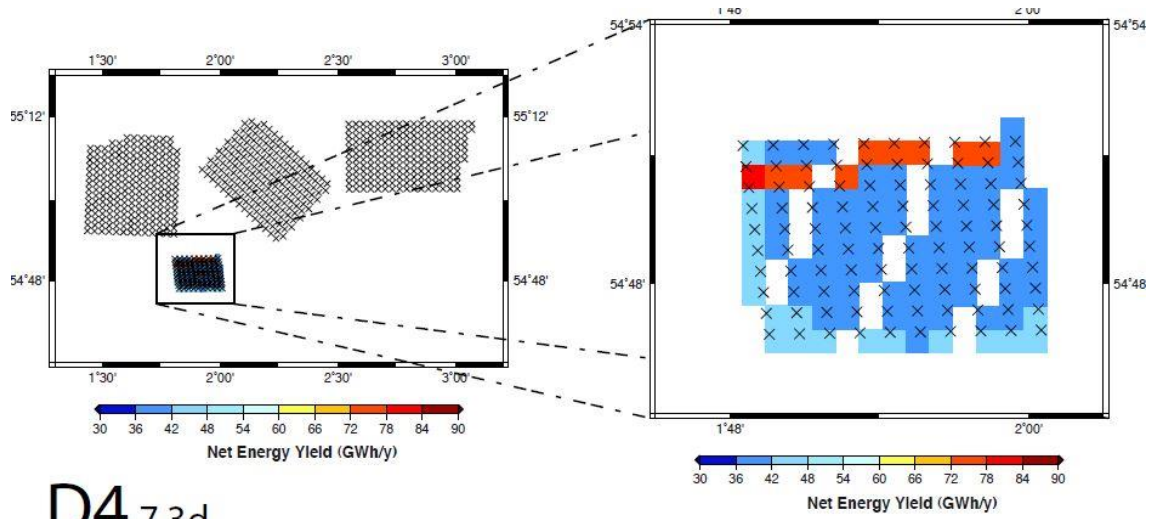
Figure 5: WRF output for the domain 4 (1km resolution) for the case with inter-turbine spacing of 7.3 rotor diameters

Figure 6: WRF output for the domain 4 (1km resolution) for the case with inter-turbine spacing of 3.85 rotor diameters

The final net energy yield for the whole wind farm (Creyke Beck A) for the year 2013, and for the different inter-turbine spacing (10, 7.3, 5.1 and 3.85 diameters) is 4240.23, 4000.15, 3837,40 and 3700,76 GWh/y, respectively.

K.5 Observations

K.5.1 Observations on results.

Deliverable 5.12 EERA DTOC calculation of scenarios

Since the fourth domain resolution is 1km and the rotor diameter is 178m., the differences among the above figures are mainly due to the fact that in some cases there are one or more wind turbines ("x") within a cell and in other cases, there is not any wind turbine in a cell (blank).

Although it would have been desirable to reach a higher resolution (in fact, the current work in these cases is focused in reaching a resolution of 333m), the above figures can give us a first idea of the influence of varying the inter-turbine spacing.

Although the difference on the annual net energy yield when changing the inter-turbine spacing does not seem to be remarkable, it is important to deepen this topic, as well as the effect of other kind of wind farm lay-outs on the net energy yield.

K.5.2 User experiences

N.r. the calculations are run off-line

K.5.3 Expert judgment

The use of the Wheather Research and Forecasting (WRF) mesoscale model (1) and the model ability to reproduce the effects of wind turbine wakes at the wind farm scale (3) seems to be appropriate to study the wake effect between different wind farms within a cluster as well as the inter turbine wakes within a wind farm (2), making it possible to simulate large areas and taking into account the actual meteorological inputs that are not accounted for, in the case of the micoscale models.

In this particular case, the main objective was to show the performance of the WRF model to simulate the average power and the annual net energy yield at each point of the cluster constituting the Near Future Scenario (Dogger Bank projects) as well as the total net energy yield of the reference wind farm (Creyke Beck A), for different layouts, varying the spacing between the wind turbines.

Although the results show the differences between the cases and the importance of the domains refinement for each case, the experts think that it is worth to go deeper by reaching higher resolution (e.g. 333m), in order to improve the analysis of the inter- turbine wakes within a windfarm, as it was performed in other analysis within the EERA-DTOC project, either increasing the resolution in the WRF Wind Farm Parameterization itself (2) or combining the WRF outputs with a Wind Farm model, like the UPM Park (13 and 14).

K.5 References

1. Skamarock WC, Klemp JB, Dudhia J, Gill DO, Barker DM, Duda M, Huang XY, Wang W, Powers JG. A description of the advanced research WRF version 3. Technical Report TN-475+STR, NCAR, 2008. [WRF is a community model provided by the National Center for Atmospheric Research, Boulder CO, sponsored by the National Science Foundation].

2. Jiménez, P.A. , Navarro, J., Palomares, A.M., Dudia, J. . Mesoscale modeling of offshore wind turbine wakes at the wind farm resolving resolving scale. Wind Enegy 2014 DOI: 10.1002/we.1708

3. Fitch AC, Olson JB, Lundquist JK, Dudhia J, Gupta AK, Michalakes J, Barstad I. Local and mesoscale impacts of wind farms as parameterized in a mesoscale NWP model. Monthly Weather Review 2012; 140: 3017–3038.

4 Fitch AC, Lundquist JK, Olson JB. Mesoscale influences of wind farms throughout a diurnal cycle. Monthly Weather Review 2013; 141: 2173–2198.

5. Dudhia J. Numerical study of convection observed during the winter monsoon experiment using a mesoscale two-dimensional model. Journal of Atmospheric Sciences 1989; 46: 3077–3107.

Deliverable 5.12 EERA DTOC calculation of scenarios

6. Mlawer EJ, Taubman SJ, Brown PD, Iacono MJ, Clough SA. Radiative transfer for inhomogeneous atmospheres: RRTM, a validated correlated-k model for the longwave. Journal of Geophysical Research 1997; 102: 16663–16682.

7. Hong SY, Noh Y, Dudhia J. A new vertical diffusion package with an explicit treatment of entrainment processes. Monthly Weather Review 2006; 134: 2318–2341.

8. Kain JS, Fritsch JM. A one-dimensional entraining/detraining plume model and its application in convective parameterization. Journal of Atmospheric Sciences 1990; 47: 2784–2802.

9. Kain JS, Fritsch JM. Convective Parameterization for Mesoscale Models: The Kain-Fritcsh Scheme. The Representation of Cumulus Convection in Numerical Models, Meteor. Monogr., No. 24. American Meteorological Society: Boston, 1993. pp. 165–170.

10. Charnock H.Wind stress on a water surface. Quarterly Journal of the Royal Meteorological Society 1955; 81: 639–640.

11. Nakanishi M, Niino H. Development of an improved turbulence closure model for the atmospheric boundary layer. Journal of the Meteorological Society of Japan 2009; 87: 895–912.

12. Mellor GL, Yamada T. Development of a turbulence closure model for geophysical fluid problems. Reviews of Geophysics and Space Physics 1982; 20: 851–875.

13. Crespo, A., Hernández, J. (1989). "Numerical modelling of the flow field in a wind turbine wake": Proceedings of the 3rd Joint ASCE/ASME Mechanics Conference, Forum on Turbulent Flows. ASME, FED-vol. 76, La Jolla, CA, USA, 1989. p. 121–7.

14. Hansen, K.S., Réthoré, P.-E., Palma; J., Hevia, B., Prospathopoulos, J., Peña, A., Ott, S., Schepers, G., Palomares, A., van der Laan, M.P., Volker, P. (2015) Simulation of wake effects between two wind farms. *Journal of Physics: Conference Series, Visby Wake Conference 2015*, vol. 625, Gotland, Sweden, 9-11 June 2015

Deliverable 5.12 EERA DTOC calculation of scenarios

L.1 Objective/user story

L.1.1 Objective

The objective of this far future scenario analysis was to address user story 2.1 using the Net-Op tool.

LI.1.2 User story and scenario

Scenario: Far future scenario
User story:
2.1 As a strategic planner I can determine the optimum strategic infrastructure to accommodate offshore wind farm clusters.

L.2 Codes

The code used in this analysis is NET-OP.
At the time of analysis, the model was not included in the web portal, so the analysis is based on offline computations, but using the to-be-implemented command-line single executive version of the program.

L.3 Input:

L.3.1 Description of wind farm

The far future scenario is described in deliverable D5.7 "EERA DTOC far future scenario". It considers three new wind farms in a post-2030 situation with a pre-existing offshore grid in the North Sea, see Figure 35.

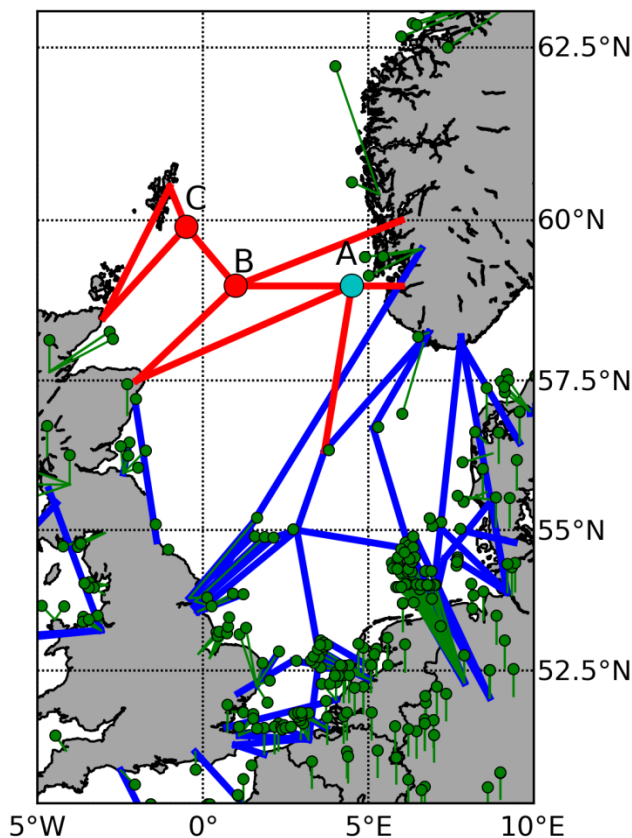*Deliverable 5.12 EERA DTOC calculation of scenarios*

Figure 35: Far future scenario overview. Three wind farm clusters A,B, and C are considered, with a presumed pre-existing offshore grid shown in blue, and potential new connections in red.

The three considered wind farms, denoted A, B and C are each 1200 MW.

L.3.2 Description of turbines:

Turbines are not represented directly. The input used is power production timeseries, which have been generated from the Reanalysis numerical weather model for the year 2012 for the given locations. Smoothed power curves representing an entire offshore wind farm has been assumed, see Figure 36.
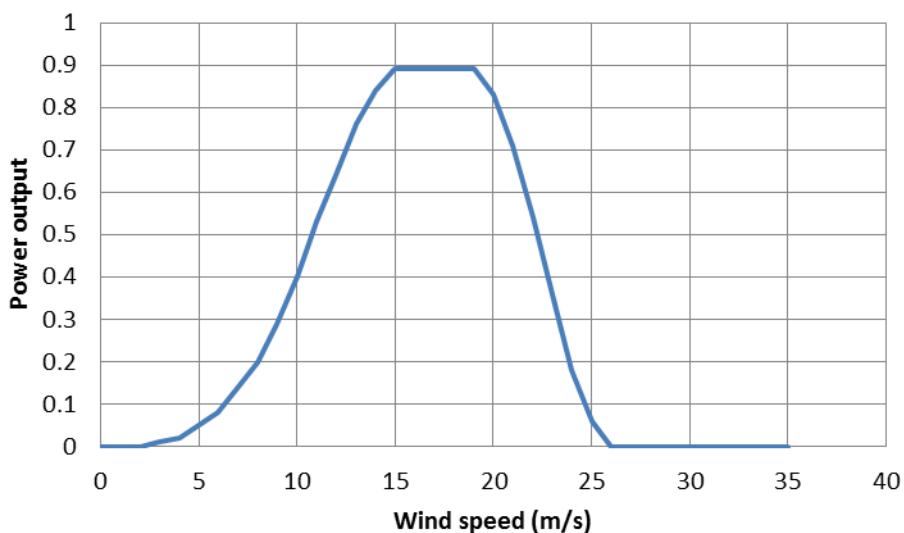
Deliverable 5.12 EERA DTOC calculation of scenarios

Figure 36: Smoothed power curve representing offshore wind farm. Vertical axis shows power output relative to installed capacity.

L.3.3 Description of wind climate

For this analysis the wind climate was based on Reanalysis numerical weather model data, generated following the procedure from the European TradeWind project. A time-series for 2012 was created with hourly resolution.

Since correlations between wind generation at other locations, both offshore and onshore are important for determining the benefit of offshore grid connections, time-series for other locations were also included. For Germany, also a time series for solar power generation was included for this reason. See Figure 37.
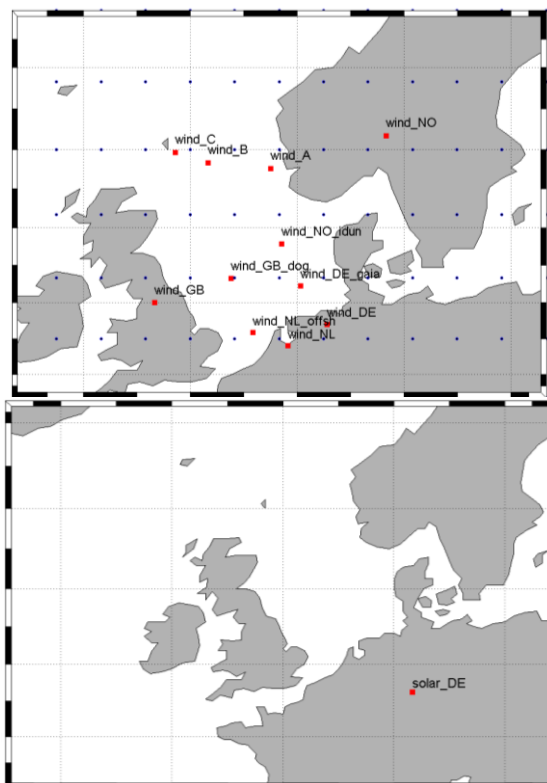

Figure 37: Points for which wind (left) and solar (right) power time series were generated.

Deliverable 5.12 EERA DTOC calculation of scenarios

L.3.4 Remarks.

Net-Op optimizes the offshore grid based on an overall socio-economic benefit, i.e. by minimizing the system cost of energy production and transmission. Therefore, not only wind, but also other generation alternatives and demand are important. As noted above, time-series for wind correlated with the time-series for wind was included. Power demand time-series with daily and seasonal variations were also included.

The annual power demand and generation capacity and price per generation type is based on the OffshoreGrid project 2030 scenario, and shown in Table 10.

Table 10: Demand and generation capacity and price

	UK	DE	NL	NO	
Demand (TWh)	436	632	139	152	
Capacity (GW)					Price (€/MWh)
Coal	15.21	42.70	8.53		62
Gas	42.60	38.19	11.51	0.93	69
Oil	2.62	10.03	1.65	0.10	162
Nuclear	12.64		1.11		11
Biofuel	8.01		2.62	0.90	50
Hydro	1.55	4.69	0.04	29.97	50
Solar		33.29			0
Wind	58.32	73.25	18.12	15.45	0

Wind farms/clusters A, B and C come in addition to this capacity.

L.4. Output/results

Results from the Net-Op pre-processing and optimisation is shown in Figure 38 and Figure 39. Regarding the A (101), B (102), C (103) wind farms, the optimal solution found is one using multi-terminal DC grid interconnecting the B and C wind farms with each other and to onshore connection points in both Norway and the UK. No connection to Shetland is included despite its proximity to wind farm C. Wind farm A is connected to the same point in Norway and also to the offshore grid in the southern parts of the North Sea.

Some detailed results in table format for cables is shown in Table 11. It shows number of new cables, new total capacity on connections and the mean power flow in both direction.

86 | P a g e

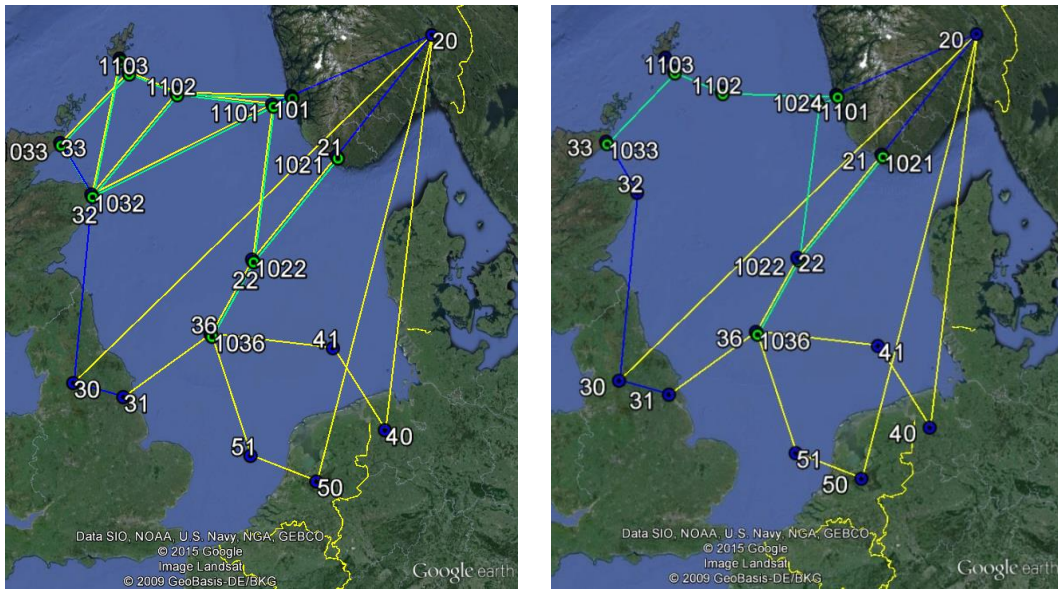*Deliverable 5.12 EERA DTOC calculation of scenarios*

Figure 38: Net-Op results. Left: Connections alternatives considered in the optimisation. Right: Optimal solution. Blue=AC connections, yellow=point-to-point DC, green=multi-terminal DC system

Figure 39: Detailed results. 101=wind cluster A, 102=wind cluster B, 103=wind cluster C.

Deliverable 5.12 EERA DTOC calculation of scenarios

Table 11: Detailed Net-Op results for cables

from node	to node	type	existing capacity	new cables	new capacity	mean flow 1->2	mean flow 2->1
21	20	AC	5000	0	5000	3327	69
24	20	AC	5000	0	5000	4315	74
31	30	AC	9000	0	9000	2115	7110
32	30	AC	4000	0	4000	192	3838
33	32	AC	1000	0	1000	285	334
41	40	MTDC	1710	3	5154	4908	170
51	50	MTDC	1800	0	1800	773	1059
30	20	MTDC	1400	0	1400	1400	0
50	20	MTDC	1400	0	1400	1400	0
40	20	MTDC	1400	0	1400	90	532
36	31	MTDC	4000	3	7444	1239	6234
36	51	MTDC	1000	0	1000	20	820
36	41	MTDC	1000	3	4444	4215	149
36	22	MTDC	2000	0	2000	1896	194
22	21	MTDC	2010	0	2010	2010	0
101	24	AC	0	1	373	219	0
1036	1022	DC	0	1	1302	1245	0
1022	1021	DC	0	1	1302	1279	0
1101	1024	DC	0	3	3906	3614	0
1101	1032	DC	0	3	3906	0	3540
1102	1024	DC	0	1	1302	484	0
1102	1103	DC	0	1	1302	9	108
1036	36	conv	0	2	2296	0	1265
1021	21	conv	0	2	2296	1269	0
1022	22	conv	0	1	1148	0	42
1024	24	conv	0	5	5740	4089	0
1032	32	conv	0	4	4592	0	3597
1101	101	conv	0	1	1148	2	124
1102	102	conv	0	1	1148	2	393
1103	103	conv	0	1	1148	15	115

L.5 Observations

L.5.1 Observations on results.

Multiple optimization runs with different assumptions have shown that the optimal solution (or course) depend on these. In all cases the solutions favour strengthened connections between the UK and Norway, and the wind farms are generally connected in a way that goves a cost-effective sharing of the offshore grid infrastructure.

L.5.2 User experiences:

Deliverable 5.12 EERA DTOC calculation of scenarios

This calculation did not use the EERA-DTOC web tool, but based on offlline use of the Net-Op model.

L5.3 Expert judgment

The results obtained are reasonable, but depends very much on the parameter values used, e.g. assumed cost for subsea cables. A valuable aspect of the tool is that it provides a simple means to quickly investigate the impact of different parameter values.

Deliverable 5.12 EERA DTOC calculation of scenarios

M.1. Introduction

This document investigates the compliance of three offshore wind clusters in the North Sea which are planned to be constructed in the far future (i.e., 2030). This comes in the frame of proposing a complete and practical tool to design the offshore wind clusters (DTOC). Applied case studies examine the stability of the grid during and after severe and moderate disturbances, and insure that the grid codes are not violated. Moreover, this document proposes a detailed procedure to deal with the outcomes of Net-OP tool which provides an optimized topology for the connection of the three wind clusters to the benchmark grid. Particularly, data files and documentation provided based on the outcomes of Net-OP tool are utilized to examine the compliance of the far future wind clusters with grid codes. The integrated simulation environment is PSS®E. The major additions and modifications which are carried on the data provided by Net-OP, and the implemented benchmark system are explained. Afterwards, the executed cases studies are presented, and finally, results are summarized and discussed.

M.2. Benchmark system

The examined benchmark system represents the major regions that will be connected directly or indirectly to the three far future wind clusters. This system is inspired from the outcome of Net-OP tool [1], which recommended certain topology to connect the three clusters as shown in Figure 1. Buses 20, 30, 40 and 50 aggregate the conventional and wind generation in Norway, UK, Germany and Netherlands respectively. In addition the average load demand at each bus location is integrated according to real chronological hourly data. Meanwhile, the far future clusters are connected to buses 101, 102 and 103. The green generators represent the aggregate wind power generation at the given buses. For the sake of simplicity, the wind generation is modelled by a single aggregate machine of type 4 (Full rated converter wind turbine generator) at each bus. Likewise, conventional generation is modelled as a single generator with a capacity equal to the generation capacity of the entire region of the bus (the parameters source reactance and resistance are assumed to be 0.3 and 0.06 per unit respectively). Table 1 describes the generation capacities at each bus, and Table 2 includes the aggregate load at each region. A limitation is applied on wind generated power through assuming that the capacity factor of any wind power plant is not exceeding 55% [2, 3].

The system shown in Figure 1 contains 12 HVDC corridors which connect the three far future clusters to the grid, and connect other commissioned or under construction offshore wind clusters. In addition, there is a DC link between UK and Norway (future expectation). As an assumption, all the corridors are 1100 kV and have rated capacity of 1500 MVA (values might seem to be high, but this system is dealing with a scenario to be executed after 15 years from now. The system dynamic model embedded in PSS®E includes detailed models for the HVDC Voltage Source Converters (VSC), wind turbine type 4 generator and electrical models (WT4G1, and WT4E1), and conventional generators are represented by round rotor model (GENROU). The numerical values of models' parameters are found in K.8.
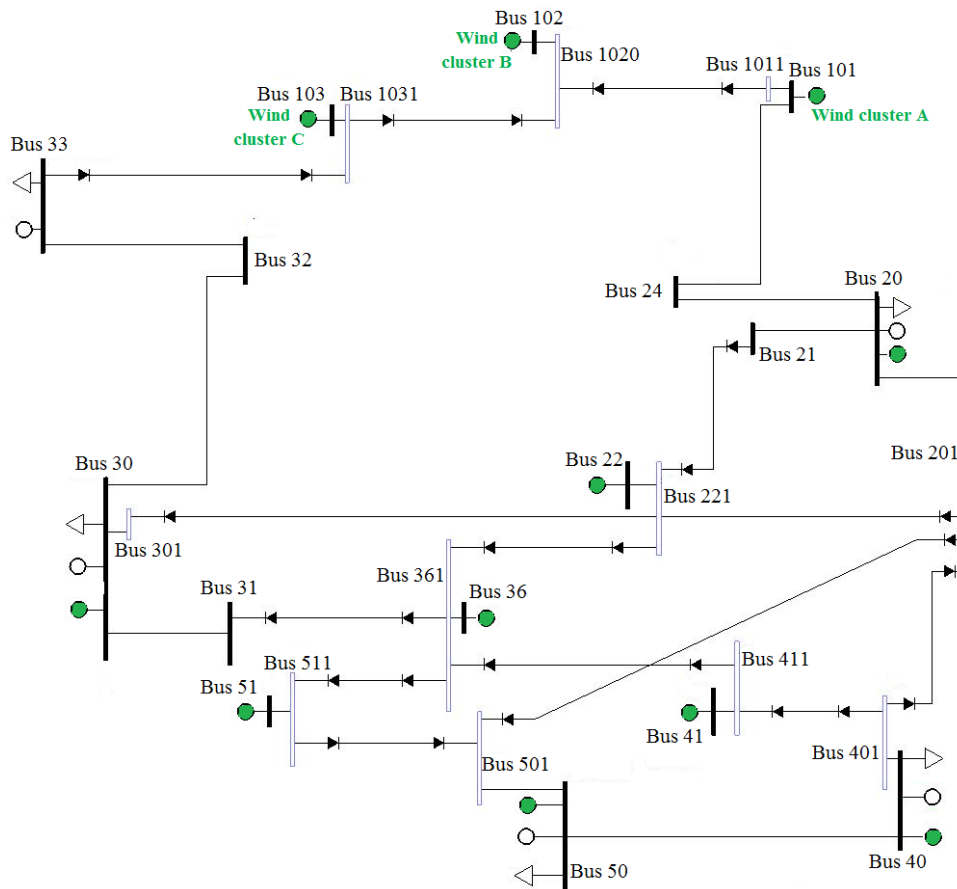
Deliverable 5.12 EERA DTOC calculation of scenarios

Figure 40 Benchmark system single line diagram

Table 12 Aggregate conventional and wind generation at different buses

Aggregate generation (MW)		Onshore wind clusters (MW)		Far future clusters (MW)	
Bus 20- Norway	31900	Bus 20-Norway	15450	Wind cluster A	1200
Bus 30- UK	82630	Bus 30-UK	58320	Wind cluster B	1200
Bus 33	1000	Bus 40-Germany	73250	Wind cluster C	1200
Bus 40- Germany	128900	Bus 50-Netherlands	18120		
Bus 50- Netherlands	25460				

Table 13 Aggregate loads at different buses

Aggregate load (MW)	
Bus 20-Norway	17352
Bus 30-UK	49772
Bus 33	49
Bus 40-Germany	72146
Bus 50-Netherlands	15868

M.3. Preparing the PSS®E File provided by Net-Op

Comprehensive changes and additions were required to prepare the *.RAW file provided by Net-OP tool before being able to reach an acceptable converging load-flow solution suitable for

Deliverable 5.12 EERA DTOC calculation of scenarios

dynamic simulations. One of the problems was the connection of wind clusters to DC links, as the PSS®E does not accept the connection of a swing bus to a DC link. To overcome this problem, a supplementary bus is added at each bus to be connected to DC link(s). The supplementary bus is connected to the main bus through a very short AC link (i.e., very low inductance). These supplementary buses are shown in violet in Figure 1.

The Net-OP tool does not provide a dynamic model for the system (i.e., *.DYR file), hence dynamic models are assigned for all the system components. A technical survey is performed to determine the appropriate numerical values for the different parameters of each model. Moreover, the following modifications are applied:

- The active and reactive power limits (Pmax, Pmin, Qmax and Qmin) of conventional and wind generation are modified to match the benchmark system documentation.
- The source reactance parameters (XSOURCE) of the generators were very high (1 pu), thus it is reduced to 0.3 pu as an assumption.
- The power factors of loads and wind plants are fixed to 0.8 and 0.9 respectively. It is of note that the wind plant power factor has an impact on the plant reactive power capability which affects its contribution in voltage support. In addition, reactive power limits of power electronics converters have a decisive influence.
- The inductances of several AC links are reduced to achieve a converging load-flow solution.
- The rated voltage levels of DC links and the rated capacity of all lines were missing. As mentioned earlier, it is assumed that all the DC links are 1100 kV and rated 1500 MVA.
- The control method used for HVDC corridors is Power-Voltage control [2]. As an illustration, one converter is responsible for matching a pre-set value of active power transmitted by the DC link (this mainly depends on the expected capacity factor of the connected wind farm/cluster). Meanwhile, the other converter maintains the DC link rated voltage level. For the sake of consistency, the wind cluster end converter is always power controlled.
- The reactive limits of converters are assumed to be +0.25 and -0.75 per unit from their rated capacities according to the real modern HVDC link fabricated by Siemens [3].
- The single line diagram in Figure 1 is drawn from scratch using PSS®E.
- The system shown in Figure 1 is based on the optimised pattern provided by Net-OP as displayed in Figure 2 (Bus 34 is ignored).
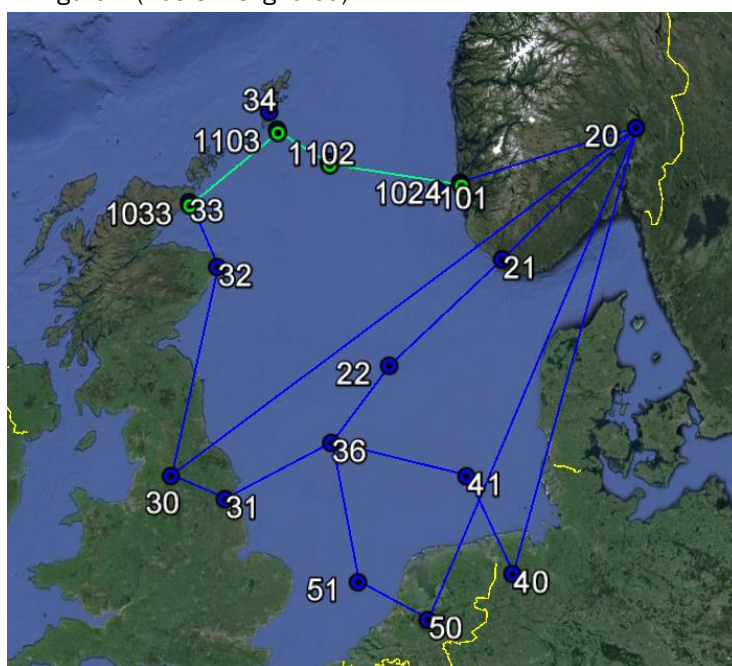

Figure 41 Geographical layout of the system provided by Net-OP tool

Deliverable 5.12 EERA DTOC calculation of scenarios

M.4. Case studies

M.4.1 Faults implication

The implemented case studies are designed to investigate the impact of integrated new wind clusters on voltage response of the connected grid areas during severe faults. In particular, each bus of the major four buses (i.e., 20, 30, 40 and 50) suffers a solid three phase fault leading to a zero-voltage dip. The voltage response at the faulted bus is compared to the voltage regime provided by the grid code. In addition, the voltage responses at some selected buses, and power flows from the faulted bus are displayed prior, during and post the dip. Two different grid codes are integrated, namely, Eon code and Norwegian code (Nord). Further details about the two codes are found in [4]. The fault is initiated at time = 1s, cleared after six cycles (i.e., system frequency is 50Hz), and the simulations continue for 3s. Table 3 summarizes the examined case studies.

Table 3 Examined case studies

Name	Faulted bus	Fault type	Clearance duration
Case A	Bus 20	3-phase	120 ms
Case B	Bus 30	3-phase	120 ms
Case C	Bus 40	3-phase	120 ms
Case D	Bus 50	3-phase	120 ms

M.4.2 User models integration

The methodology provided in Deliverable 2.5 is applied [4]. In particular, the voltage at the bus which should suffer the fault is forced to follow the voltage regime provided by the grid code. During the dip, the voltage responses at other buses, and the reactive currents injected by wind clusters are monitored. Bus 20 is selected to connect the user model which makes the bus voltage follow Eon and Nordic codes in two separate case studies. In addition, a user model is integrated to Bus 33 to imitate the Eon code in a third case study. The concept of user models is also applied to examine the impact of a sudden phase shift and frequency step on the system performance. Two case studies are implemented at t = 0s, Bus 20; 1) phase-shift step rise of 20 degrees, and 2) frequency step increase by 0.2 Hz

M.5. Results and discussion

M.5.1 Faults implication

The four cases proved to be coping with the grid codes, namely, Case A is compared to Nordic code as in Figure 3, meanwhile Cases B to D are assessed against Eon code as in Figure 4. Actually, this is highly expected as most of the offshore wind clusters (i.e., the operative and under commissioning or the far future) are connected through HVDC corridors. Thus, the reactive capability mainly depends on the reactive limits of the DC link inverter not on the wind turbines installed in the wind clusters. It is expected that after fifteen years, special codes will be needed to deal with such advanced renewable energy integration. It is also interesting to highlight the slight differences between the responses of voltage dips at the three buses in Figure 3. Case D records a slow initial recovery, which might be due to the lower generation capacity connected at bus 50. Meanwhile, Bus 30 exploited a minor overshoot, where the high wind power penetration is a possible cause. Among the three responses, Case C achieved the best response since the voltage recovered after fault clearance very fast with minimum oscillations and avoided any overshoots. Likewise, the response at Bus 20 is promising and there is an acceptable safe time-margin between the code requirements and the actual recovery response after voltage dip.
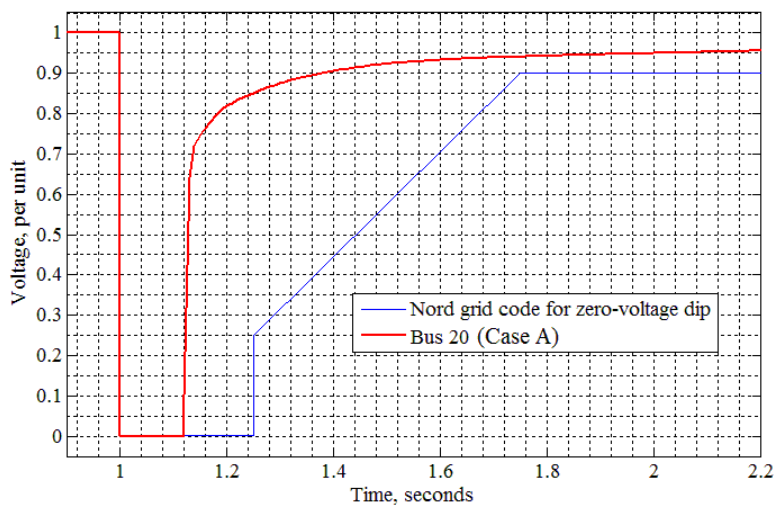
Deliverable 5.12 EERA DTOC calculation of scenarios

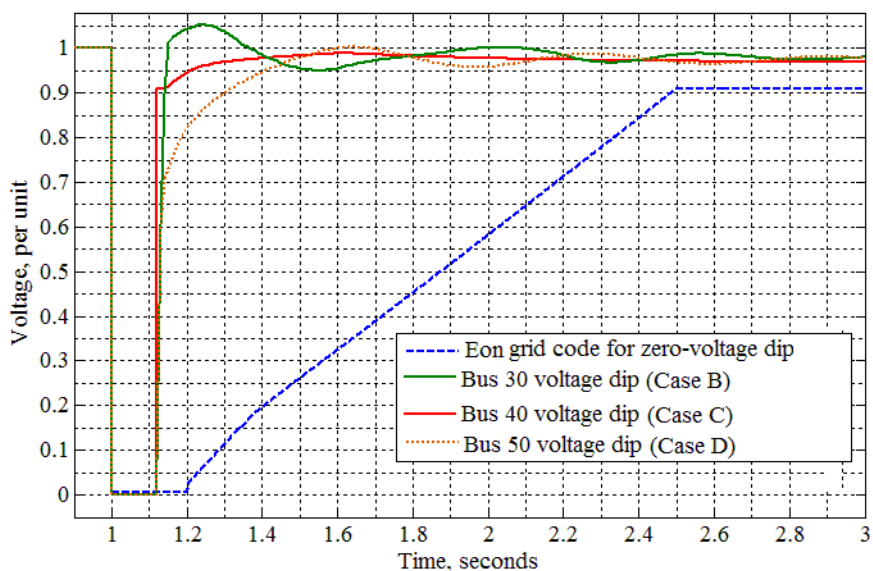**Figure 42 Case A voltage dip compared to Nord grid code**

Figure 43 Cases B to D voltage dips compared to Eon grid code

Next, separate analysis for each case study is conducted. The voltage responses at two near buses to the faulted bus are investigated. Buses 24 and 101 are selected for Case A as shown in Figure 5. Bus 24 is considerably affected as it is has no generation and is close to the faulted bus, meanwhile Bus 101 is more robust as it is connected to Wind cluster A. However, Bus 101 suffers minor oscillations before it stabilizes (note that this bus is also connected to HVDC link). In Case B, Buses 361 (the supplementary bus connecting offshore wind plant at Bus 36) and 24 are selected as shown in Figure 6. Bus 361 does not sense the voltage dip as it is connected to the grid only through DC links; but Bus 32 is slightly affected. Similar results are achieved in Case C, in which the voltage at Buses 50 and 411 are displayed in Figure 7.
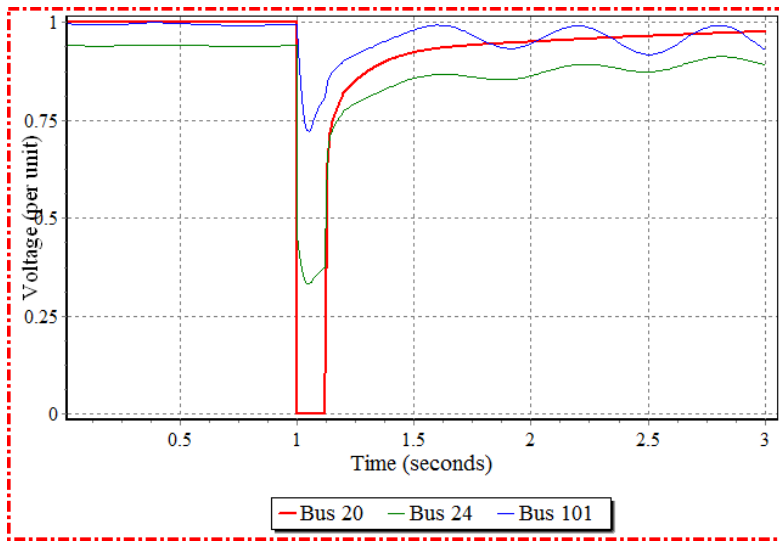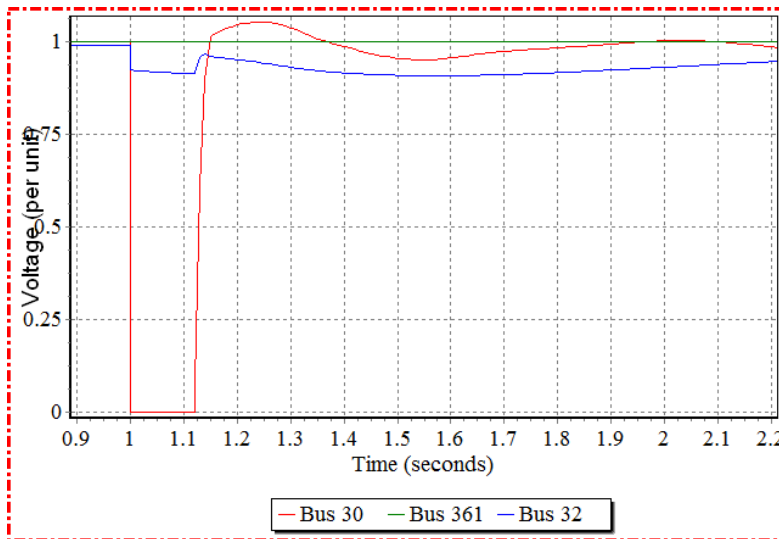
Deliverable 5.12 EERA DTOC calculation of scenarios

Figure 44 Voltage responses of Case A

Figure 45 Voltage responses of Case B

Figure 46 Voltage responses of Case C

Deliverable 5.12 EERA DTOC calculation of scenarios
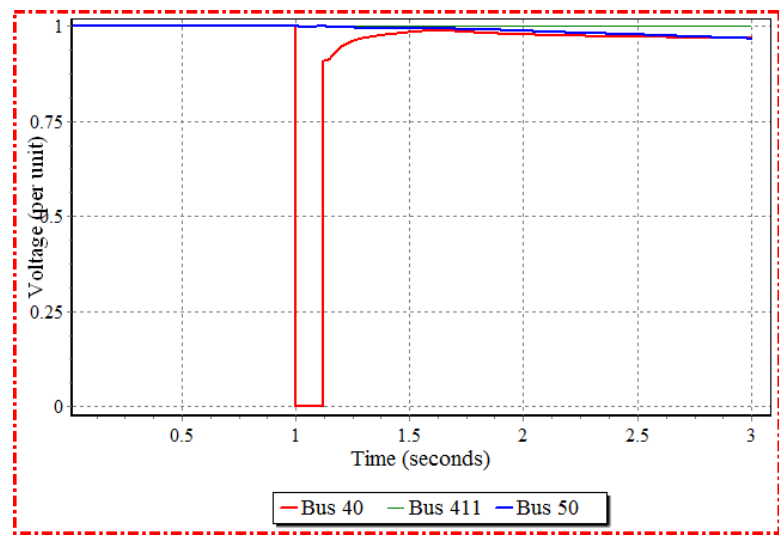
Conventional generator speed at the faulted bus is also examined in Figures 8 to 10. Cases A and C are characterized with very small deviations. However, Case B reached a speed dip of about 0.75 Hz which might generate a frequency event in this area of the grid. But this dip continues for a very short duration with respect to the thresholds of dead-bands of frequency sensors. Thus, frequency drops procedures should not be initiated.
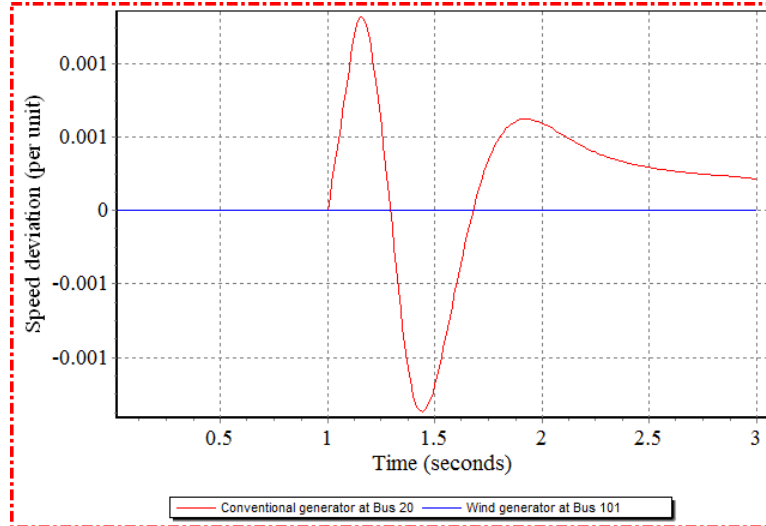

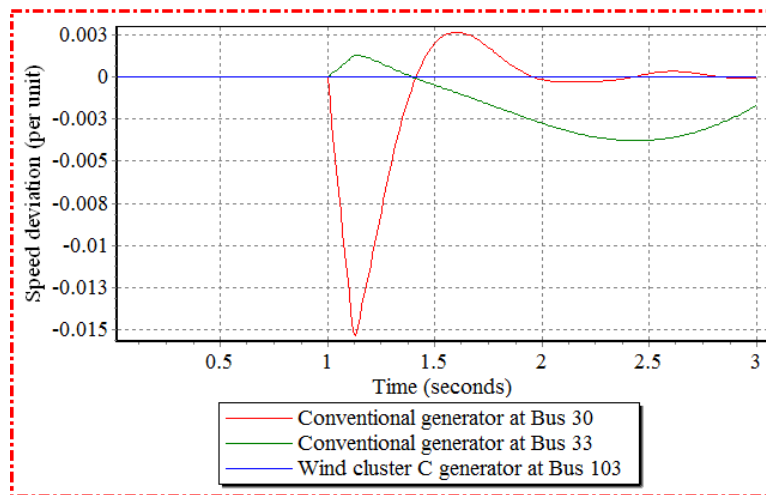**Figure 47 Case A-Conventional generators speed deviations**

Figure 48 Case B-Conventional generators speed deviations

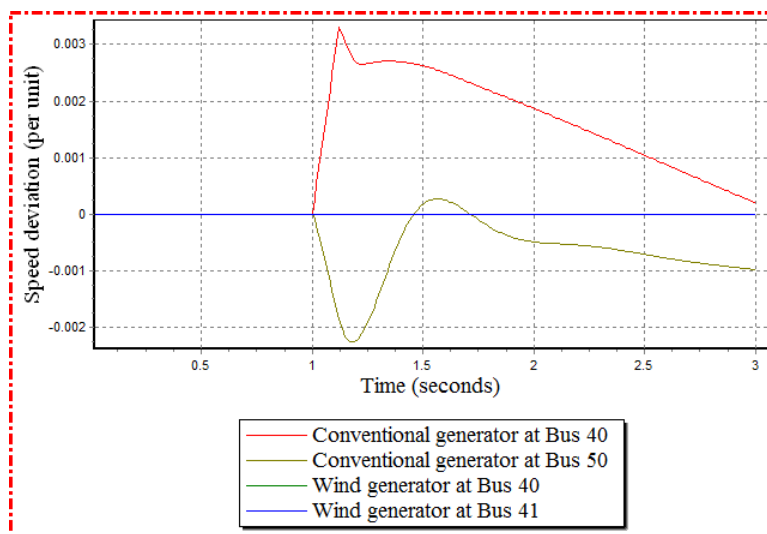*Deliverable 5.12 EERA DTOC calculation of scenarios*

Figure 49 Case C-Conventional generators speed deviations

The power flow from/to the faulted bus is analysed in Cases A and D. The power drops naturally to zero during fault duration; however it builds up again very rapidly as shown in Figure 11. Bus 20 is feeding power to Bus 201 (supplementary connected to DC links), as Bus 201 is transmitting power to Bus 30 (UK) through a DC link. In addition, Bus 20 is receiving power from Bus 21, where an offshore wind cluster is generating power through the DC link between Buses 21and 221. Once again, the fact that the future wind clusters are not affected by the voltage dip is clear where the output of Wind cluster B is fixed all the time.

In Figure 12 (Case D), the generation of wind cluster at Bus 51 is not delivered, hence the converter is forced to supress the output gradually, and it builds up again after the fault is cleared. As an illustration, the output of Bus 51 is consumed mainly through Bus 50, but the fault avoided this consumption (i.e., the pre-set active power delivery of DC link between Buses 511 and 361 is maintained). It is of note that all the power flows through the bus are following the trend of wind generation building up at Bus 51, until the pre-fault values are retained. The recovery of normal operation for the flow through the AC link between Netherlands and Germany (Buses 50 and 40) is slower due to the huge conventional and renewable capacities integrated at both buses.
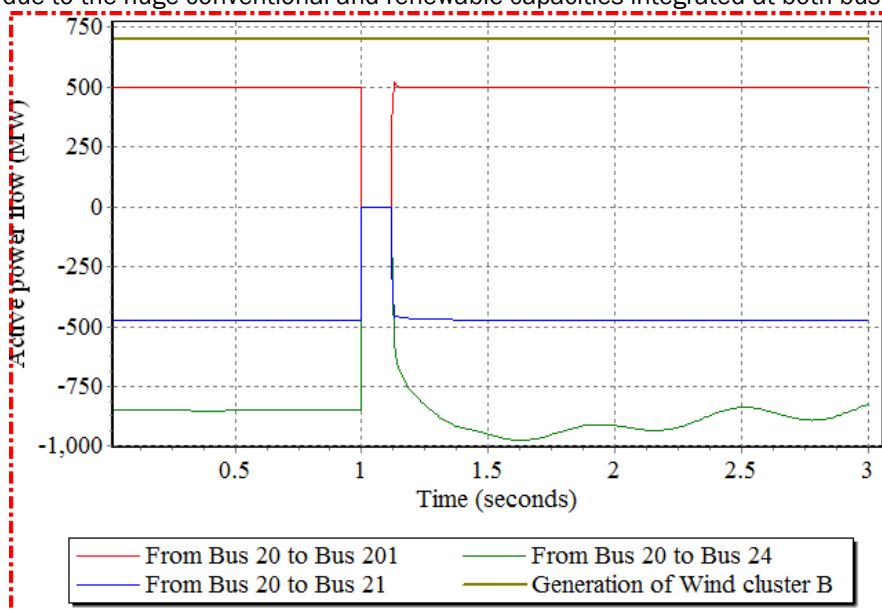

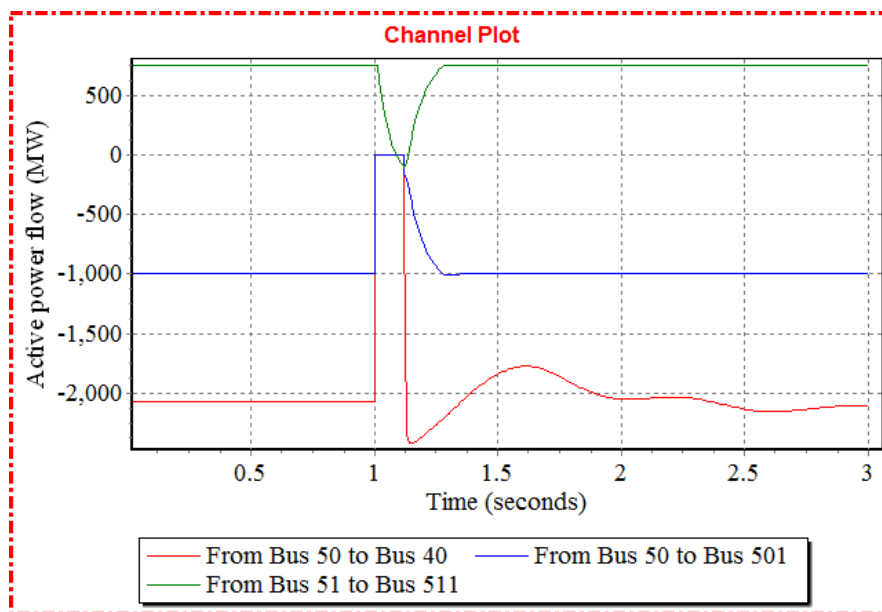**Figure 50 Examples for power flow at Case A**

Deliverable 5.12 EERA DTOC calculation of scenarios

Figure 51 Examples for power flow at Case D

M.5.2 User models integration

As explained in Section 4.2, the impacts of applying grid codes voltage dips at Buses 20 and 33 are investigated. In the cases studies of Bus 20, simulations show that, according to the nature of the examined system, the fault affects only Buses 24 and 101; meanwhile the other buses are not affected as they are connected through HVDC corridors. This is illustrated through Figure 13 (Bus 102) and Figure 14 (Buses 101 and 103). The major difference between the two dips is in the first stage, where the Nordic code dip is severer (voltage drops to almost 0), therefore, other buses (i.e., 24 and 101) drops to the same level. Conversely, in Eon case study, the voltage nadir is different between the three buses, where the worst deviation occurs at the faulted bus, namely, Bus 20. Meanwhile, in Bus 33 case study, Bus 30 is unaffected by the voltage dip as shown in Figure 15.
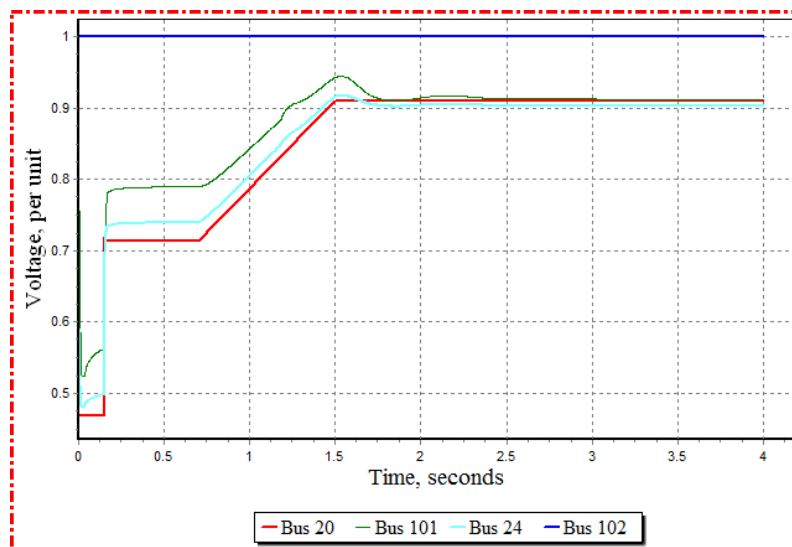

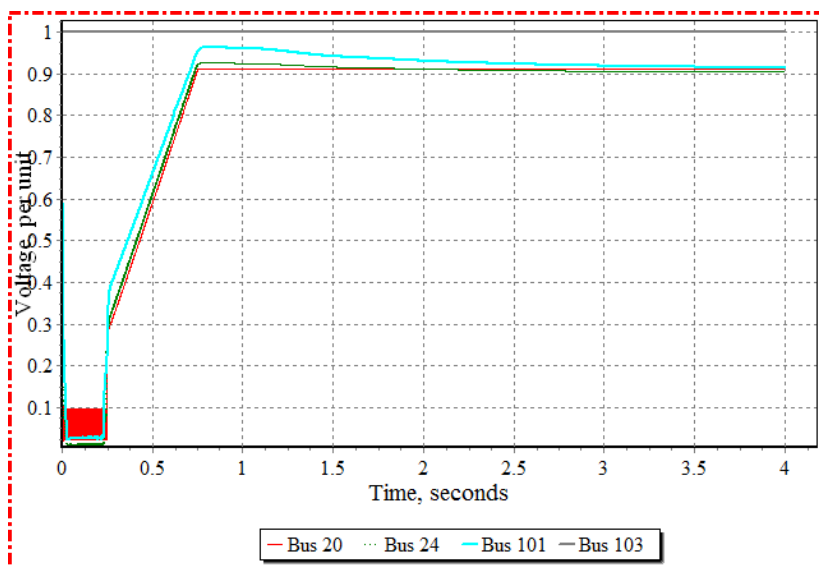**Figure 52 Voltage responses at several busses (Eon voltage dip at Bus 20)**

Deliverable 5.12 EERA DTOC calculation of scenarios

Figure 53 Voltage responses at several busses (Nordic voltage dip at Bus 20)

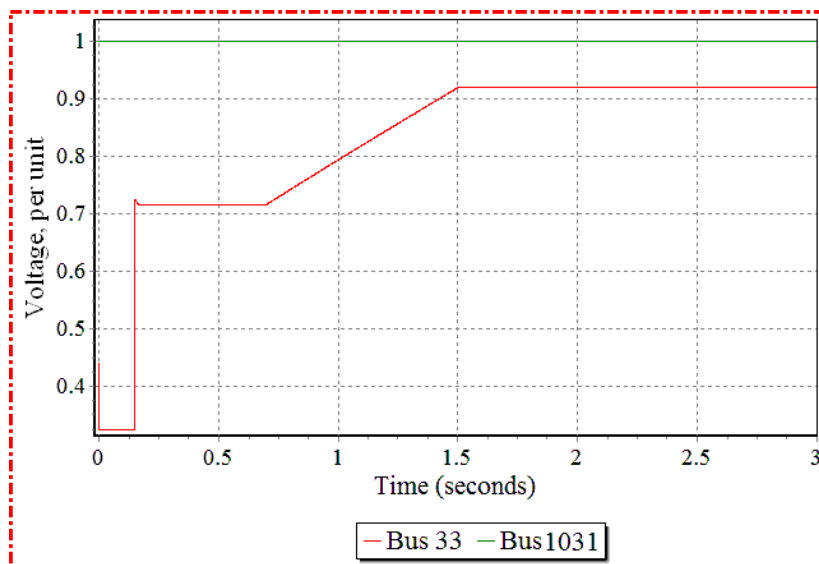**Figure 54 Voltage responses at Buses 33 and 30 (Eon voltage dip at Bus 33)**

The reactive current grid requirement is fulfilled by the wind clusters as shown in Figure 16, where the reactive current is always higher than the red threshold. However, the reactive power slightly violates the code limit after the fault is almost cleared as shown in Figure 17.
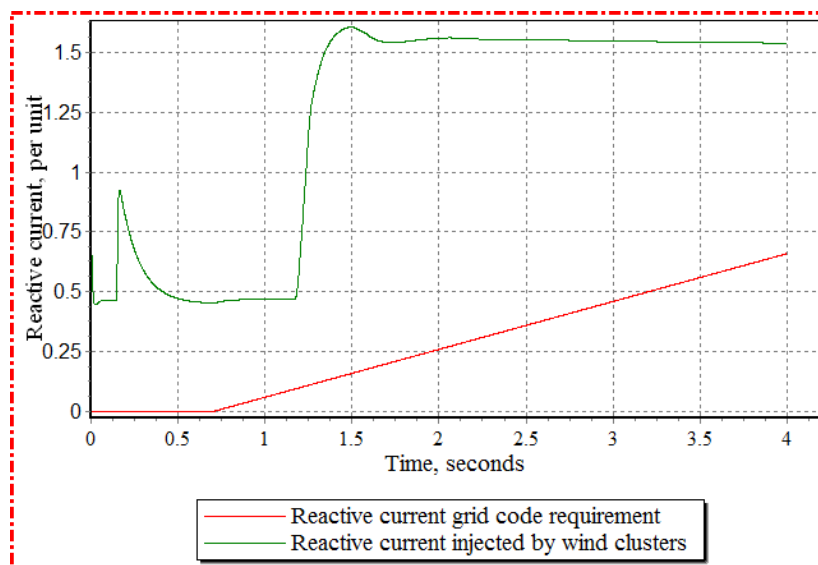
Deliverable 5.12 EERA DTOC calculation of scenarios

Figure 55 Reactive current code requirements and actually injected (Eon voltage dip at Bus 20)
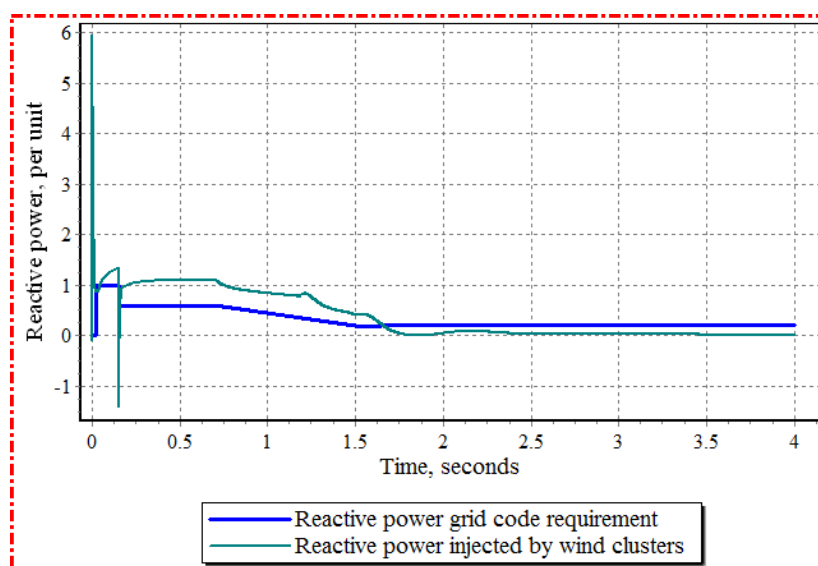

Figure 56 Reactive power code requirements and actually injected (Eon voltage dip at Bus 20)

Conversely, in case of Bus 33 dip, the reactive current violates the grid requirements as shown in Figure 18. As an illustration, the power electronics converters of the DC link corridor at Bus 103 are not equipped with special controller algorithms to provide reactive current during dips. On the contrary, in Bus 20 case study, the onshore WFs provided suitable reactive currents based on their controllers. However, reactive power provided to Bus 33 is acceptable as shown in Figure 18. The sudden steep rise in reactive power is most probably caused by a numerical solution issue of PSS®E. It is worth mentioning that the applied codes are dealing with wind farms connected at a certain point of common coupling in an AC grid. But in the given cases, there are several wind farms which form wind clusters. In addition they are linked through HVDC corridors. Thus, the reactive capability mainly depends on the reactive limits of the DC link inverter, not on the wind turbines installed in the wind clusters. The steep drops and peaks in Figure 18 are most probably caused by numerical solutions obtained from the mathematical methods implied by the PSS®E, and should not be considered a violation of the grid code.
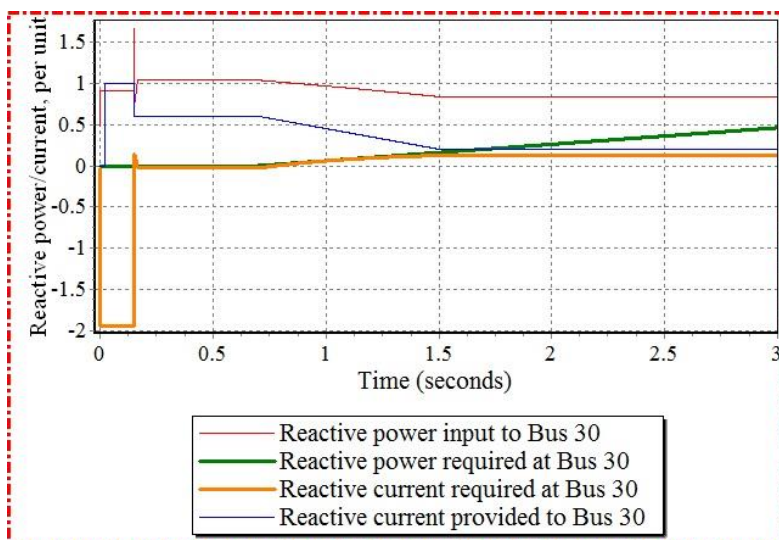
Deliverable 5.12 EERA DTOC calculation of scenarios

Figure 57 Reactive power and current requirements and actually injected (Eon voltage dip at Bus 33)

The active power provided by the wind clusters in the second case study (Nordic code dip at Bus 20) is highlighted. As shown in Figure 19, the active power flows continuously even during the dip. However, it suffers a moderate drop (i.e., the reactive power increases during the dip). Afterwards, it returns back to the initial value after the dip ends.
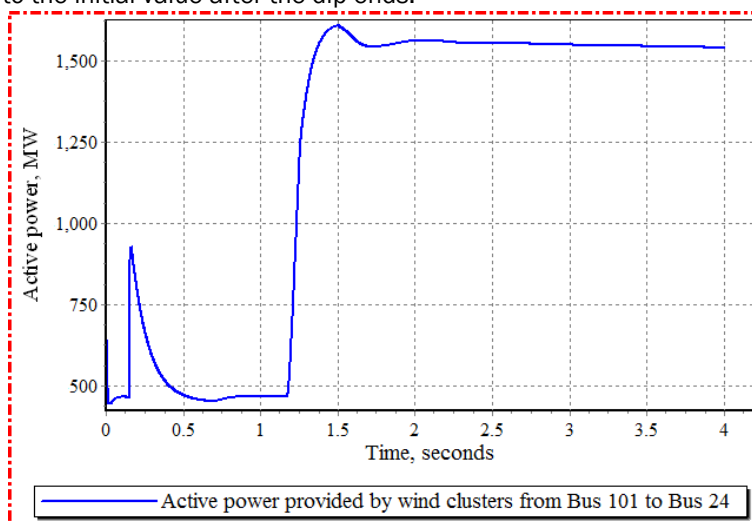
Figure 58 Active power from wind clusters at Bus 101 (Nordic voltage dip at Bus 20)

The frequency rise by 0.2 Hz at Bus 20 causes a continuous increase in absolute phase angles at the buses which are connected to Bus 20 (i.e. Bus 24 and 21) as shown in Figure 20-a. The sudden speed deviation between the voltage vector at Bus 20 and the corresponding voltage vectors at Buses 21 and 24 forced their phase angles to keep rising. The sudden rise of frequency forced the generator at Bus 20 to accelerate; so that its speed deviates from the nominal value by 0.004 per unit (0.2 Hz) as shown in Figure 20-b. The voltages and power delivered/consumed by these buses are almost not affected (i.e. minor smooth oscillations in the range of 0.0001 per unit).

Deliverable 5.12 EERA DTOC calculation of scenarios

Figure 59 a) phase angles responses at disturbed Bus 20 and near Buses, b) speed deviation of generator at the disturbed Bus 20

M.6. Conclusions and recommendations

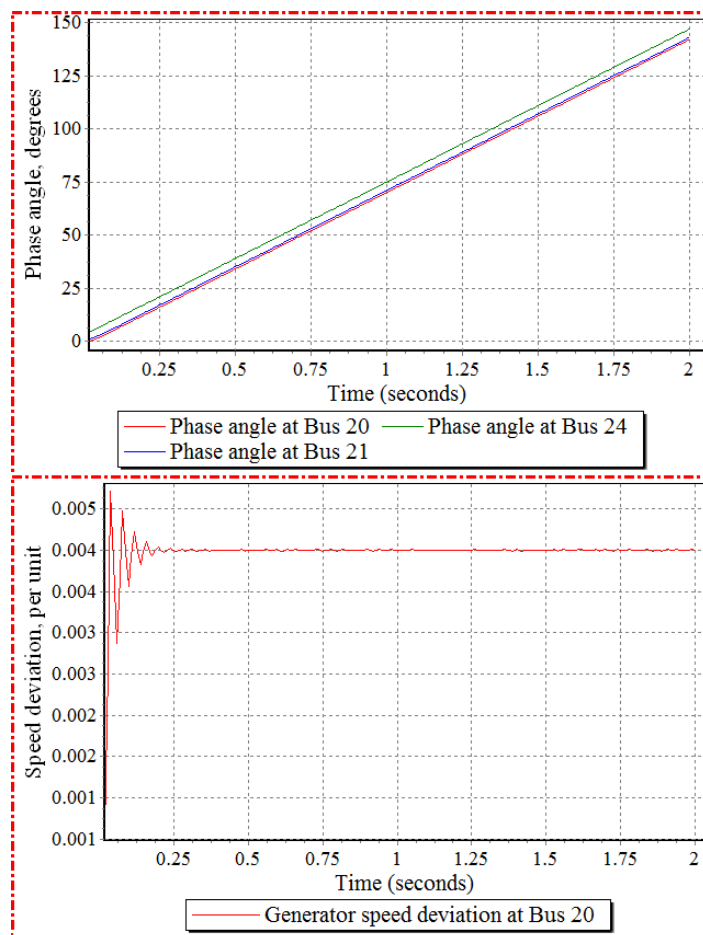This report investigates the impact of three large offshore wind clusters (aggregate capacity of 3 GW) on the stability of a grid. This grid connects the major power systems which might be supplied by these clusters directly or indirectly through AC lines or DC links. The Net-OP suggested an optimized topology to connect the wind clusters to this grid to form a 15-bus benchmark system. The first step was to deal with the *.RAW file provided by Net-OP tool in the frame of DTOC. Afterwards, a dynamic model for the whole system is prepared (*.DYR) to perform several case studies. Most of the case studies focused on the voltage issues when a given bus suffers a severe voltage dip. The grid code compliance at the faulted bus and the nearby buses is investigated. All the case studies proved an acceptable pattern for voltage recovery after the faults. However, the DC link converters failed to provide the required reactive current to the nearby faulted bus as they are not equipped with the suitable control algorithms in the applied dynamic models installed in PSS®E. The integrated grid codes are designed for WFs which are connected through AC lines; hence the voltage support capabilities are mainly based on WFs/WTGs reactive power limits. Conversely, in the case of offshore clusters which are connected through DC links, voltage support is dependent on the control methods and the ratings of the power electronic converters of the DC link.

The authors' recommendations concerning the DTOC and the robust integration of Net-OP and PSS®E are summarized in four points:

Deliverable 5.12 EERA DTOC calculation of scenarios

- The outcomes of Net-OP tool should be refined, so that the PSS®E file can be directly used in static and dynamic simulations. The PSS®E *.RAW file used in this report can be used as a template, because the solution provided by Net-OP affects only few buses and lines. The template file can be then updated when more detailed data are available. Additionally, the aggregate generation capacities and load demand need to be updated frequently according to their present values.
- The suggested topology by Net-OP is based on the current values of generation and load demand at the major zones in benchmark system. However, the examined scenario deals with a far future study. Thus, to improve the accreditation of obtained results, a forecasting process for the generation and loads in year 2030 is required.
- Special attention should be paid to the dynamic modelling of the converters in the DC-lines, because the play a critical role in the provision of reactive current during voltage dips. In addition, advanced user models could be implemented to provide the converters with the capability of supporting voltage during dips.
- The dynamic simulation is based on generic values for all the parameters of the controller models integrated to the PSS®E dynamic model. However, real values for these parameters will be very beneficial, and could be obtained through cooperation channels with the related industrial parties.

Finally, comprehensive efforts are required to design new grid codes which specify clearly the role of DC links converters in providing ancillary services, including voltage and frequency support during unusual events.

M.7. References

[1]   H. G. Svendsen, "Planning Tool for Clustering and Optimised Grid Connection of Offshore Wind Farms," *Deepwind'2013 - Selected Papers from 10th Deep Sea Offshore Wind R&D Conference,* vol. 35, pp. 297-306, 2013 2013.

[2]   "Lecture: VSC-HVDC, Course: EG2070 FACTS and HVDC in Electric Power Systems," Royal Institute of Technology (KTH), Sweden2012.

[3]   M. Davies, M. Dommaschk, J. Dorn, J. Lang, D. Retzmann, and D. Soerangr, "HVDC PLUS – Basics and Principle of Operation," E. S. Siemens AG, Ed., ed. Germany, 2011.

[4]   O. Anaya-Lara and P. Ledesma, "D2.5 Procedure for Verification of Grid Code Compliance," University of Strathclyde2012.

[5]   Siemens Power Technologies International, "PSS®E Documentation," Siemens Industry Inc., 2012.

[6]   C. Du, "VSC-HVDC for Industrial Power Systems," Thesis for the degree of Doctor of Philosophy, Energy and Environment, Chalmers University of Technology, 2007.

Deliverable 5.12 EERA DTOC calculation of scenarios

M.8: Additional numerical values used in the study

Table A. 1 Numerical values of WT4E1 parameters

WT4E1 (GE 2.5 MW)	
Tfv, Filter time constant in Voltage regulator (sec)	0.15
J+1 KPV, Proportional gain in Voltage regulator(pu)	18
J+2 KIV, Integrator gain in Voltage regulator (pu)	5
J+3 Kpp, Proportional gain in Active Power regulator(pu)	0.05
J+4 KIP, Integrator gain in Active Power regulator (pu)	0.1
J+5 Kf, Rate feedback gain (pu)	0
J+6 Tf, Rate feedback time constant (sec.)	0.08
J+7 QMX, Max limit in Voltage regulator (pu)	0.47
J+8 QMN, Min limit in Voltage regulator (pu)	-0.47
J+9 IPmax, Max active current limit	1.1
J+10 TRV, Voltage sensor time constant	0
J+11 dPMX, Max limit in power PI controller (pu)	0.5
J+12 dPMN, Min limit in power PI controller (pu)	-0.5
J+13 T_Power, Power filter time constant	0.05
J+14 KQI, MVAR/Voltage gain	0.1
J+15 VMINCL, Min. voltage limit	0.9
J+16 VMAXCL, Max. voltage limit	1.1
J+17 KVI, Voltage/MVAR Gain	120
J+18 Tv, Lag time constant in WindVar controller	0.05
J+19 Tp, Pelec filter in fast PF controller	0.05
J+20 ImaxTD, Converter current limit	1.7
J+21 Iphl, Hard active current limit	1.11
J+22 Iqhl, Hard reactive current limit	1.11

Table A. 2 Numerical values of GENROU and WT4G1 parameters [5]

GENROU			WT4G1	
J T´do (>0) (sec)	7		J TIQCmd, Converter time constant for IQcmd	0.02
J+1 T²´do (>0) (sec)	0.05		J+1 TIPCmd, Converter time constant for IPcmd	0.02
J+2 T´qo (>0) (sec)	1.5		J+2 VLVPL1, LVPL voltage 1 (Low voltage power logic)	0.87537
J+3 T²qo (>0) (sec)	0.05		J+3 VLVPL2, LVPL voltage 2	0.898853
J+4 H, Inertia	6		J+4 GLVPL, LVPL gain	1.111951
J+5 D, Speed damping	0		J+5 VHVRCR, HVRCR voltage	1.12
J+6 Xd	2.2		J+6 CURHVRCR, HVRCR current	2
J+7 Xq	2		J+7 RIp_LVPL, Rate of LVACR active current change	10
J+8 X´d	0.35		J+8 T_LVPL, Voltage sensor for LVACR time constant	0.02
J+9 X´q	0.4			
J+10 $X^2d = X^2q$	0.3			
J+11 Xl	0.15			
J+12 S(1.0)	0.1			
J+13 S(1.2)	0.3			

Table A. 3 Numerical values of VSCDCT parameters [6]

VSCDCT	
J Tpo_1, Time constant of active power order controller, sec (For VSC # 1).	0.05

Deliverable 5.12 EERA DTOC calculation of scenarios

J+1 AC_VC_Limits_1, Reactive power limit for ac voltage control, pu on converter MVA rating.	0
J+2 AC_Vctrl_kp_1, AC Voltage control proportional gain, converter MVA rating/BASEKV (For VSC # 1).	2.4
J+3 Tac_1 > 0.0, Time constant for AC voltage PI integral, sec (For VSC # 1).	0.01
J+4 Tacm_1, Time constant of the ac voltage transducer, sec (For VSC # 1), must be longer than simulation step	0.05
J+5 Iacmax_1, Current Limit, pu on converter MVA rating (For VSC # 1).	1
J+6 Droop_1, AC Voltage control droop, converter MVA rating/BASEKV (For VSC # 1).	0
J+7 VCMX_1, Maximum VSC Bridge Internal Voltage (For VSC # 1).	1.07
J+8 XREACT_1 > 0.0, Pu reactance of the ac series reactor on converter MVA rating (For VSC # 1).	0.17
J+9 QMAX_1, Maximum system reactive limits in MVAR (For VSC # 1)	240
J+10 QMIN_1, Minimum system reactive limits in MVAR (For VSC # 1).	-740
J+11 AC_VC_KT_1, feedback from reactive power limiter to ac voltage controller (For VSC #1).	1.2
J+12 AC_VC_KTP_1, feedback from current order limiter to ac voltage controller (For VSC #1).	1
J+13 Tpo_2, Time constant of active power order controller, sec (For VSC # 2).	0.05
J+14 AC_VC_Limits_2, Reactive power limit for ac voltage control, pu on converter MVA rating	0
J+15 AC_Vctrl_kp_2, AC Voltage control proportional gain, converter MVA rating/BASEKV (For VSC # 2).	2.4
J+16 Tac_2 > 0.0, Time constant for AC voltage PI integral, sec (For VSC # 2). When 0, VSC#2 is ignored.	0.01
J+17 Tacm_2, Time constant of the ac voltage transducer, sec (For VSC # 2), must be longer than simulation step	0.05
J+18 Iacmax_2, Current Limit, pu on converter MVA rating (For VSC # 2).	1
J+19 Droop_2, AC Voltage control droop, converter MVA rating/BASEKV (For VSC # 2).	0
J+20 VCMX_2, Maximum VSC Bridge Internal Voltage (For VSC # 2).	1.07
J+21 XREACT_2 > 0.0, Pu reactance of the ac series reactor on converter MVA rating (For VSC # 2)	0.17
J+22 QMAX_2, Maximum system reactive limits in MVAR (For VSC # 2).	240
J+23 QMIN_2, Minimum system reactive limits in MVAR (For VSC # 2).	-740
J+24 AC_VC_KT_2, feedback from reactive power limiter to ac voltage controller (For VSC #2).	1.2
J+25 AC_VC_KTP_2, feedback from current order limiter to ac voltage controller (For VSC #2).	1
J+26 Tpo_DCL, Time constant of the power order controller, sec (For DC Line).	0.05
J+27 Tpo_lim, Time constant of the power order limit controller, sec (For DC Line).	0.05

Deliverable 5.12 EERA DTOC calculation of scenarios

N.1 Objective/user story

N1.1 Objective

Evaluate the impact of the combinations for the wind resource and wake models using the standard layout.

N1.2 User story and scenario

Base scenario (Race Bank)
User story
3.1 As a developer I can determine the wake effects of neighbouring wind farm clusters on a single wind farm (meso and/or micro).

N.2 Codes

WAsP-Park and Levellised Cost Of Energy (LCOE) models

N.3 Input:

N.3.1 Description of wind farm

The Race Bank wind farm, located 27 km from the North Norfolk coast, has a planned capacity of 580 MW. Approximately 94 to 116 turbines in the range of 5-6.15 MW will be founded. The scenario assumes the farm to consist of 100 UPWIND 5MW reference turbines, since this type is well documented. The Race Bank wind farm is surrounded by several other wind farms which are either in operation already or they are in the planning phase. These surrounding farms are included in the scenario description.

The suggested layout of the farms (Figure 1) it based on the layout of the Horns Rev wind farm modified to 10x10 wind turbines. One main 'wind farm line' is oriented in the East-West direction and the other main wind farm line slightly skewed compared to the North-South direction. In Figure 1 the direction of the main wind farm lines is 5.1 rotor diameters but scenarios will be considered with different distances between the turbines ranging from 3.65 to 10 rotor diameters.
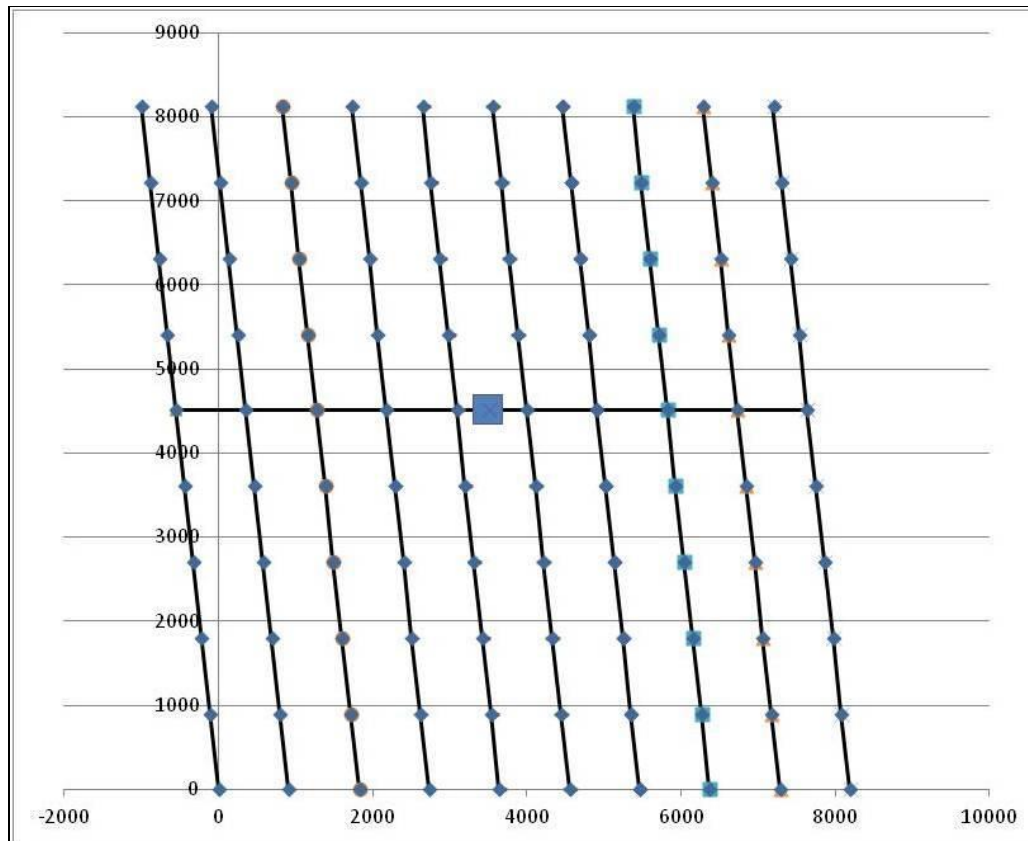
Deliverable 5.12 EERA DTOC calculation of scenarios

Figure 60 Layout of wind farm including electrical cables and transformers and 5.1 D distance between the turbines.

N.3.2 Description of turbines:

The wind turbines from the base scenario have a rated power of 5 MW with a rotor diameter of 126 m at a hub height of 90 m.

- Wind class: IEC class Ib

- Regulation: Variable speed, collective pitch

- Orientation of rotor: Upwind, overhang 5 meter

- Rated wind speed 11.4 m/s

- Cut-out wind speed 25 m/s

- Maximum rotor speed: 12.1 rpm (maximum tip speed: 80 m/s)

N.3.3 Description of wind climate

Because we seek to evaluate the impact of neighbouring wind farms on the wind farm of interest, new wind climates without any wake effects were used. For this scenario, the 100 m wind resource from the CENER reference run, i.e. no wakes included, was used.

N.3.4 Remarks.

Deliverable 5.12 EERA DTOC calculation of scenarios

In order to evaluate the impact of neighbouring wind farms, the scenario was originally calculated as is. Neighbouring wind farms were removed consecutively and the scenario was calculated after the removal of each wind farm. Figure shows the location of the wind farms in the North Sea (top) and a close view of each wind farm in relation to the others (bottom).

The order by which wind farms were removed was:

- Dudgeon
- Sheringham Shoal
- Triton Knoll A
- Triton Knoll B
- Lincs
- Inner Drowsing
- Lynn

Due to the special format of this scenario, all wind turbines of all wind farms were considered active for the calculations. Therefore, in order to derive estimates of Net and Farm Annual Energy Production for the Race Bank case, the scenario was edited in QGIS, and only the relevant turbines of RB were selected and their performance statistics were summarized separately.
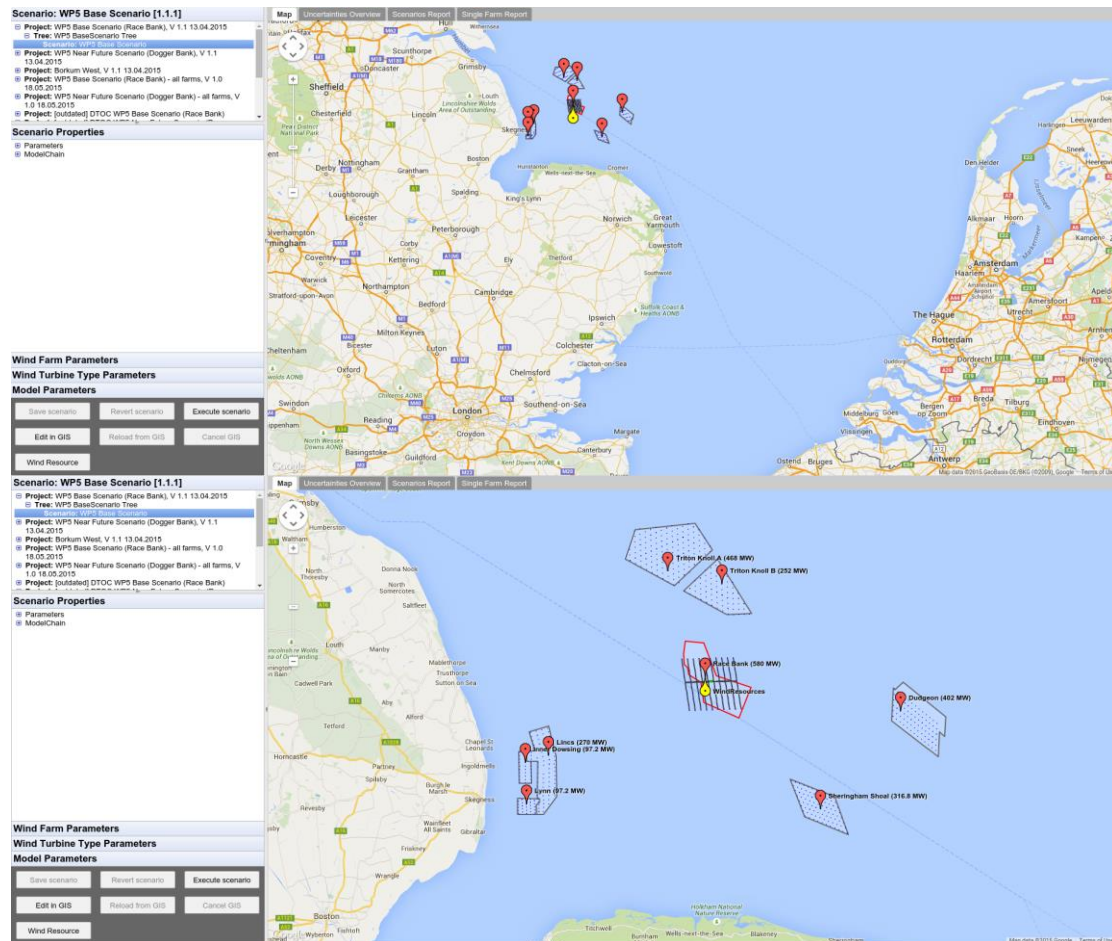

Figure 61. Position of the Race Bank wind farm in the North Sea (top), with a detailed layout (bottom)

Deliverable 5.12 EERA DTOC calculation of scenarios

N.4 Output/results

Scenario	Total Farm AEP (GWh/a)	Total Net AEP (GWh/a)	LCOE (Eur/MWh) * For all farms
All farms included	2391.080	2664.510	85.29
Remove: Dudgeon	2391.492	2664.510	85.69
Sheringham Shoal	2602.992	2664.509	85.71
Triton Knoll A	2393.919	2664.509	86.44
Triton Knoll B	2372.220	2664.509	87.54
Lincs	2397.720	2664.509	88.09
Inner Drowsing	2397.958	2664.509	88.71
Lynn	2398.102	2664.505	89.22

N.5 Observations

N.5.1 Observations on results.

Since the neighbouring wind farms in this scenario are at various distances from the Race Bank wind farm, their impact is expected to vary. Indeed, removing Dudgeon which is one of the farms furthest away has a minimal impact on the Total AEP of RB (increase of 0.4 GWh/a). Sheringham Shoal's removal increases the total AEP of RB significantly, 204 GWh/a, more than any other wind farm. While the removal of Triton Knoll A increases the AEP of RB, by no more than 3 GWh/a, the removal of Triton Knoll B decreases it by almost 20 GWh/a. Lincs, Inner Drowsing and Lynn also have an impact on Race Bank's AEP, their removal increases it by 7 GWh/a.
The total net AEP for Race Bank remains practically unchanged, independent of the surrounding wind farms.

N.5.2 User experiences:

At this point, the way to evaluate the impact of neighbouring wind farms is not properly integrated in the tool since
- Included wind resources have been evaluated accounting for the wake losses. Thus editing wind farm locations in the tool, will not change anything as the underlying wind climate already includes the wake effects from such farms.
- Even if the wind climate did not include the wake effects. It is not possible to remove neighbouring wind farms as the tool is now, since they are considered inactive layers and can not be edited.

N.5.3 Expert judgement

While the total farm AEP of Race Bank increases when the neighbouring wind farms are removed, the LCOE decreases by 4 Eur/MWh when all farms are included.

Deliverable 5.12 EERA DTOC calculation of scenarios

O.1 Objective/user story

O.1.1 Objective

Evaluate the impact of the surrounding wind farms using the standard layout.

O.1.2 User story and scenario

Near future scenario (Dogger Bank)

User story
3.1 As a developer I can determine the wake effects of neighbouring wind farm clusters on a single wind farm (meso and/or micro).

O.2 Codes

WAsP-Park and Levellised Cost Of Energy (LCOE) models

O.3 Input:

O.3.1 Description of wind farm

This scenario is connected to the plan for an off-shore cluster at Dogger Bank. It starts with a 1GW wind farm consisting of 100 turbines with a rated power of 10 MW using the well documented INNWIND.EU reference turbine. The farm is assumed to be located at the southern part of the Dogger Bank area and is surrounded by other wind farms similar to the planned situation for Dogger Bank.

The suggested layout of the farms (Figure 62) it based on the layout of the Horns Rev wind farm modified to 10x10 wind turbines. One main 'wind farm line' is oriented in the East-West direction and the other main wind farm line slightly skewed compared to the North-South direction. In Figure 1 the direction of the main wind farm lines is 5.1 rotor diameters but scenarios will be considered with different distances between the turbines ranging from 3.65 to 10 rotor diameters.
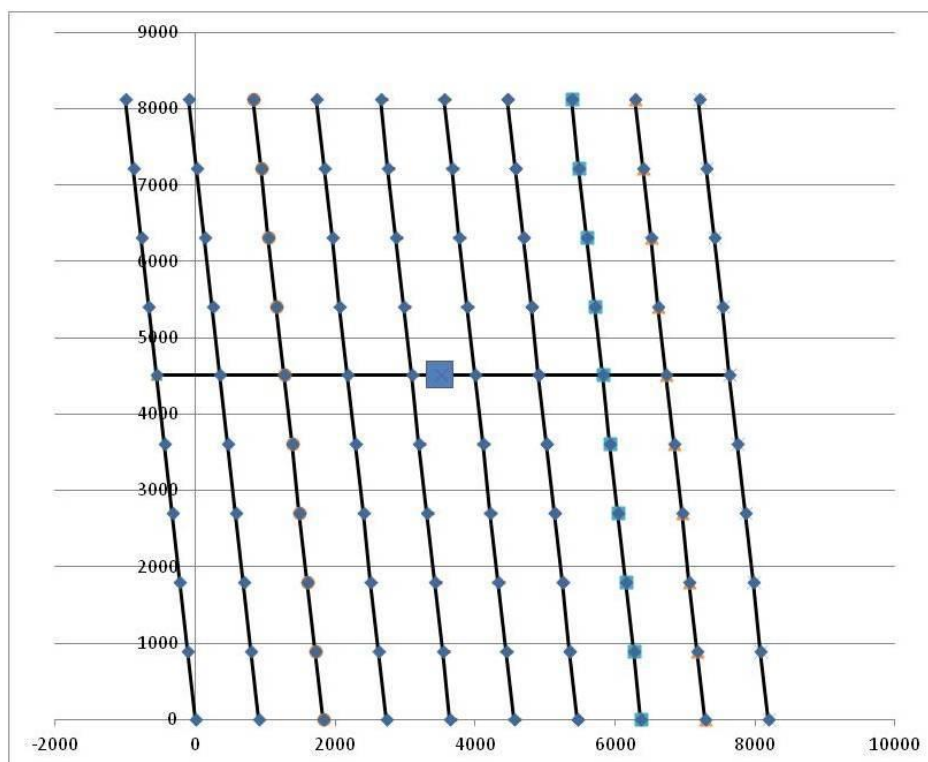
Figure 62.Layout of wind farm including electrical cables and transformers with 5.1 D distance between the turbines

0.3.2 Description of turbines:

The wind turbines from the near-future scenario have a rated power of 10 MW with a rotor diameter of 178.3 m at a hub height of 119 m.

- Wind class: IEC class Ia

- Regulation: Variable speed, collective pitch

- Orientation of rotor: Upwind, overhang 7.1 meter

- Cut in wind speed: 4 m/s

- Rated wind speed 11.4 m/s

- Cut-out wind speed 25 m/s

- Minimum rotor speed 6 rpm

- Maximum rotor speed: 9.6 rpm (maximum tip speed: 90 m/s)

- Gearbox: Medium speed, Multiple stage generator

0.3.3 Description of wind climate

Because we seek to evaluate the impact of neighbouring wind farms on the wind farm of interest, new wind climates without any wake effects were used. For this scenario, the 100 m wind resource from the DTU reference run, i.e. no wakes included, was used.

0.3.4 Remarks

Deliverable 5.12 EERA DTOC calculation of scenarios

In order to evaluate the impact of neighbouring wind farms, the scenario was originally calculated as is. Neighbouring wind farms were removed consecutively and the scenario was calculated after the removal of each wind farm. Figure shows the location of the wind farms in the North Sea (top) and a close view of each wind farm in relation to the others (bottom).

The order by which wind farms were removed was:
- Dogger Bank Teesside-A
- Dogger Bank Teesside-B
- Dogger Bank Creyke Beck-B

Due to the special format of this scenario, all wind turbines of all wind farms were considered active for the calculations. Therefore, in order to derive estimates of Net and Farm Annual Energy Production for the Dogger Bank case, the scenario was edited in QGIS, and only the relevant turbines of DB were selected and their performance statistics were summarized separately.
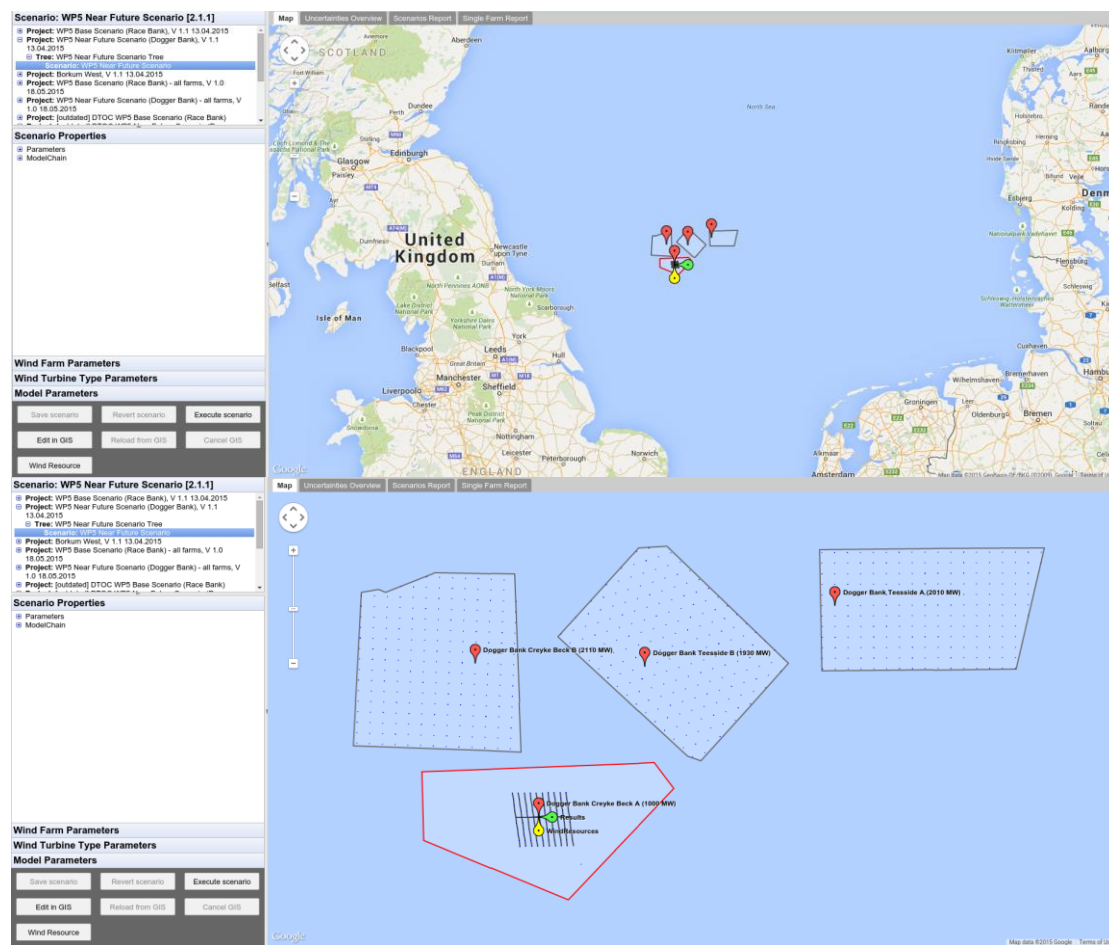

Figure 63. Position of the Dogger Bank wind farms in the North Sea (top), with a detailed layout (bottom).

0.4 Output/results

Scenario	Total Farm AEP (GWh/a)	Total Net AEP (GWh/a)	LCOE (Eur/MWh) *For all wind farms
All farms included	4315.901	5224.624	79.78

Deliverable 5.12 EERA DTOC calculation of scenarios

Remove:			
DB-TS-A	4316.135	5224.624	80.3
DB-TS-B	4320.175	5224.624	81.48
DB-CB-B	4333.063	5224.624	87.89

0.5 Observations

0.5.1 Observations on results.

What is found from the results is that there is an increase in the total Farm AEP as wind farms are removed. When DB-TS-A is removed, this increase is the smallest, less than 0.5 GWh/a, possibly justified by the larger distance to DB-CB-A, compared to the others. Removing DB-TS-B increases the farm's AEP by approximately 4 GWh/a, compared to the all-included-farms case, while having all other farms removed increases the AEP by 17 GWh/a, compared to the all-included-farms case, and by 13 GWh/a compared to having the DB-CB-B farm present.
In addition, an increase in the LCOE is observed when wind farms are being removed, but this calculation is based on all available wind turbines from all wind farms and not only on the DB one. The total net AEP for DB remains the same, independent of surrounding wind farms.

0.5.2 User experiences:

At this point, the way to evaluate the impact of neighbouring wind farms is not properly integrated in the tool since
- Included wind resources have been evaluated accounting for the wake losses. Thus editing wind farm locations in the tool, will not change anything as the underlying wind climate already includes the wake effects from such farms.
- Even if the wind climate did not include the wake effects. It is not possible to remove neighbouring wind farms as the tool is now, since they are considered inactive layers and can not be edited.

0.5.3 Expert judgement

While the total farm AEP of Dogger Bank CB-A increases when the neighbouring wind farms are removed, the LCOE decreases by 8 Eur/MWh when all farms are included.

Deliverable 5.12 EERA DTOC calculation of scenarios

P.1 Objective/user story

P.1.1 Objective

Evaluate the impact of the surrounding wind farms using the floating farm layout.

P.1.2 User story and scenario

Near future scenario (Dogger Bank) – Floating wind farm layout

User story
3.1 As a developer I can determine the wake effects of neighbouring wind farm clusters on a single wind farm (meso and/or micro).

P.2 Codes

WAsP-Park

P.3 Input:

P.3.1 Description of wind farm

This scenario is connected to the evaluation of the floating wind turbine layout for a cluster at Dogger Bank. It starts with a 1GW wind farm consisting of 104 turbines with a rated power of 10 MW using the well-documented INNWIND.EU reference turbine. The farm is assumed to be located at the southern part of the Dogger Bank area and is surrounded by other wind farms similar to the planned situation for Dogger Bank.

The suggested layout of the farm (Figure 64) is based on the hypothetical, optimal layout of a floating wind farm, designed for great depths, i.e. more than 100 meters. The mooring system of the wind farm becomes an important aspect for the electrical grid layout in field. Following the mooring system of Hywind, which includes 3 lines to minimise the cost and to enable its simple installation method, 2 wind farm clusters are designed. Since one single turbine is assumed to require three anchors, when multiple floating turbines are installed, it is cost effective to share the installation of the anchors. Since, one anchor might host three moorings a potential layout of 104 units has a celluloid shape.
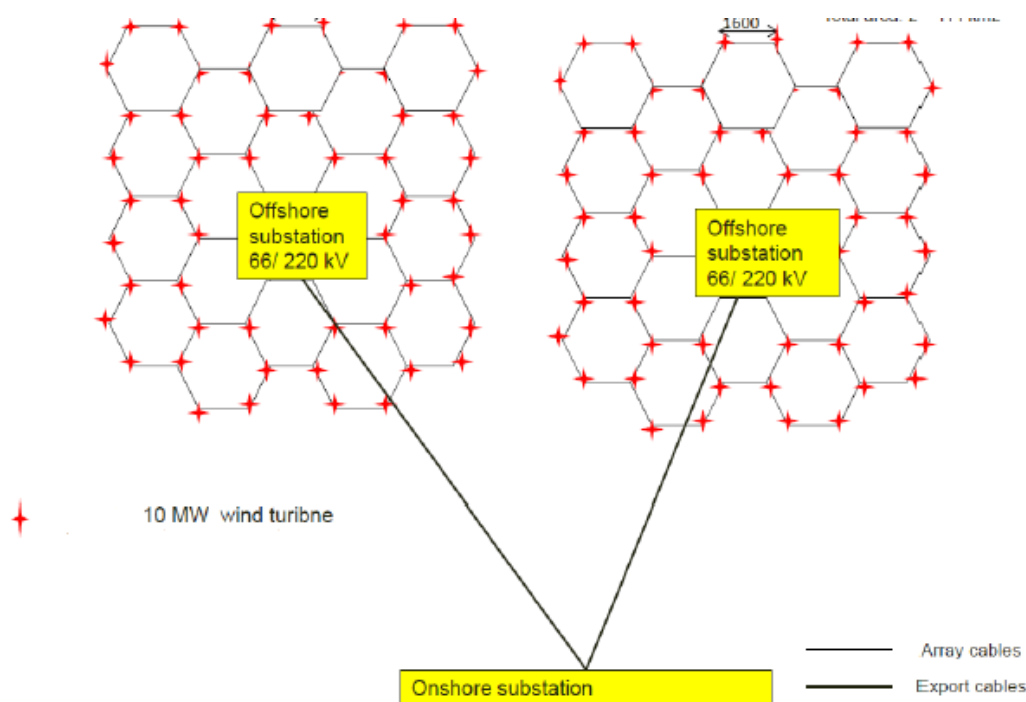
Deliverable 5.12 EERA DTOC calculation of scenarios

Figure 64.Layout of wind farm including electrical cables and transformers with 8.97 D distance between the turbines.

P.3.2 Description of turbines:

The wind turbines from the near-future scenario have a rated power of 10 MW with a rotor diameter of 178.3 m at a hub height of 119 m.

- Wind class: IEC class Ia

- Regulation: Variable speed, collective pitch

- Orientation of rotor: Upwind, overhang 7.1 meter

- Cut in wind speed: 4 m/s

- Rated wind speed 11.4 m/s

- Cut-out wind speed 25 m/s

- Minimum rotor speed 6 rpm

- Maximum rotor speed: 9.6 rpm (maximum tip speed: 90 m/s)

- Gearbox: Medium speed, Multiple stage generator

P.3.3 Description of wind climate

Because we seek to evaluate the impact of neighbouring wind farms on the wind farm of interest, new wind climates without any wake effects were used. For this scenario, the 100 m wind resource from the DTU reference run, i.e. no wakes included, was used.

P.3.4 Remarks

A major consideration regarding this scenario is that it assumes a floating farm layout suitable for depths greater than 100 meters. Nonetheless, it is calculated for Dogger Bank, where the water

Deliverable 5.12 EERA DTOC calculation of scenarios

depth is from 20 to 60 meters. Therefore, the bathymetry of the area is not relevant for such a scenario. In addition, the wind climate was simulated using the current, shallow depth bathymetry, rather than the assumed deep-water conditions.

In order to evaluate the impact of neighbouring wind farms, the scenario was originally calculated as is. Neighbouring wind farms were removed consecutively and the scenario was calculated after the removal of each wind farm. Figure shows the location of the wind farms in the North Sea (top) and a close view of each wind farm in relation to the others (bottom).

The order by which wind farms were removed was:
- Dogger Bank Teesside-A
- Dogger Bank Teesside-B
- Dogger Bank Creyke Beck-B

Due to the special format of this scenario, all wind turbines of all wind farms were considered active for the calculations. Therefore, in order to derive estimates of Net and Farm Annual Energy Production for the Dogger Bank case, the scenario was edited in QGIS, and only the relevant turbines of DB were selected and their performance statistics were summarized separately.
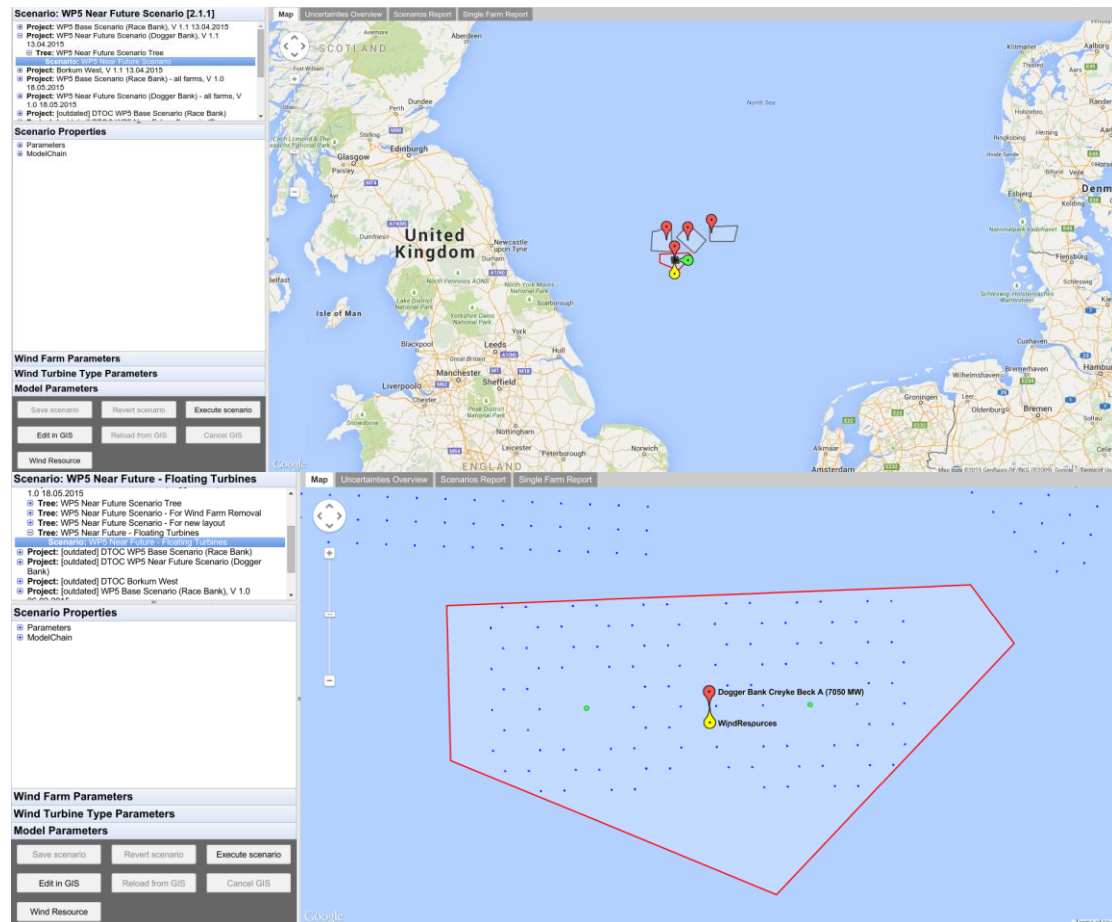

Figure 65. Position of the Dogger Bank wind farms in the North Sea (top), with a detailed layout (bottom).

Deliverable 5.12 EERA DTOC calculation of scenarios

P.4 Output/results

Scenario	Total Farm AEP (GWh/a)	Total Net AEP (GWh/a)
All farms included	5433,650	5103,366
Remove: DB-TS-A	5433,650	5103,679
DB-TS-B	5433,650	5110,862
DB-CB-B	5433,650	5139,449

P.5 Observations

P.5.1 Observations on results.

What is found from the results is that there is an increase in the total Net AEP as wind farms are removed. When DB-TS-A is removed, this increase is the smallest. Removing DB-TS-B increases the farm's AEP by approximately 7 GWh/a, compared to the all-included-farms case, while having all other farms removed increases the AEP by 36 GWh/a, compared to the all-included-farms case, and by 29 GWh/a compared to having the DB-CB-B farm present.
The total net AEP for DB remains the same, independent of surrounding wind farms.

From a comparison with the results presented in Appendix O: DTU: Near Future Scenario – Standard Layout, the total Net AEP is higher by approximately 800 GWh/a, keeping in mind that the floating scenario includes 4 additional wind turbines compared to the standard layout case.

P.5.2 User experiences:

At this point, the way to evaluate the impact of neighbouring wind farms is not properly integrated in the tool since
- Included wind resources have been evaluated accounting for the wake losses. Thus editing wind farm locations in the tool, will not change anything as the underlying wind climate already includes the wake effects from such farms.
- Even if the wind climate did not include the wake effects. It is not possible to remove neighbouring wind farms as the tool is now, since they are considered inactive layers and can not be edited.

P.5.3 Expert judgement

No LCOE model could be evaluated.

Q.1 Objective/user story

Q.1.1 Objective

Within the European Energy Research Alliance (EERA) Design Tool for Offshore wind farm Cluster (DTOC) project, three different institutes implemented the Weather Research & Forecasting (WRF) meso-scale model to produce wind climates for different areas of interest in the North Sea and spanning different time periods. At DTU Wind Energy two consecutive years were simulated, the National Renewable Energy Centre (CENER) modelled a representative meteorological year using a 10-year period while the Centro de Investigaciones Energéticas, Medioambientales y Tecnológicas (CIEMAT) modelled winds for 2013. Validation of such wind climates is essential but unfortunately, in situ measurements of the wind speed and direction at different atmospheric heights are only limited to those obtained from meteorological masts. Such datasets, while being optimal for validation purposes are available for few point locations, which are typically not representative of large spatial scales.

Surface winds retrieved from space borne sensors offer a wide spatial coverage but typically suffer from low spatial and temporal resolution, compared to the in situ observations and the modelled winds. In an effort to evaluate the accuracy of the model outputs, the 10-m winds from WRF were used to estimate the Equivalent Neutral Wind (ENW) at 10 meters, using the friction velocity at the surface and the logarithmic wind profile and assuming neutral atmospheric stratification. Two different scatterometer-retrieved 10-meter wind products were used, i.e. QuikSCAT and ASCAT, for comparisons with the WRF derived ENW. This report summarises the validation results in terms of general statistics, scatter plots and spatial comparisons.

Q.1.2 User story and scenario

Q.2 Codes

WRF, Matlab

Q.3 Input

Q.3.1 Data

In this section, the different WRF simulated winds produced at the three institutes are presented along with the two different types of scatterometer winds. In addition, the methodology for estimating the Equivalent Neutral Wind is described along with some considerations on the statistical comparisons.

Deliverable 5.12 EERA DTOC calculation of scenarios

WRF DTU

DTU Wind Energy provided almost two years of hourly WRF simulations, starting on January 11, 2006 and ending on December 31, 2007 with a 3-km grid spacing. In total, 1431 hourly fields were compared with QuikSCAT. Because the WRF domain is very large compared to the Dogger Bank area, two comparisons were performed. The first included the full WRF domain (DTU$_{FD}$) and a second comparison was performed only for the area around the wind farm (DTU$_{DB}$), i.e. two QuikSCAT grid cells compared to the closest WRF grid points (54.4–54.0°N, 1.7–2.1°E).

WRF CENER

For the Race Bank test case, CENER simulated a typical meteorological year, representative of a 10-year period. In total, they have provided 352 days of hourly WRF outputs, spanning over different calendar years with a spatial resolution of 3 km. After matching-up with QuikSCAT overpass times, 563 hourly fields were used (CENER$_{RB}$).

WRF CIEMAT

For the near future scenario, CIEMAT simulated 2013 using 4 domains around the area of interest with increasing spatial resolution from the outer towards the inner domain (27, 9, 3 and 1km) and an hourly temporal resolution. For comparisons with ASCAT, the 9 km domain outputs were used.

QuikSCAT

NASA's QuikSCAT mission carried on board SeaWinds, a pencil beam, wide swath scatterometer and was the first to operate for 10 consecutive years (99-09). It provided daily global coverage of the ocean with a repeat period of twice a day for the mid-latitudes. Wind measurements were routinely assimilated into weather models and used for hurricane monitoring. It provided valuable, consistent and frequent observations of the global ocean both in terms of speed and direction. QuikSCAT was launched in June 1999 with a design life-time of 3 years, as a quick recovery mission to fill the gap from the loss of NSCAT. The scatterometer's antenna failed rotating on the 23rd of November 2009, far exceeding the design life-time.

At an altitude of 803 km, QuikSCAT completed each orbit in approximately 101 minutes, ascending in the morning and descending in the afternoon (see Figure 1 for an example). With a wide swath of 1800 km it covered 93% of the global ocean each day. SeaWinds was an active microwave radar operating at 13.4 GHz (Ku band), radiating microwave pulses through a 1 m diameter antenna, and measuring the power of the signal returning back to the instrument (σ_0). The σ_0 "footprint" cell had dimensions of 25·37 km and the averaging area, the Wind Vector Cell was a square box of 25·25 km. The mission was managed by the Jet Propulsion Laboratory (JPL), operational products were produced at the National Oceanic Atmospheric Administration (NOAA) for the international meteorological community and were released near real time, i.e. within 3 hours of the data collection. More information can be found in http://winds.jpl.nasa.gov/missions/quikscat/index.cfm.

The mission requirements were i) an r.m.s. of 2 m/s for a wind speed range between 3-20 m/s and 10% within the 20-30 m/s range and ii) an r.m.s. of 20° for the direction within the wind speed range 3-30 m/s. Science products were distributed through the Physical Oceanography Data Archive Center (PODAAC). More information on the science data products can be found in JPL (2006). Karagali et al. (2014) used the full QuikSCAT archive from RSS processed with the Ku-2001 GMF, which is a descendant of the NSCAT-2 GMF, the improved version of the NSCAT-1 (GMF) (Wentz and Smith, 1999), where σ_0 values were mapped to a 0.25° Earth grid. This L3 product was compared with in situ derived ENW in the North Sea. Overall biases for the wind speed were found in the order of zero (±1.2 m/s), and 2.3° (±15°) for the wind direction.

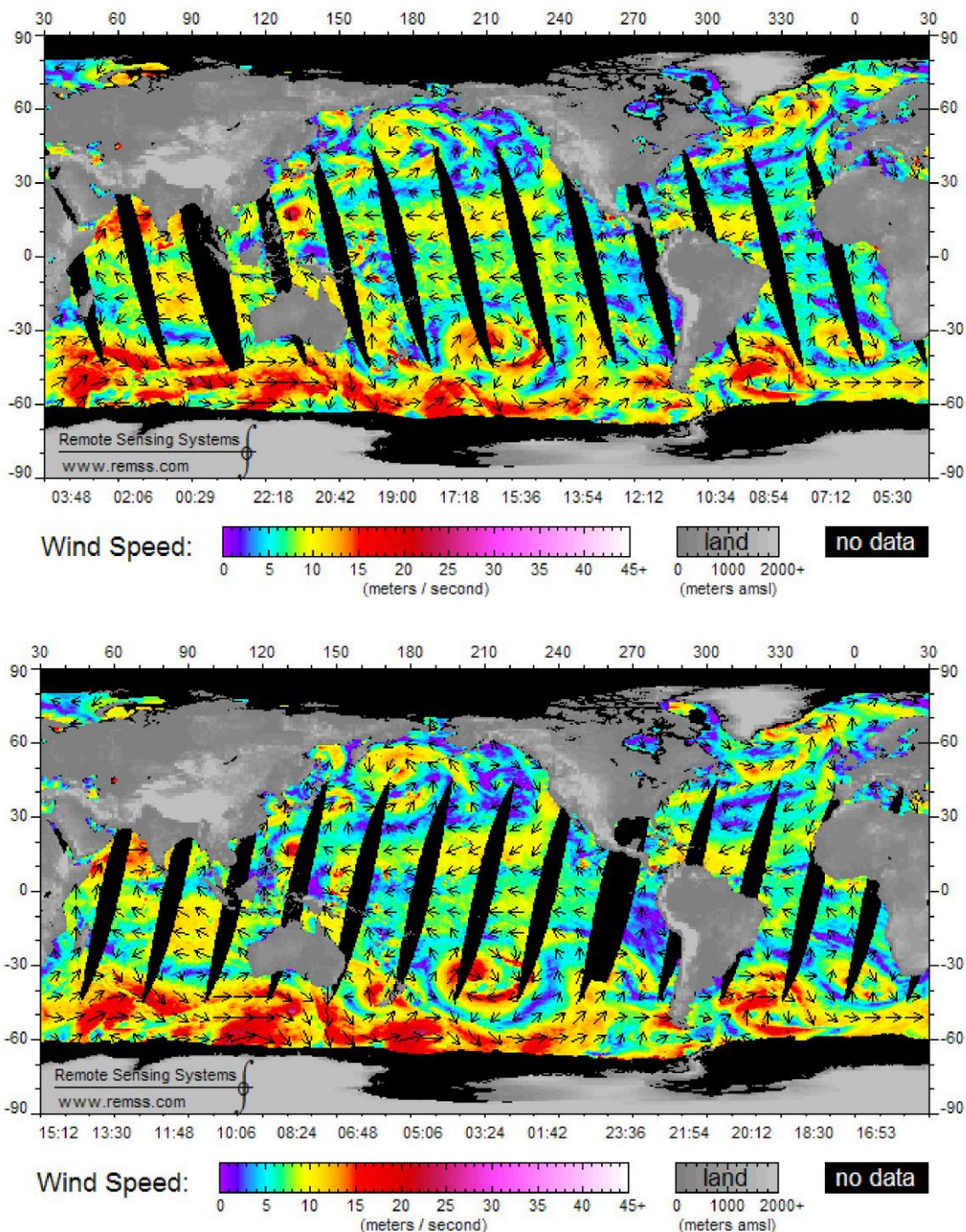*Deliverable 5.12 EERA DTOC calculation of scenarios*

Figure 66 Examples of the ascending, in the morning (top) and descending, in the afternoon (bottom) swath modes of QuikSCAT on the 4th of July 2006. Images are courtesy of RSS.

ASCAT

The first ASCAT instrument was launched in 2006, on board MetOp-A (operational since 2007), Europe's first polar orbiting satellite used for operational meteorology. Another ASCAT instrument is also available, on board the MetOp-B satellite (operational since April 2013), with a 3rd one being scheduled for launch in 2018. Currently, ASCAT is the longer available scatterometer in orbit. It is a C-band instrument, operating at 5.255 GHz and due to the longer wavelength, ASCAT is much less sensitive to rain compared to Ku band instruments like QuikSCAT. Because of this, C-

Deliverable 5.12 EERA DTOC calculation of scenarios

band instruments are also less responsive to very small changes of the surface roughness. At a mean altitude of 817 km, ASCAT has a 550 km wide swath on each side of the platform ground track. An example from an ASCAT wind retrieval is shown in Figure 2. The data are obtained from the coastal product developed at KNMI (http://www.knmi.nl/scatterometer/ascat_osi_co_prod/ascat_app.cgi). The missing data in the North Sea are due to the nadir gap. Note the high resolution features, showing an area of high winds between Denmark and Norway.
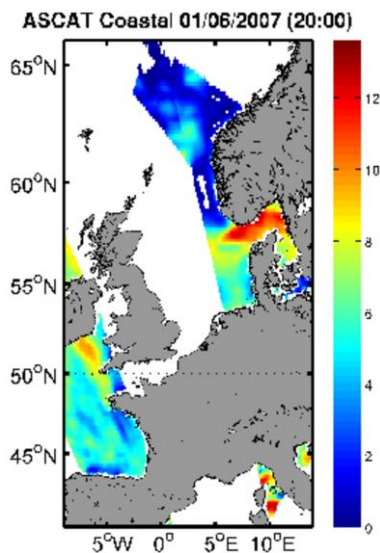

Figure 67 Example of an ASCAT coastal product from KNMI over the European Seas, taken from 01/06/2007 at 20:00. The wind speed is in m/s.

Q.3.2 Methods

The modified logarithmic wind profile accounting for the atmospheric stratification is defined in Equation 1 where u is the wind speed at height z, z_0 is the sea roughness length, u_* is the friction velocity, κ is the von Kármán constant (0.4) and Ψ_M the stability correction. The ENW is computed using u_* and z_0 consistent with the actual stratification and setting the Ψ_M function to zero.

$$u = u_*/\kappa \ln(z/z_0)-\Psi_M \qquad (1)$$

Wind observations from buoys, models or other satellite winds are used to estimate the friction velocity using the observed stability. The friction velocity is then used to estimate the 10 m wind assuming a neutral atmosphere. Finally, this neutral 10 m wind is related to the observed σ_0. The GMF resulting from the SASS scatterometer (Ku band) are tuned to ENW. The GMF of the CMOD family were tuned to non-neutral winds until CMOD5.N which is currently being used for the ASCAT scatterometer (Hersbach, 2010). The atmospheric stability is not always neutral. Figure 3 shows how the stability can influence the difference between the ENW and the true wind. When the stratification is neutral (green line), the difference between the ENW and the true wind is negligible. When the stratification is stable (blue lines) the true wind is higher than the ENW. When the stratification is unstable (red lines) the ENW is higher than the true wind but the differences are much smaller compared to the stable cases. Brown et al. (2006) found that the globally averaged 10 m neutral winds from the European Centre for Medium Range Weather Forecasting (ECMWF) were 0.19 m/s stronger than the ECMWF standard 10 m winds and concluded that the marine boundary layer is overall slightly unstable.
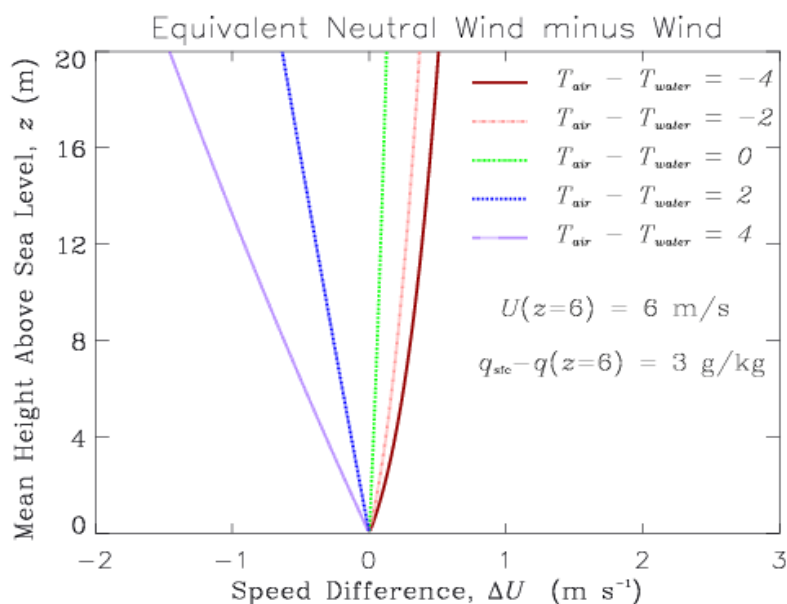
Deliverable 5.12 EERA DTOC calculation of scenarios

To directly compare WRF and scatterometer winds, the former were converted to Equivalent Neutral Winds. This was performed using the WRF friction velocity u_* along with Charnock's surface roughness value, z_0, from WRF and assuming neutral atmospheric stability. For the wind direction comparisons, all match-ups for which the WRF-QSCAT difference is larger than 90 degrees, were excluded. In addition, to filter for spurious match ups the $\mu \pm 4\sigma$ threshold was applied, in certain cases.

Q.4 Results:

Q.4.1 Statistics

All statistics between WRF and the scatterometer winds, i.e. QuikSCAT and ASCAT, shown in Table 14 are derived by matching the scatterometer value of speed or direction at a specific point with the corresponding WRF value of the closest time and grid point, for the entire area and period of WRF runs, unless otherwise stated. Due to the very large number of collocated QuikSCAT and DTU WRF points, the wind speed match-ups have been filtered for extreme values using the threshold $\mu \pm 4\sigma$.

The collocated and time coincident QuikSCAT and CENER WRF wind speeds and directions at each grid point for the entire domain and all available hourly outputs, are shown in Figure 69. The left panel shows the scatter plot of speed, with the black line representing the linear fit. A large scatter is found, while the overall bias is only 0.1 m/s but the standard deviation of 2.4 m/s is rather high. For the wind direction, the scatter is again relatively large, with a bias of 5.2° and σ of almost 30°.

Deliverable 5.12 EERA DTOC calculation of scenarios

Table 14 Statistics between WRF hourly wind speed (U) and direction (Dir) and ocean surface winds from scatterometers, including the mean bias (μ), standard deviation (σ), root mean square error (RMSE), correlation coefficient (r), number of collocated samples (N).

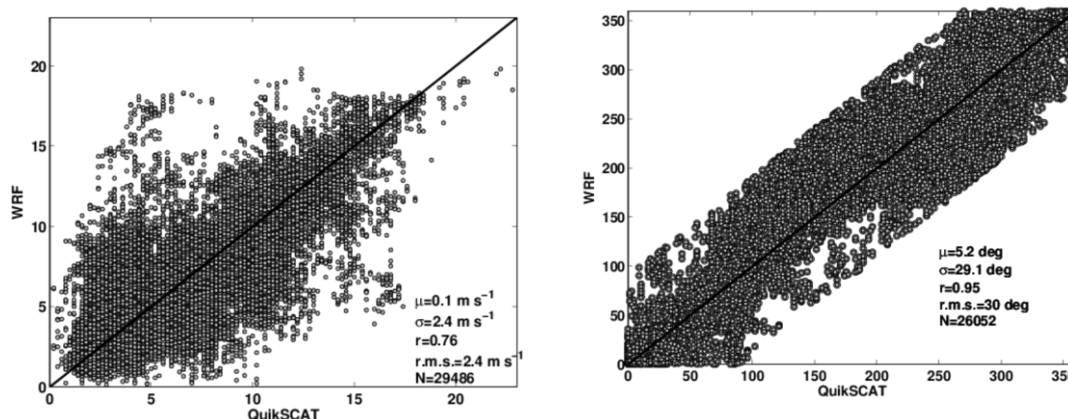| Datasets	μ		σ		RMSE		r		N	
	U(m/s)	Dir (deg)	U(m/s)	Dir (deg)	U(m/s)	Dir (deg)	U(m/s)	Dir (deg)	U(m/s)	Dir (deg)
CENER$_{RB}$-QSCAT	0.08	5.20	2.43	29.14	2.43	29.60	0.76	0.95	29486	26052
DTU$_{FD}$-QSCAT	0.41	10.11	2.62	29.80	2.66	31.54	0.77	0.94	884597	786227
DTU$_{DB}$-QSCAT	0.78	9.58	2.57	78.93	2.69	79.49	0.78	0.65	2519	2220
CIEMAT-ASCAT	0.17	4.35	1.54	18.65	1.55	19.15	0.91	0.98	37136	35417

Figure 69 Scatterplots of collocated match-ups of wind speed (left) and direction (right), between QuikSCAT (bottom) and the CENER WRF runs (vertical).

Due to the extended area of the DTU WRF domain and the large number of match-ups with QuikSCAT, the scatter plots of speed and direction are shown as colour-coded density plots, where each coloured box represents the number of match-ups at a specific range of speeds or directions. The left panel of Figure 70 shows the density plot of all the wind speed match-ups between QuikSCAT (horizontal) and DTU WRF (vertical), for the entire domain and binned every 1 m/s from 0 to 20 m/s. Most match-ups occur within the range 5-12 m/s, with a slight overestimation of WRF winds in this range. For the wind direction (right panel), almost all match-ups occur within the 180° to 360° interval.

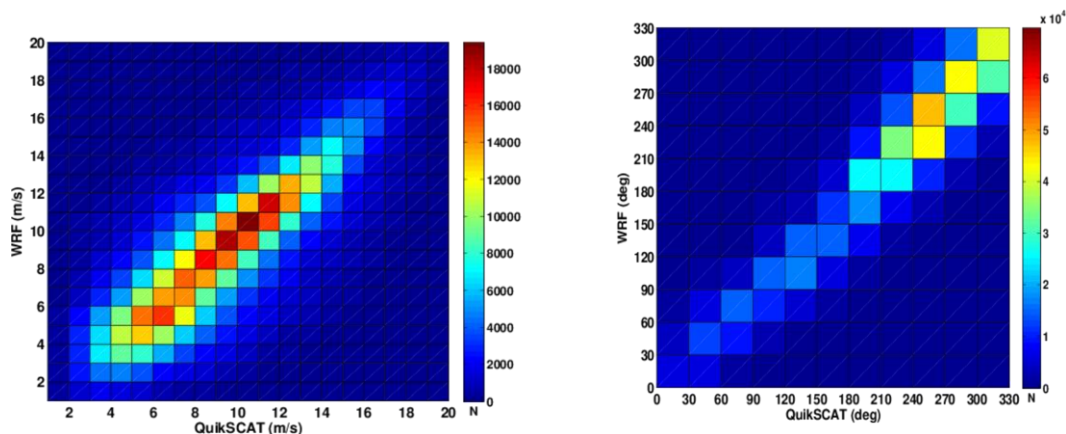*Deliverable 5.12 EERA DTOC calculation of scenarios*

Figure 70 Density plots of the collocated match-ups of wind speed (left) and direction (right), between QuikSCAT (horizontal axis) and the DTU WRF runs (vertical) for the entire domain.

The scatter plot of wind speed and direction match-ups between QuikSCAT (horizontal) and DTU WRF (vertical), only around the Dogger Bank wind farm are shown in Figure 71. Most match-ups occur within the 2-12 m/s interval and there is a significant scatter above the 1:1 line, showing higher WRF speeds which is also evident from the μ value. At the higher wind speed ranges though, QuikSCAT shows higher values compared to WRF. The wind direction scatter (right panel) is also relatively large, while most match ups occur in the range between 150° and 360°, showing westerlies and northern directions.
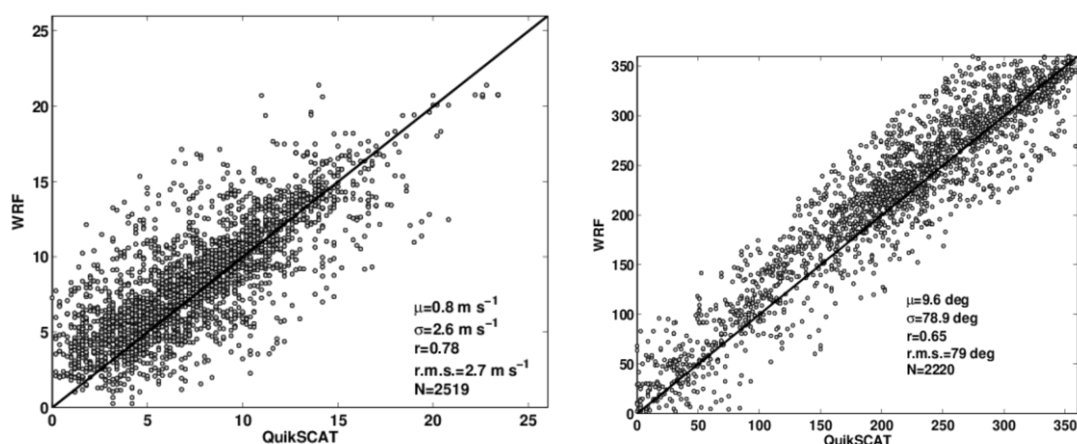

Figure 71 Scatterplots of the collocated match-ups of wind speed (left) and direction (right), between QuikSCAT (horizontal axis) and the DTU WRF runs (vertical) only for a small area around the wind farm.

Finally, the scatter plots of wind speed (left) and direction (right) match-ups between ASCAT (horizontal) and CIEMAT WRF (vertical) for 2013 are presented in Figure 72. The scatter is somewhat less for the speed, compared to the cases of the QuikSCAT comparisons, with a lower standard deviation value of 1.5 m/s and μ of 0.2 m/s while the correlation coefficient is also high. A slight overestimation of WRF winds is identified, particularly for the lower and higher wind speed ranges. The wind direction scatter plot also shows a slight overestimation of WRF directions.

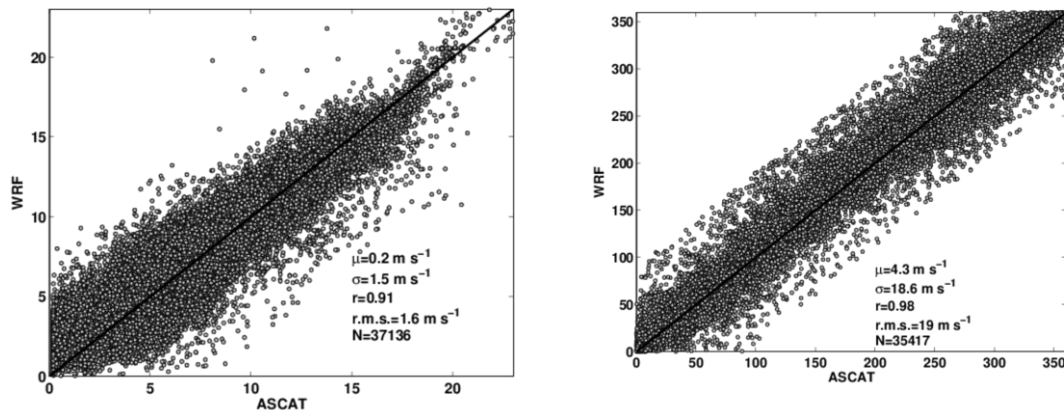*Deliverable 5.12 EERA DTOC calculation of scenarios*

Figure 72 Scatterplots of the collocated match-ups of wind speed (left) and direction (right), between ASCAT (horizontal axis) and the CIEMAT WRF runs (vertical).

Q.4.2 Spatial Comparisons

The mean wind speed from the time-coincident QuikSCAT and CENER WRF wind speeds are shown in Figure 73. The lack of information near the coast of the satellite scatterometer is evident, shown with white. Highest QuikSCAT speeds are identified at the south-east part of the domain, ranging between 7.5 and 8 m/s. At the same region, WRF winds are slightly lower around 7.5 m/s, while the spatial variability is much higher due to the higher spatial resolution of WRF. The opposite trend is identified at the north-east part of the domain, where QuikSCAT winds are around 7.5 m/s while WRF shows higher wind speeds, up to 8 m/s.

The bottom panels of Figure 73 show the number of wind speed observations at each grid cell, used for the estimation of the mean wind speed. At the left panel, QuikSCAT shows spatial variability in the number of observations per grid cell, related to the presence of rain which contaminates the wind retrieval and the proximity to the land which alters the scattering properties thus making the retrieval of wind information highly ambiguous. The right panel, shows the number of wind speed "observations" from WRF, which being a model provides full temporal and spatial coverage.

Figure 74 shows the mean wind speed (top panels) from QuikSCAT (left) and DTU WRF (right), for the entire North Sea domain modelled by DTU Wind Energy. Spatial agreement is generally found between WRF and QuikSCAT, with the area of lower speeds off the central part of the UK appearing also in WRF but with a reduced magnitude of wind speed variability. Higher wind speeds at the north part of the domain are retrieved from QuikSCAT and modelled by WRF but with some spatial mismatch, which is to be expected if one considers the difference in spatial resolution between QuikSCAT and WRF.

The bottom panels of Figure 74 show the available QuikSCAT wind retrievals for each grid cell, ranging between zero retrievals very close to and on land, to 1400 retrievals at some parts of the North Sea. WRF available wind speeds (right panel) have a constant amount of 1400 at each grid cell.

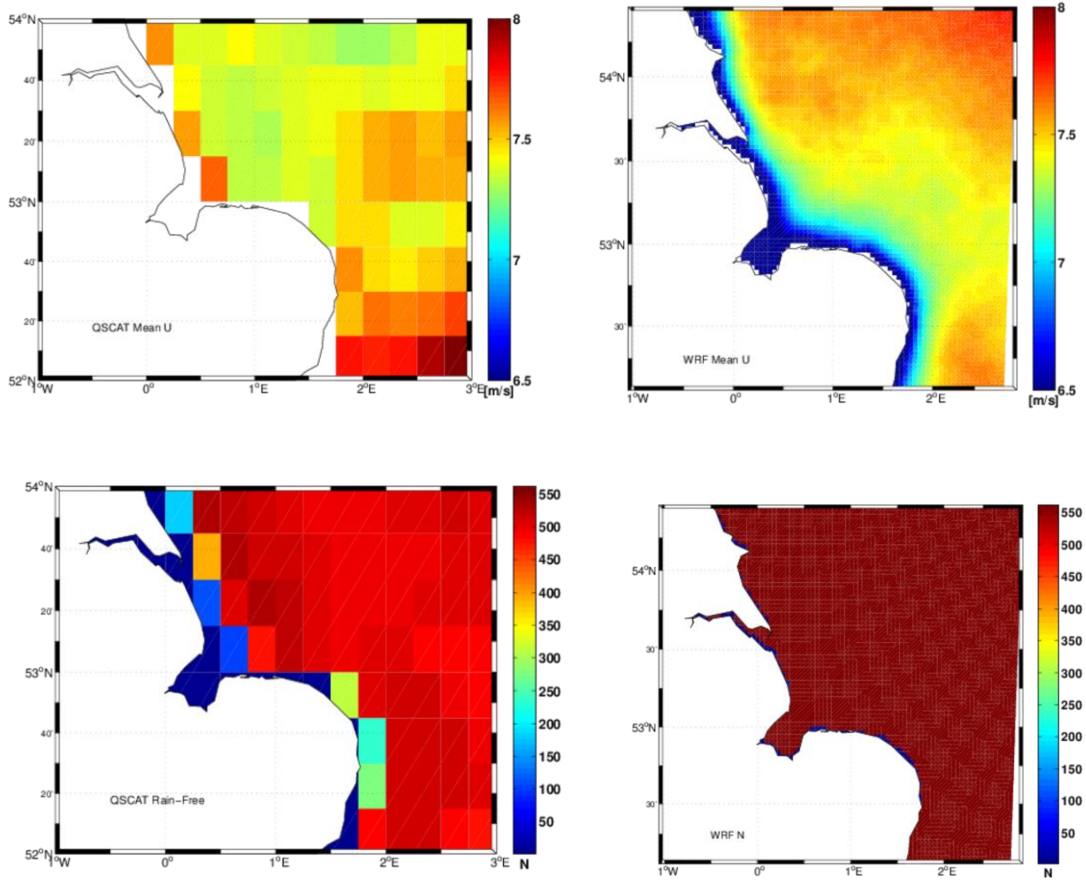*Deliverable 5.12 EERA DTOC calculation of scenarios*

Figure 73 Top: Mean wind speed from QuikSCAT (left) and WRF (right). Bottom: Number of available wind retrievals for QuikSCAT (left) and WRF (right).

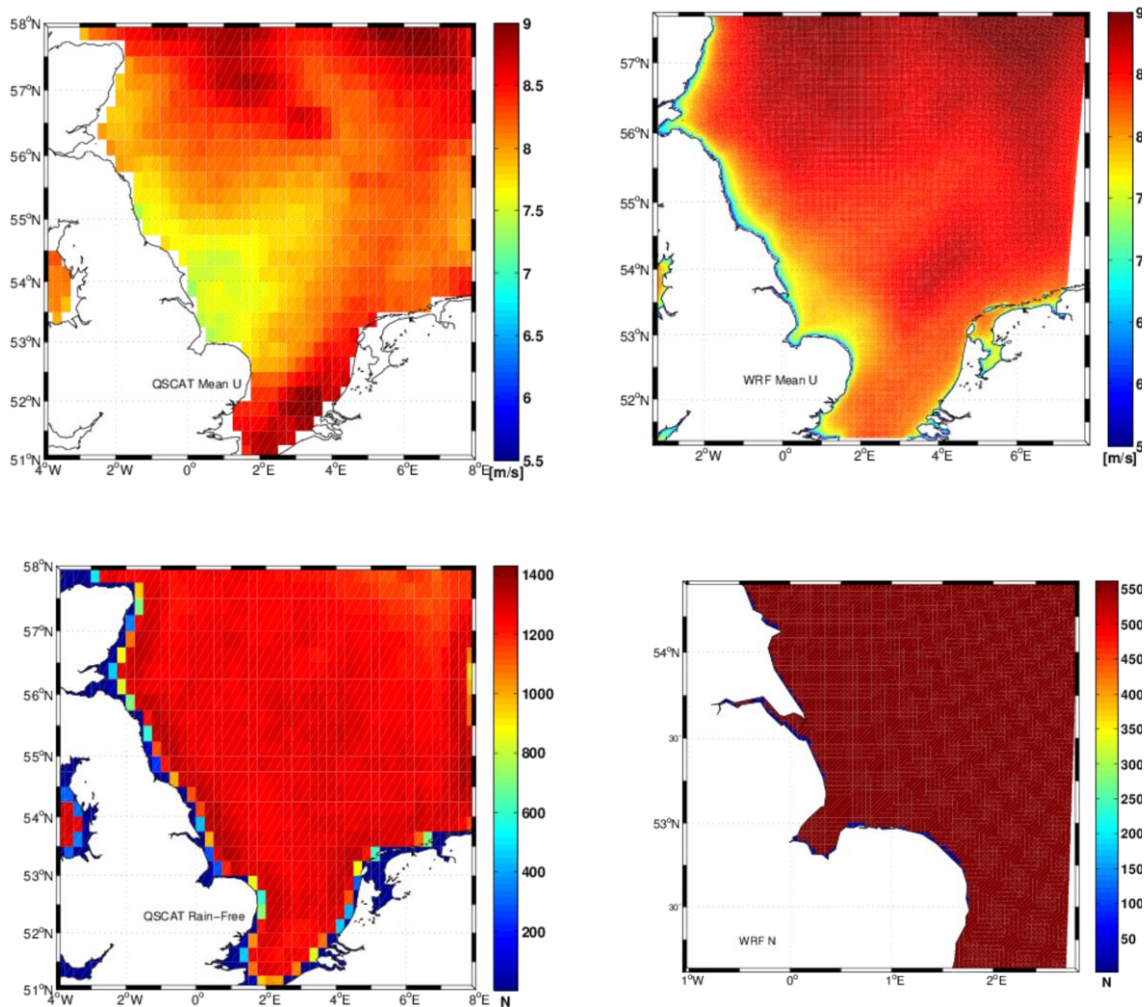*Deliverable 5.12 EERA DTOC calculation of scenarios*

Figure 74 Top: Mean wind speed from QuikSCAT (left) and WRF (right). Bottom: Number of available wind retrievals for QuikSCAT (left) and WRF (right).

Due to the non-gridded nature of the ASCAT wind product, no direct spatial comparisons between ASCAT and CIEMAT WRF could be performed. Instead, the wind speed and direction from the WRF model and ASCAT were averaged based on latitude and longitude bins of 12.5 km, in accordance with the lower ASCAT spatial resolution. Figure 75 shows the comparisons for the latitudinal (top) and longitudinal (bottom) averages.

The maximum deviation in speed reaches 0.3 m/s between 53.5° N and 54.5° N, where also the direction deviation is highest. A slight increase of wind speed and a turning of the wind direction from southerly to westerly winds, is also noted as the latitude increases.

For the longitudinal direction, the maximum wind speed difference is slightly higher, 0.4 m/s, and occurs between 1° E and 3° E. A sharp increase of the speed between 1 and 1.5° E is noted both in ASCAT and WRF.

This peak also appears in the wind directions that show a larger difference in the longitudinal direction compared to the latitudinal, as well as a milder turning of the winds towards westerlies as the longitude increases, i.e. towards the East.

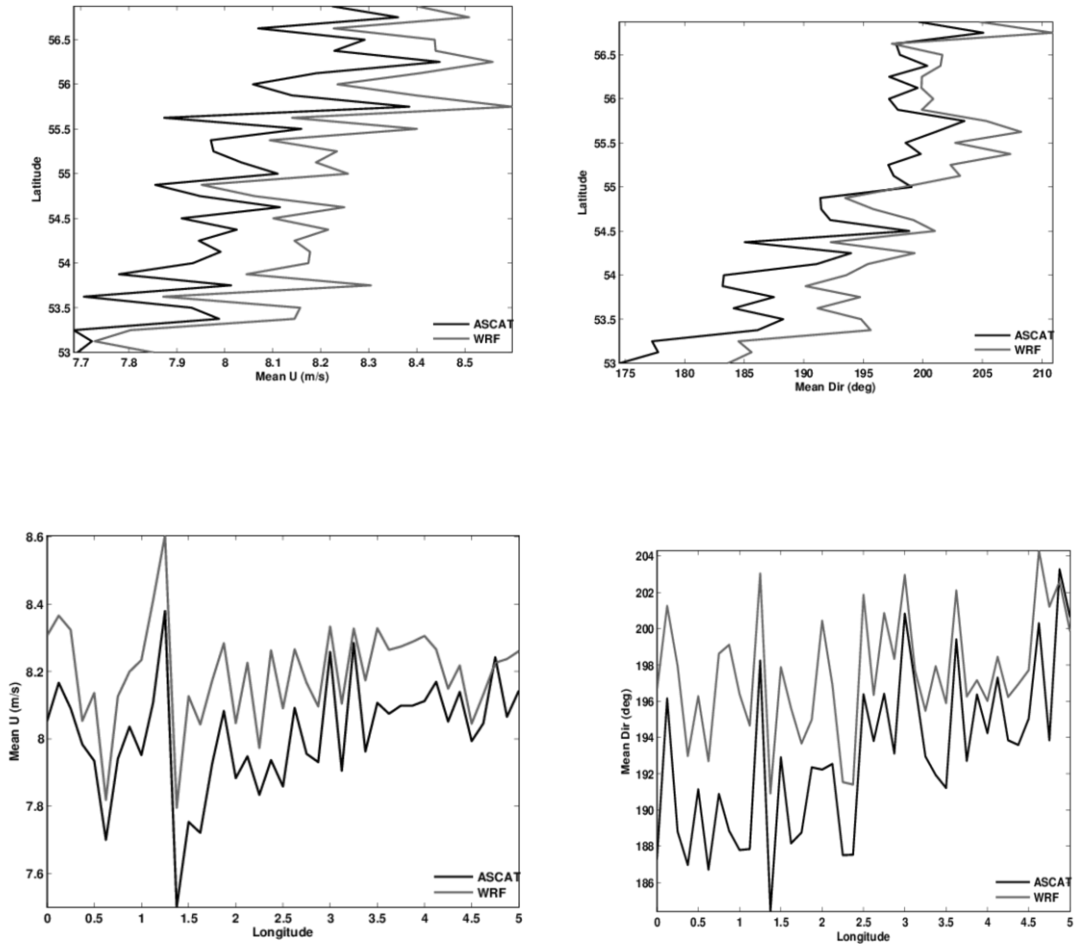*Deliverable 5.12 EERA DTOC calculation of scenarios*

Figure 75 Top: Mean wind speed from QuikSCAT (left) and WRF (right). Bottom: Number of available wind retrievals for QuikSCAT (left) and WRF (right).

Deliverable 5.12 EERA DTOC calculation of scenarios

Q.4 Discussion and Conclusions

The wind speed at 10-m above the sea surface is not directly relevant for offshore wind energy related activities, as typically wind turbine hub heights offshore reach up to 80 meters or more. In situ measurements from tall meteorological masts are ideal for validation purposes but the availability of such datasets is scarce and very often restricted. Satellite winds offer an extended spatial coverage, comparable to that of modelled winds, but typically have a significantly lower temporal and spatial, depending on the type of sensor, resolution.

From the comparisons presented in this study, the overall conclusion is an overestimation of the model 10-m neutral winds compared to the scatterometer derived ones, independent of the domain, period of time and model set-up. This may be associated with an underestimation of the surface roughness in WRF. A study comparing a WRF re-analysis dataset with QuikSCAT (Karagali et al., 2013) found on average higher WRF winds by approximately 1 m/s with a standard deviation in the order of 2 m/s for the south part of the North Sea basin. For a particular location in the German Bight, the FINO-1 platform, Karagali et al. (2013) reported a 0.5 m/s higher WRF mean wind speed, compared to the mean QuikSCAT wind speed and 0.6 m/s higher than the in situ measured mean wind speed.

From the two different types of scatterometer datasets used, QuikSCAT has a coarser resolution of 25 km compared to the 12.5 km resolution of ASCAT. While the comparisons with both DTU WRF and CENER WRF were performed by selecting the model grid point closest to the QuikSCAT grid cell centre, that value represents an average wind speed derived by averaging multiple σ_0 values before the wind retrieval is performed.

The much higher resolution of the WRF DTU and CENER set-ups, can be a partial source for the statistical deviations shown in Table 1. The similar spatial resolution of ASCAT (12.5 km) and the CIEMAT WRF (9 km), also compared in a similar manner, resulted in generally better statistics with significantly lower μ and **σ** values.

One more parameter that can lead to disagreement between the model and the satellite winds, is related to the timing of observations and model outputs. While the latter are available hourly, typically at the start of the hour, the former can be retrieved at some other point during the hour, which means that model and satellite winds may have a time difference up to 30 minutes.

The results reported here can be supplemented with comparisons between WRF and in situ measurements from offshore meteorological masts at point locations. The results of such comparisons can aid understanding the nature of the comparisons presented in this study, for example to validate if indeed there is a tendency for WRF to overestimate the wind speed, as reported above.

Q.5 References

[1] Bourassa M.A. (2013)
http://coaps.fsu.edu/~bourassa/BVW_html/eqv_neut_winds.shtml

[2] Boutin J., Quilfen Y., Merlivat L., and Piolle J.F. (2009) Global average of air-sea CO2 transfer velocity from QuikSCAT scatterometer wind speeds. J. Geophys. Res. 114:C04007.

[3] Brown A.R., Beljaars A.C.M., and Hersbach H. (2006) Errors in parametrizations of convective boundary-layer turbulent momentum mixing. Q. J. R. Meteorol. Soc. 132:1859–1876.

[4] Hersbach H. (2010) Comparison of C-band Scatterometer CMOD5.N equivalent neutral winds with ECMWF. J. Atmos. Ocean. Techn. 27:721–736.

Deliverable 5.12 EERA DTOC calculation of scenarios

[5] Jet Propulsion Laboratory (2006) NASA Quikck Scatterometer - QuikSCAT science data product user's manual: overview and geophysical data products. JPL, California Institute of Technology 2006(V3.0):D-18053-RevA.

[6] Kara A.B., Wallcraft A.J., and Bourassa M.A. (2008) Air-sea stability effects on the 10-m winds over the global ocean: Evaluation of air-sea flux algorithms. J. Geophys. Res, 113:C04009.

[7] Karagali I., Peña A., Badger M., and Hasager C.B. (2014) Wind characteristics in the North and Baltic Seas from the QuikSCAT satellite. Wind Energy 17(1):123–140.

[8] Karagali I., Badger M., Peña A., Hahmann A., Hasager C.B., and Sempreviva A.M. (2013) Spatial and temporal variability of winds in the Northern European Seas. Renewable Energy 2013(57):200-210.

[9] Liu W.T. (2002) Progress in Scatterometer Application J. Oceanogr. 58: 121–136.

[10] Liu W.T., Tang W. (1996) Equivalent neutral wind. National Aeronautics and Space Administration, Jet Propulsion Laboratory, California Institute of Technology, National Technical Information Service, distributor.

[11] Wentz F.J., and Smith D.K. (1999) A model function for the ocean-normalized radar cross section at 14GHz derived from NSCAT observations. J. Geophys. Res. 1999(104):11499-11514.

Deliverable 5.12 EERA DTOC calculation of scenarios